

THE INSTITUTE OF PAPER CHEMISTRY, APPLETON, WISCONSIN

STATUS REPORTS

To The  
Engineering Project Advisory Committee

October 22-23, 1986  
The Institute of Paper Chemistry  
Continuing Education Center  
Appleton, Wisconsin

#### NOTICE & DISCLAIMER

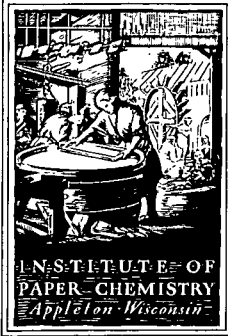
The Institute of Paper Chemistry (IPC) has provided a high standard of professional service and has exerted its best efforts within the time and funds available for this project. The information and conclusions are advisory and are intended only for the internal use by any company who may receive this report. Each company must decide for itself the best approach to solving any problems it may have and how, or whether, this reported information should be considered in its approach.

IPC does not recommend particular products, procedures, materials, or services. These are included only in the interest of completeness within a laboratory context and budgetary constraint. Actual products, procedures, materials, and services used may differ and are peculiar to the operations of each company.

In no event shall IPC or its employees and agents have any obligation or liability for damages, including, but not limited to, consequential damages, arising out of or in connection with any company's use of, or inability to use, the reported information. IPC provides no warranty or guaranty of results.

This information represents a review of on-going research for use by the Project Advisory Committees. The information is not intended to be a definitive progress report on any of the projects and should not be cited or referenced in any paper or correspondence external to your company.

Your advice and suggestions on any of the projects will be most welcome.



THE INSTITUTE OF PAPER CHEMISTRY  
Post Office Box 1039  
Appleton, Wisconsin 54912  
Phone: 414/734-9251  
Telex: 469289

October 3, 1986

TO: Members of the Engineering Project Advisory Committee

Enclosed is advance reading material for the October 22-23 meeting of the Engineering Project Advisory Committee. Included are status reports for active projects, an agenda, and a current committee membership list.

Rooms have been reserved in the Continuing Education Center, and meals will be provided as stated on the agenda. If you haven't already indicated your attendance, please do so at your earliest convenience by calling Barbara Bisby at (414)738-3328.

For all Project Advisory Committee meetings, the Institute invites its member companies to send one or more representatives to attend the review sessions (first day) of any or all of the meetings. These invitations were mailed in early August. PAC members from member companies are also welcome to attend these other meetings, and may stay in the CEC and attend meetings and meals of their choice at no cost. If you wish to attend any of these other meetings but haven't registered, please call Barbara Bisby to do so. A meeting schedule is enclosed for your information.

We look forward to meeting with you on October 22-23.

Sincerely,

Clyde H. Sprague, Director  
Engineering Division

CHS/e1  
Enclosures

TABLE OF CONTENTS

	<u>Page</u>
TABLE OF CONTENTS . . . . .	i
AGENDA . . . . .	ii
COMMITTEE LIST . . . . .	iv
Project 3309: Fundamentals of Corrosion Control in Paper Mills . . .	1
Project 3556: Fundamentals of Kraft Liquor Corrosivity . . . . .	42
Project 3607: Evaluation of Structural Coatings for Pulp and Paper Mill Service . . . . .	69
Project 3606: Corrosion in High Yield Pulping Processes. . . . .	74
Project 3384: Refining of Chemical Pulps for Improved Physical Properties. . . . .	83
Project 3479: Higher Consistency Processing . . . . .	89
Project 3470: Fundamentals of Drying . . . . .	98

\* \* \* PRELIMINARY AGENDA \* \* \*

ENGINEERING  
PROJECT ADVISORY COMMITTEE

October 22-23, 1986

Continuing Education Center (CEC)  
The Institute of Paper Chemistry  
Appleton, Wisconsin

Wednesday, October 22, 1986

PROJECT REVIEWS

10:00am --	INTRODUCTION	Sprague/Rugowski
10:15am --	CORROSION AND MATERIALS ENGINEERING SECTION	
	- Fundamentals of Corrosion Control in Paper Mills	Yeske
	- Fundamentals of Kraft Liquor Corrosivity	Crowe
12:00pm --	LUNCH	
1:00pm	- Evaluation of Structural Coatings for Pulp and Paper Mill Service	Yeske
	- Corrosion in High Yield Pulping Processes	Crowe
1:45pm --	PAPERMAKING PROCESSES GROUP	
	- Refining of Chemical Pulps for Improved Physical Properties	Farrington
	- Higher Consistency Processing	Farrington
	Applications of X-Ray Imaging	Farrington
2:45pm --	BREAK	
3:15pm --	- Impulse Drying	
	Mechanisms	Sprague
	Performance	Lavery
	Pilot Impulse Dryer Design	Kloth
5:30pm --	COCKTAILS	
6:00pm --	DINNER - CEC Dining Room	
7:15pm --	LABORATORIES	
	- X-Ray Imaging	
	- Roll Impulse Dryer	
	- Refining System	

Thursday, October 23, 1986

7:15am -- BREAKFAST -- CEC Dining Room

COMMITTEE ACTIVITIES

8:00am -- Discussion of Projects

Committee &  
Research Staff

9:30am -- BREAK

9:45am -- Continued Discussion of Projects

10:30am -- Report Preparation

Committee

11:30am -- Adjourn

-- LUNCH - CEC Dining Room

NOTE: The spring Engineering PAC meeting is scheduled for March 26-27, 1987.

ENGINEERING

Project Advisory Committee

Mr. James Rugowski (Chairman) - 6/88\*  
Engineering Consultant  
Kimberly-Clark Corporation  
2100 Winchester Road  
Neenah, WI 54956  
(414) 721-2000

Mr. LeRoy H. Busker - 6/88  
Director, Research & Planning  
Beloit Corporation  
Rockton R & D Center  
1165 Prairie Hill Road  
Rockton, IL 61072  
(608) 364-7961

Dr. Gerard P. Closset - 6/88  
Director, Papermaking and  
Coating Technology  
Champion International  
Technical Center  
West Nyack Road  
West Nyack, NY 10994  
(914) 578-7142

Dr. John W. Glomb - 6/88  
Vice President and  
Corporate Research Director  
Research Department  
Westvaco Corporation  
299 Park Avenue  
New York, NY 10171  
(212) 688-5000

Mr. Max D. Moskal - 6/88  
Sr. Project Manager  
Stone Container Corporation  
616 Executive Drive  
Willowbrook, IL 60521  
(312) 655-6949

Mr. M. Thomas Neill - 6/88  
Vice President R&D  
Abitibi-Price, Inc.  
Research Centre  
Sheridan Park  
Mississauga, Ontario L5K 1A9  
CANADA  
(416) 822-4770

\*date of retirement  
10/1/86

Dr. Robert Rounsley - 6/89  
Research Fellow  
Mead Corporation  
8th & Hickory Street  
Chillicothe, OH 45601  
(614) 772-3581

Dr. John Smuk - 6/89  
Manager of Process Engineering  
Research and Development Center  
Potlatch Corporation  
P.O. Box 510  
Cloquet, MN 55720  
(218) 879-2393

Dr. Ronald E. Swanson - 6/88  
Manager, Corporate Research  
Hammermill Paper Company  
P.O. Box 10050  
Erie, PA 16533  
(814) 456-8811

Mr. Benjamin Thorp - 6/89  
Senior Vice President  
Research and Engineering  
James River Corp. of Virginia  
P.O. Box 2218  
Richmond, VA 23217  
(804) 644-5411

Mr. David E. White - 6/87  
Group Leader  
Research & Development  
Union Camp Corporation  
P. O. Box 3301  
Princeton, NJ 08543-3301  
(609) 896-1200

Dr. Jerry Wallace - 6/89  
Mill Manager  
Appleton Papers Inc.  
100 Paper Mill Road  
Roaring Springs, PA 16673-1480  
(814) 224-2131

Dr. Yung Duk Woo - 6/89  
Senior Engineer  
Papermaking R&D Department  
Weyerhaeuser Paper Company  
Tacoma, WA 98477  
(206) 924-6428

THE INSTITUTE OF PAPER CHEMISTRY

Project Advisory Committee Fall Meetings  
Member Dues - Funded Research Reviews

October 20, 21, 22, 23 and 28

1986

Continuing Education Center  
Appleton, Wisconsin  
(414) 734-9251

<u>Committee</u>	<u>Review Schedule</u>	<u>Research Area*</u>
Pulping Processes	Monday, October 20 8:30 AM - evening	Chemical Recovery: Recovery Furnace Processes Bleached Chemical Pulp: Lignin/Carbohydrate Reactions Oxygen Bleaching Chemistry High Lignin Pulps: Brightness Stability Strength Development Micro Structure of Wood Fibers Analytical Techniques
Paper Properties	Tuesday, October 21 8:30 AM - evening	Strength Improvement and Failure Mechanisms Board Properties and Performance Student Research Process, Properties, Product Relationships Internal Strength Enhancement On-line Measurement of Paper Mechanical Properties Tour of Paper Materials Division Labs
Engineering	Wednesday, October 22 10:00 AM - evening	Corrosion: Kraft Liquor Corrosivity Corrosion Control in Paper Mills Papermaking: Mechanics of Refining Higher Consistency Processing Wet Pressing New Drying Concepts

\*NOT IN ORDER OF AGENDA



<u>Committee</u>	<u>Review Schedule</u>	<u>Research Area*</u>
Systems Analysis	Thursday, October 23 1:00 PM - evening	MAPPS Simulator Development MAPPS Applications and Field Experience
Forest Genetics	Tuesday, October 28 8:30 AM - evening	Optimum Developmental Window for Somatic Embryogenesis, Norway Spruce Progress on Inducing Embryo- genesis in other Conifers Update on Primary Biochemical Markers New Findings in Loblolly Pine Reproductive Biology Discussion of Plantlet Develop- ment and Transfer Review of Molecular Biology-- Technique and Implications Preliminary Results from Exploratory Efforts: Embryogenesis from Older Seed Additional Biochemical Markers Student Research

---

\*NOT IN ORDER OF AGENDA

STATUS REPORTS

To The  
Engineering Project Advisory Committee

THE INSTITUTE OF PAPER CHEMISTRY  
Appleton, Wisconsin

Status Report  
to the  
ENGINEERING PROJECT ADVISORY COMMITTEE

Project 3309  
FUNDAMENTALS OF CORROSION CONTROL IN PAPER MILLS

October 22, 1986

## PROJECTS SUMMARY FORM

DATE: September 20, 1986

PROJECT NO.: 3309 - Fundamentals of Corrosion Control in Paper Mills

PROJECT LEADER: Ronald A. Yeske

IPC GOAL:

Increase the useful life of equipment by proper selection of materials of construction and by identifying suitable process conditions.

OBJECTIVE:

Improve the useful life of paper machine suction rolls by conducting corrosion and corrosion fatigue studies to establish the mechanisms of failure as the basis for developing approaches for prolonging roll life.

CURRENT FISCAL BUDGET: \$150,000

SUMMARY OF RESULTS SINCE LAST REPORT: (February, 1986 - September, 1986)

Near-threshold crack growth tests have been completed in several simulated paper machine whitewaters using five alloys whose service performance ranges from good to poor. A significant effect of a tensile mean stress and a corrosive whitewater on cracking susceptibility has been observed. This measure of cracking susceptibility correlates with the service performance of the five alloys tested, provided that the residual stresses present in suction rolls are taken into account.

High cycle fatigue testing continues in an effort to characterize crack initiation processes in suction roll alloys. S-N curves have been completed for tests in air on all five alloys in the current program, but these results do not

correlate with service performance of these alloys. S-N curves have also been completed for A63 and A75 alloys in simulated whitewaters. Rotating bending tests on smooth specimens and alternating bending tests on notched specimens are included in this test program. A significant environmental effect is seen in both types of fatigue test, but no correlation has yet been found which links the high cycle fatigue behavior of these alloys with their service performance record. The testing effort continues in a search for crack initiation processes that control cracking resistance in the field.

Testing to characterize stress corrosion cracking resistance continues, with special emphasis on cracking in the vicinity of cosmetic repair welds. High tensile residual stresses have been measured in a simulated repair weld, and tests are planned to expose welded coupons to simulated whitewater environments to learn whether cracking will occur as predicted by slow strain rate tests.

## INTRODUCTION

Corrosion assisted cracking of suction rolls continues to be a costly problem for the paper industry. Garner(1) has documented failures of a large number of suction rolls in recent years. Failure occurs when cracks initiate at the edge of a drilled hole and then propagate through the shell in a longitudinal or circumferential direction. The mechanism of failure is corrosion fatigue, wherein the fluctuating stresses imposed on the roll during use result in initiation and propagation of a crack. The corrosive conditions present in the whitewater promote initiation at pits and other corrosion-related defects, and, therefore, stimulate accelerated growth of cracks. Tensile residual stresses remaining in rolls as a result of fabricating practices have also been implicated as a contributing factor in roll failure.

A number of factors have contributed to the large number of suction roll failures. Paper machine speeds have increased, resulting in more stress cycles per unit time and higher nip loading (and multiple nips). The distance between bearing supports has increased on wider paper machines, leading to larger moments and higher fluctuating stresses on rolls. Closure of paper-making processes has also resulted in an environment that is more corrosive and therefore more likely to promote crack initiation.

While other avenues may be available for reducing the cost of suction roll failure, the most attractive remedy appears to be development of suction roll alloys with improved resistance to corrosion-assisted cracking. In recent years, duplex stainless steels with low residual stress levels have been offered commercially, with a marked improvement in the durability of rolls. However, further work is needed to optimize resistance to corrosion and cracking while minimizing alloy cost.

Although improved suction roll alloys are sought by the paper industry, the prediction of improved resistance to corrosion-assisted cracking is not easily accomplished. New alloys have been identified only after a lengthy process of laboratory development followed by prolonged testing in prototype roll applications.

In general, the laboratory tests used to predict suction roll performance in the field have not been very successful. Traditionally, tests are used to evaluate the mechanical strength, toughness, and corrosion resistance of candidate alloys, as well as the resistance to fatigue failure of smooth test specimens. A detailed treatment of suction roll testing methods was presented in a recent Project 3309 progress report(2).

Mechanical properties are usually determined in simple tensile tests to evaluate strength and ductility. Impact and fracture mechanics testing may be conducted to establish the toughness of candidate alloys. These tests are conducted to insure that the mechanical properties of the roll are adequate for the desired loading configuration.

Corrosion resistance of roll alloys is also of critical importance. Corrosion resistance is usually established by exposing coupons to actual or simulated paper machine whitewater, and using visual inspection and/or weight loss measurements to characterize corrosion resistance. Electrochemical tests may be used to supplement the coupon exposure testing. Resistance to pitting, crevice corrosion and general corrosion is sought in suction roll materials.

The resistance to corrosion fatigue failure is usually assessed by conducting high cycle fatigue tests on specimens exposed to real or simulated paper machine whitewaters. In this test, smooth or notched test specimens exposed to white-water are subjected to cyclic stresses in order to initiate a fatigue

crack which will grow to failure of the specimen. As the magnitude of the alternating stress,  $S$ , decreases, the number of stress cycles,  $N$ , required to cause failure of a test specimen increases. A plot of the alternating stress versus the (logarithm of the) number of cycles to failure,  $N$ , is the S-N curve, as shown schematically in Fig. 1. Materials with improved resistance to corrosion fatigue have S-N curves that are above (or shifted to the right) compared to curves for less resistant materials. That is, resistant materials can withstand more stress cycles of a given amplitude before failure occurs. Since a typical suction roll will experience more than  $10^8$  cycles per year of service, it is necessary to conduct S-N tests at extremely long lifetimes — typically  $10^8$  or  $10^9$  cycles to failure — to quantify the cracking resistance of any material.

The S-N behavior of any alloy is affected by a number of variables, including the level of superimposed tensile mean stress, test environment, surface finish, frequency of cyclic loading, and the metallurgical composition and structure of the test alloy. Accelerated failure is usually achieved by testing with a high frequency applied stress, although this raises questions regarding the corrosion influence on the S-N behavior and proper simulation of low frequency loading that occurs in actual rolls.

Fatigue crack propagation behavior may also be examined in characterizing corrosion fatigue failure of suction roll alloys. In this type of test, the rate of growth of a crack is determined visually during application of a fluctuating load on a fracture mechanics specimen. The driving force for cracking is a combination of the cyclic forces applied to the specimen, the geometry of the specimen, and the instantaneous length of the crack. These factors are combined in a parameter known as the cyclic stress intensity range,  $\Delta K$ , which determines the driving force for crack growth. Crack growth rates can vary significantly, so the results of crack propagation tests are usually plotted on



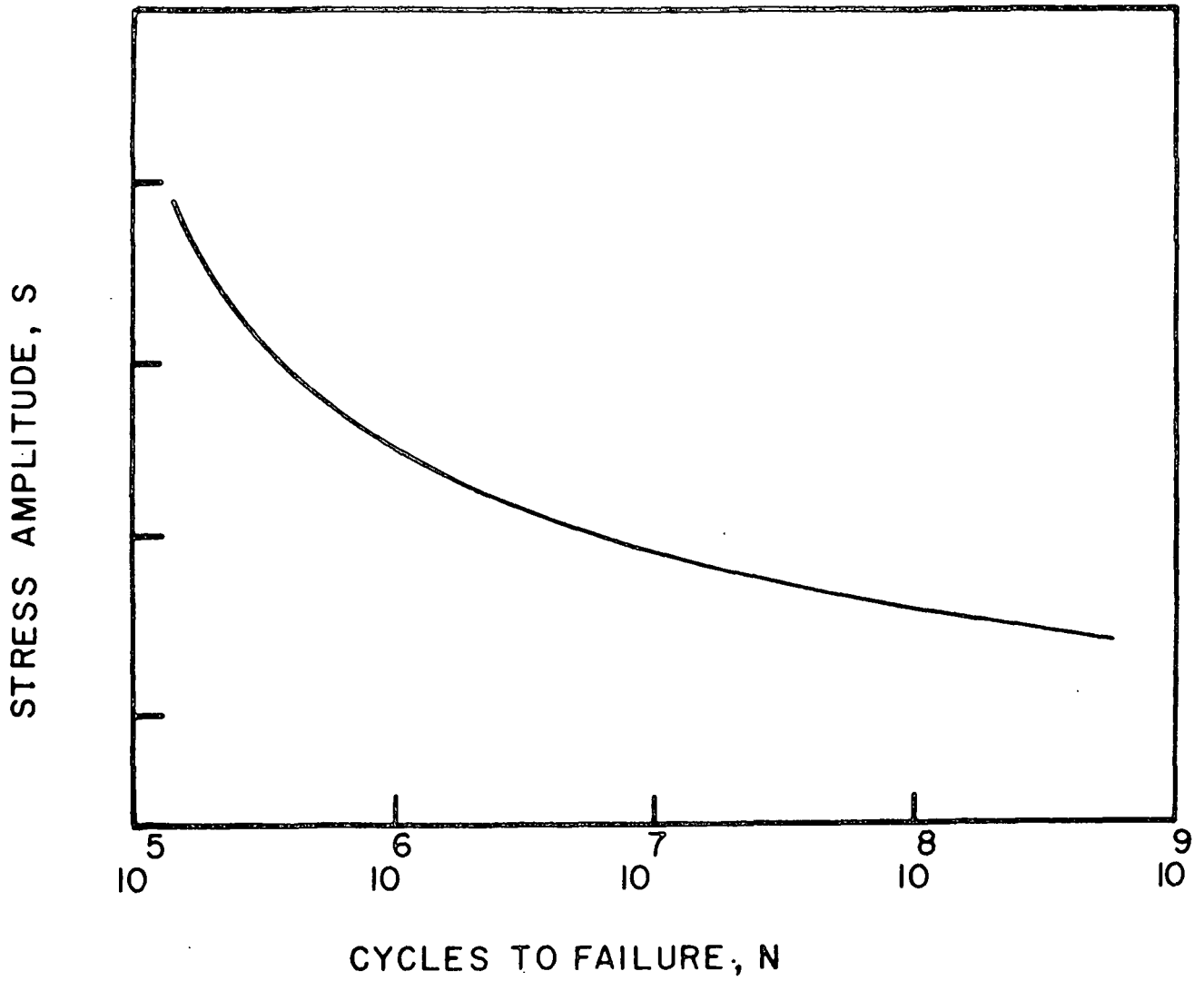


Figure 1. Schematic S-N curve.

a log-log scale. A schematic plot of a typical crack growth curve is shown in Fig. 2, where three stages of growth are apparent. At high  $\Delta K$  levels, the driving force for cracking is large, and the rates are high and devoid of a significant environmental effect (Stage III). At somewhat lower  $\Delta K$  levels, there is a linear regime where the (log) rate of crack growth is related directly to the (log) stress intensity range (Stage II). At still lower  $\Delta K$  levels, the linear relationship disappears and the rate of growth becomes vanishingly small ( $10^{-9}$  in/cycle) at lower stress intensity ranges (Stage I). If the stress intensity range is lowered below a threshold value,  $\Delta K_{th}$ , no crack growth is apparent. Since suction rolls accumulate large numbers of cycles in routine service, very little of the lifetime is spent in Stage II or III growth; rather, most of the crack propagation lifetime is spent in Stage I growth where rates are low. For example, one inch of crack growth might be expected in only one year of operation if the growth rate is as low as  $10^{-8}$  in/cycle. As a result, crack growth behavior is relevant to suction roll applications only in the near-threshold regime where growth rates are so low that structures of suction roll dimensions are not severed by a few years of stress cycling in routine operation.

Determination of the threshold stress intensity involves a complicated experimental method. If a notched or pre-cracked test specimen is simply subjected to larger and larger stress intensity ranges until cracking occurs, the threshold stress intensities measured would be very dependent on the details of the notch or pre-crack geometry. Furthermore, experience has shown that stress intensity thresholds determined by the rising load method would be higher — and therefore not conservative — compared to thresholds determined by gradually reducing the stress intensity range until cracking ceases.

The preferred method for determining the threshold stress intensity is a "load-shedding" approach, wherein the cyclic load applied to a specimen is

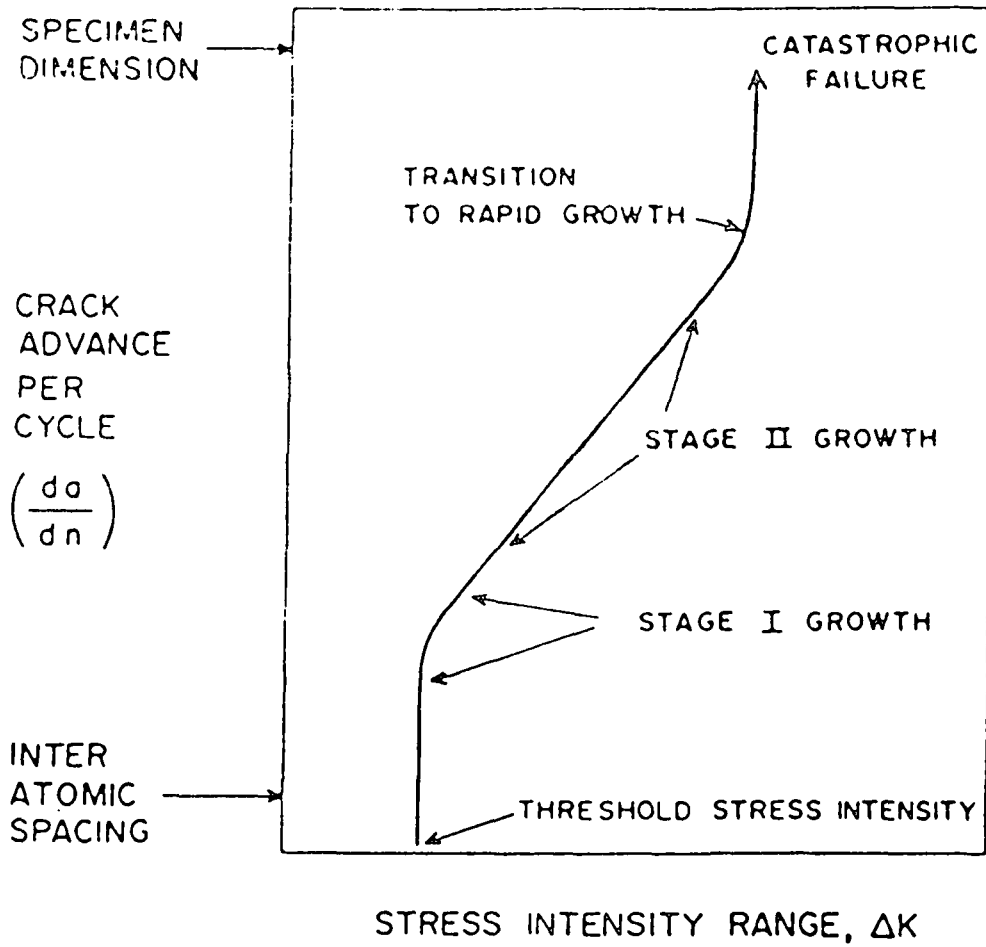


Figure 2. Schematic plot of crack growth rate vs. cyclic stress intensity range.

exposed to an aggressive environment simulating service conditions and subjected to a slow tensile test to failure. Stress corrosion cracking susceptibility is established by comparing the results of this tensile test with an identical test conducted in an inert environment. If stress corrosion is possible, it will be revealed as a loss of ductility, elongation, or strength in the test involving environmental exposure, or by the appearance of numerous cracks in the gage section of the test specimen.

#### LABORATORY PREDICTION OF SUCTION ROLL PERFORMANCE

Several of the laboratory tests described above are used in the development of new suction roll alloys, together with extensive testing of prototype rolls fabricated from the candidate material. Candidate rolls are evaluated based on corrosion resistance, mechanical strength and toughness, corrosion fatigue resistance and fabricability.

Although there are broad correlations between the service performance of alloys in the field and their performance in laboratory tests, the ability of existing laboratory tests to predict suction roll performance has not been very good. The tests have been able to document significant differences between classes of suction roll alloys — bronze versus duplex stainless steels, for example — but unable to identify improved suction roll alloys within alloy classes. This has led to a greater reliance on prototype roll testing over several years as the final arbiter of the worth of a new roll material.

This reliance on prototype roll testing impedes the development of new and improved rolls in a variety of ways. First, the time required for identification of an improved alloy is lengthy, since new but inferior rolls may not fail for several years. This limits the number of candidate alloys that can be

examined. Furthermore, little is gained by using prototype rolls to qualify improved rolls, since there is no feedback to guide the development of still better rolls. A roll that performs well in service may do so because of improved corrosion resistance, better fatigue resistance, lower design stresses, higher strength, etc. Successful rolls are never removed for investigation of the causes of their success; rather, laboratory tests are needed which can push the materials to their limits in order to identify those characteristics required of improved roll materials. A good predictive laboratory test that will evaluate new roll alloys is an important need for continued development of the suction roll materials of the future.

There is some evidence that the corrosion resistance of a suction roll material does not correlate with the performance of that alloy in the field. For example, Alloy 63 (A63) has superior corrosion resistance in real and simulated whitewaters compared to Alloy 75 (A75), yet the latter material has a far better record as a suction roll alloy.

Corrosion fatigue behavior in whitewaters is likewise a poor predictor of suction roll performance in the field. As shown in Fig. 3, the endurance limit for Alloy 75 is lower than that of Alloy 63 in a simulated whitewater, yet the Alloy 75 is a far better suction roll alloy.

Very limited data are available regarding the fatigue crack growth rate behavior of suction roll alloys, but the available data do not discriminate between inferior and superior suction roll materials. The available data shows little difference among suction roll alloys in near threshold crack growth behavior, in spite of considerable differences in the field performance of these alloys.

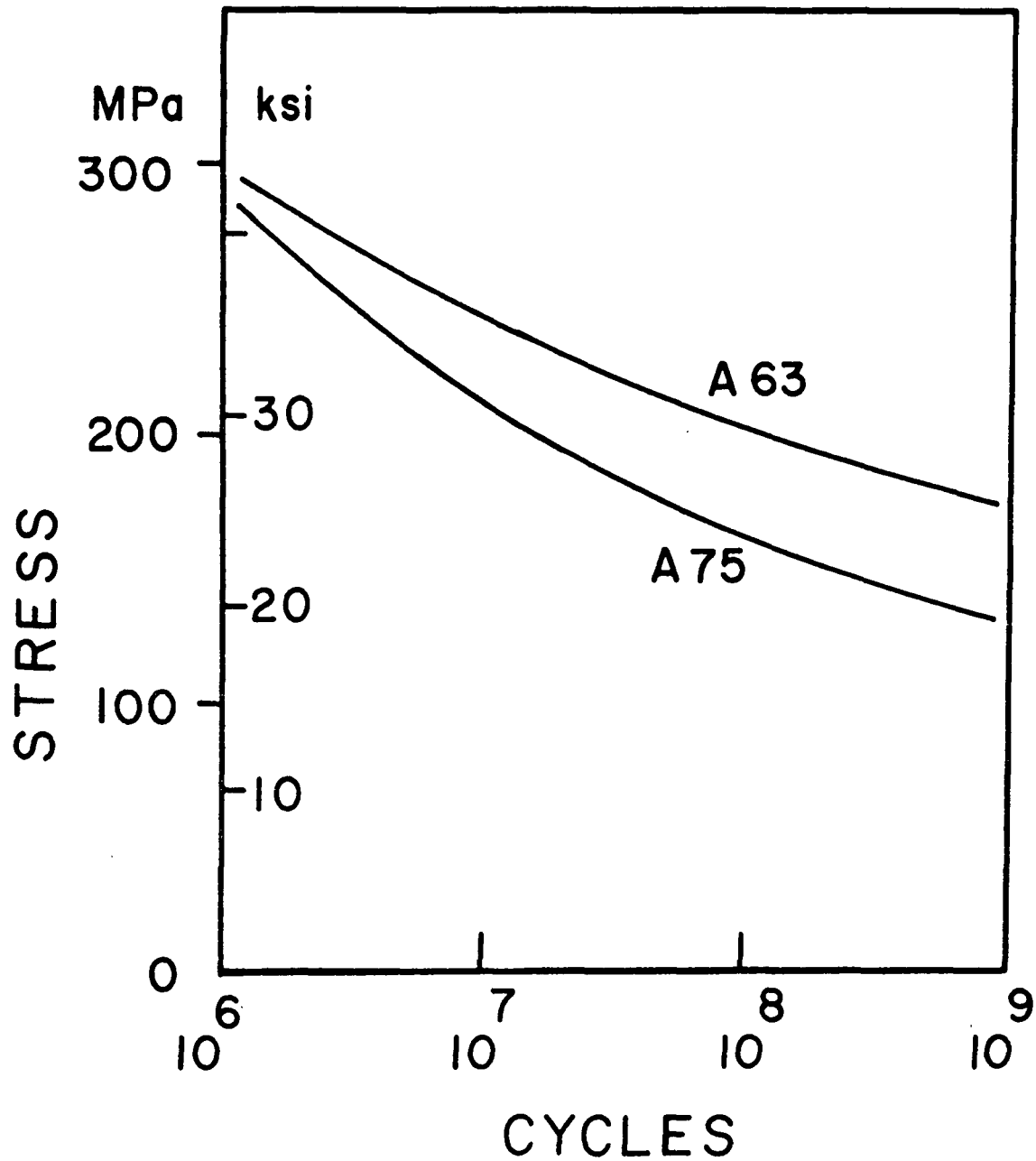


Figure 3. S-N curve for Alloys 63 and 75 in a simulated whitewater environment.

Thus, it is clear that the laboratory tests currently used to evaluate suction roll alloys — while providing some insight into overall performance — do not discriminate between superior and inferior suction roll alloys as determined by field performance. As a result, laboratory testing offers little guidance regarding desirable attributes of improved suction roll alloys. A significant improvement in the predictability of laboratory tests must be developed if insight is to be gained in development of improved, crack-resistant suction roll alloys.

#### SHORT TERM OBJECTIVES

The principal effort on this project has been focused on developing a laboratory test for suction roll alloys that offers a better correlation with service performance. A variety of suction rolls with known service histories is being subjected to various laboratory tests in an attempt to identify a test that correlates with service performance. Corrosion, stress corrosion, and corrosion fatigue tests are being conducted in this search for an improved laboratory test.

Five alloys are currently being investigated — Sandusky Alloys A75 and A63, Valmet Kubota VK-A171 and VK-A378, and Avesta 3RE60. The A75 and A378 alloys have had good service performance records in recent years, while 3RE60 and VK-A171 have experienced several failures. Alloy 63 was removed from the market because of severe cracking problems. The 3RE60 is a wrought material whereas the other four are centrifugally cast. All of the alloys are in the same class of duplex stainless steels for which design rules are relatively constant.

## PREVIOUS WORK

A detailed report summarizing the current status of suction roll cracking has been distributed to IPC member companies(2). This report also describes the results of corrosion tests in simulated whitewaters on several suction roll alloys. There is no apparent correlation between (pitting) corrosion resistance and suction roll performance.

Near-threshold fatigue tests have been conducted in simulated white-water in order to compare the threshold stress intensities for crack growth with the ranking of alloy service performance. In these tests, little difference was found among alloys in less aggressive simulated whitewaters, but differences did appear in more aggressive conditions. In particular, lowering the pH to the 3.0-3.5 range allowed some discrimination between alloys. In this environment, the A75 and VK-A378 alloys exhibited good resistance to near threshold crack growth, but VK-A171 was as good as VK-A378. Alloy 63 was decidedly inferior to the other cast alloys, as expected. The wrought 3RE60 alloy exhibited the poorest resistance to near-threshold fatigue crack growth in this simulated whitewater.

A number of screening tests have been conducted to examine the reproducibility of near-threshold fatigue testing and to explore the limits of the method. As expected, there was little difference in crack growth rates for tests conducted at the same stress intensity range, but with different crack lengths (compensated by different cyclic loads). Moreover, a small cyclic frequency effect was noted when the test frequency was reduced from 25Hz (where most testing has been done) to 5Hz. A slight reduction in threshold was detected at the lower frequency. Sulfate present in the test environment was shown to inhibit the crack acceleration effect attributed to chlorides.



No significant differences were observed in S-N curves generated on Alloys 63 and 75, which are at the ends of the service performance spectrum. Tests have been conducted by rotating bending on smooth specimens and by alternating bending on notched specimens in an environment containing 1000 ppm  $\text{Cl}^-$  and a pH of 3.0-3.5. Alternating bending tests on notched specimens produced higher endurance limits than rotating bending tests on smooth specimens.

Slow strain rate tests have been conducted on the five suction roll alloys in a simulated whitewater containing  $\text{Cl}^-$  and  $\text{S}_2\text{O}_3^{2-}$  (thiosulfate) ions. Of the five alloys tested, only A75 exhibited any evidence of pitting and stress corrosion cracking, in apparent contradiction to the service performance records for these alloys.

## PROGRESS

### Near-threshold Fatigue Testing

The effect of a superimposed tensile mean stress on near-threshold crack growth behavior has been investigated in Environment E for all five of the roll alloys in the current program. Environment E contains 1000 ppm  $\text{Cl}^-$ , at a pH of 3.0-3.5. Tests were conducted at R ratios of 0.04, 0.10, and 0.50, where R is the ratio of the maximum load to the minimum load. Thus, an R value of 0.04 represents a small superimposed tensile mean stress, whereas  $R = 0.5$  represents a significant tensile mean stress component. The results of the near-threshold crack growth rate measurements are shown in Figs. 4-8.

With the exception of Alloy 75, increased tensile mean stress resulted in a decrease in the threshold stress intensity for crack growth in this simulated whitewater environment. For Alloy 75, the high threshold stress intensity exhibited by this alloy endured when significant tensile mean stresses were imposed on the specimen during crack growth. For A63, VK-A171, VK-A378, and

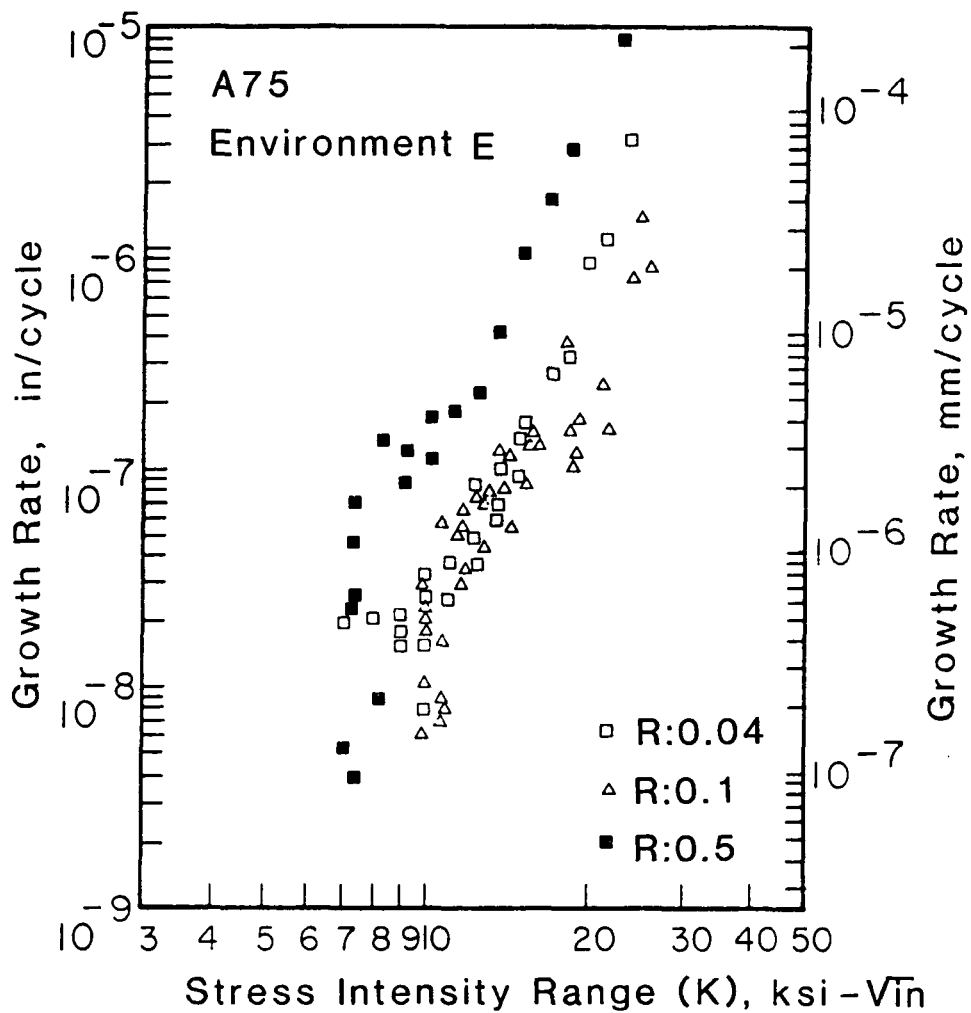


Figure 4. Near-threshold fatigue crack growth behavior for Alloy 75 in a 1000 ppm Cl<sup>-</sup>, pH 3 - 3.5 environment.

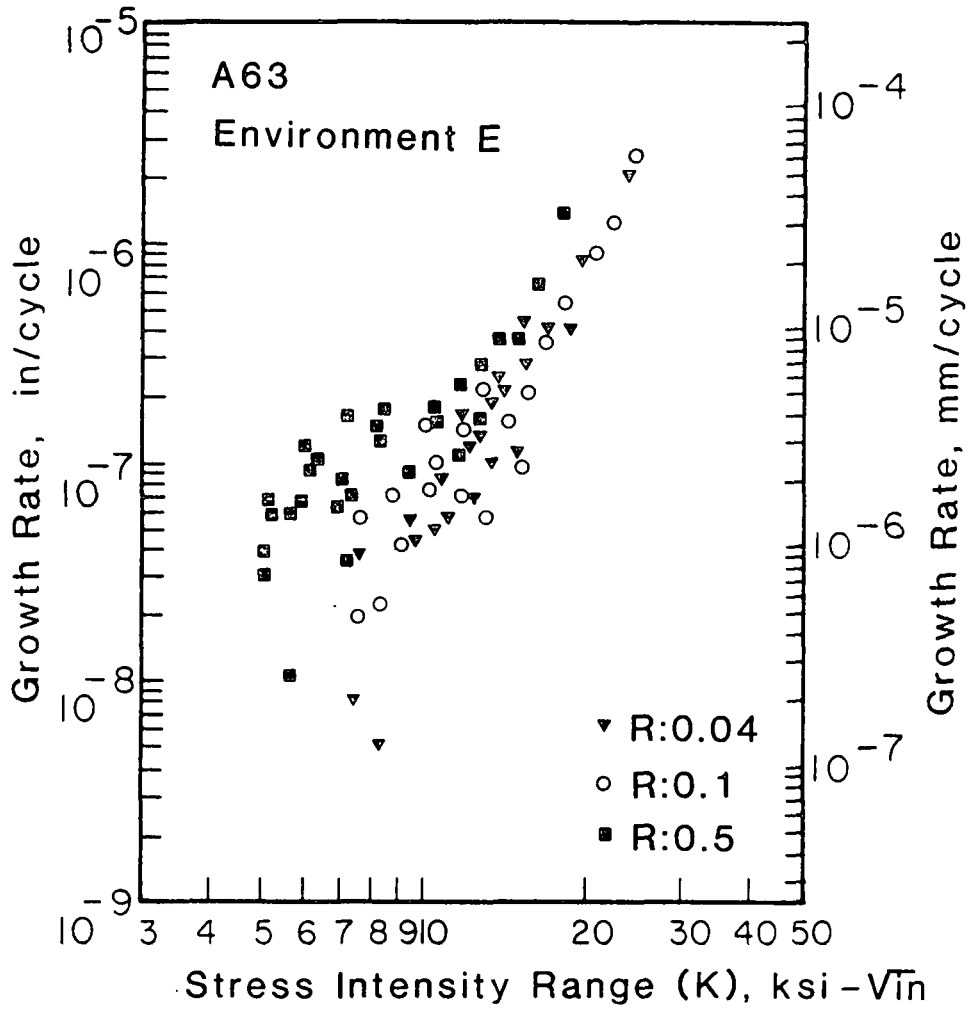


Figure 5. Near-threshold fatigue crack growth behavior for Alloy 63 in a 1000 ppm Cl<sup>-</sup>, pH 3 - 3.5 environment.

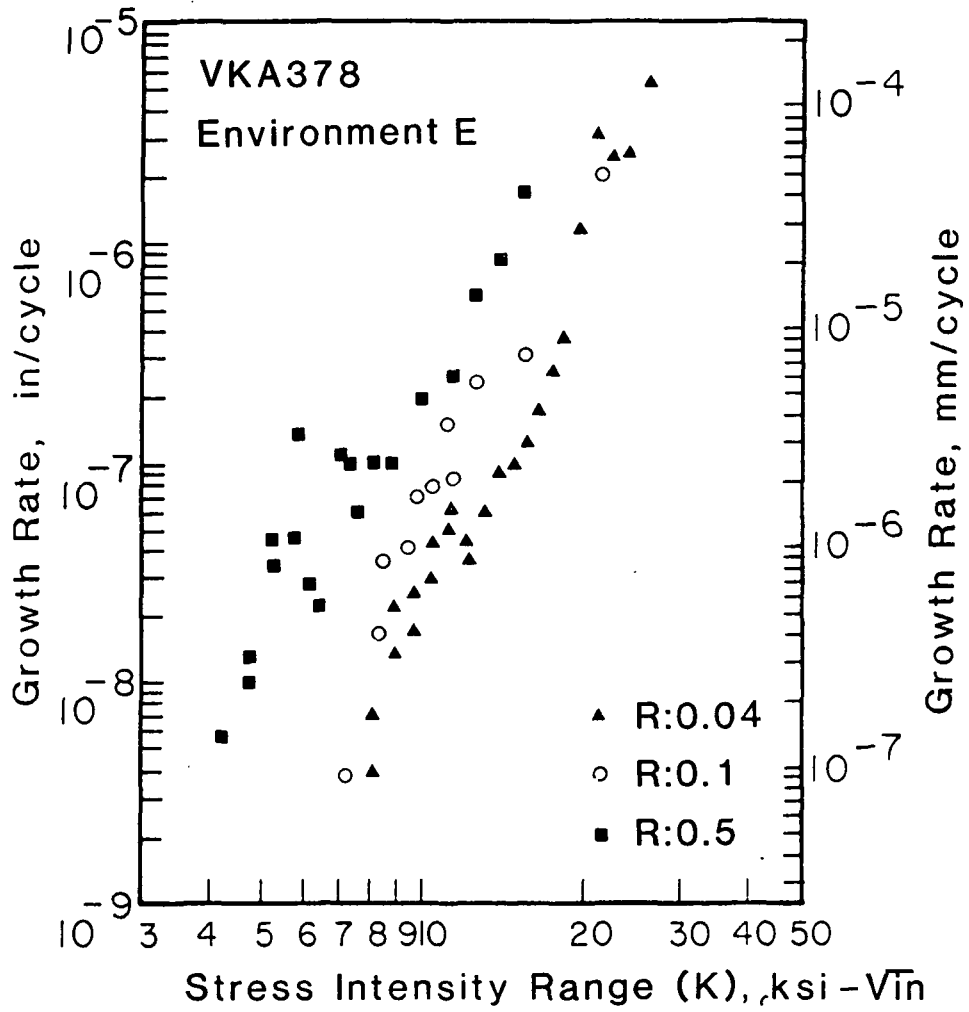


Figure 6. Near-threshold fatigue crack growth behavior for Alloy VK-A378 in a 1000 ppm  $\text{Cl}^-$ , pH 3 - 3.5 environment.

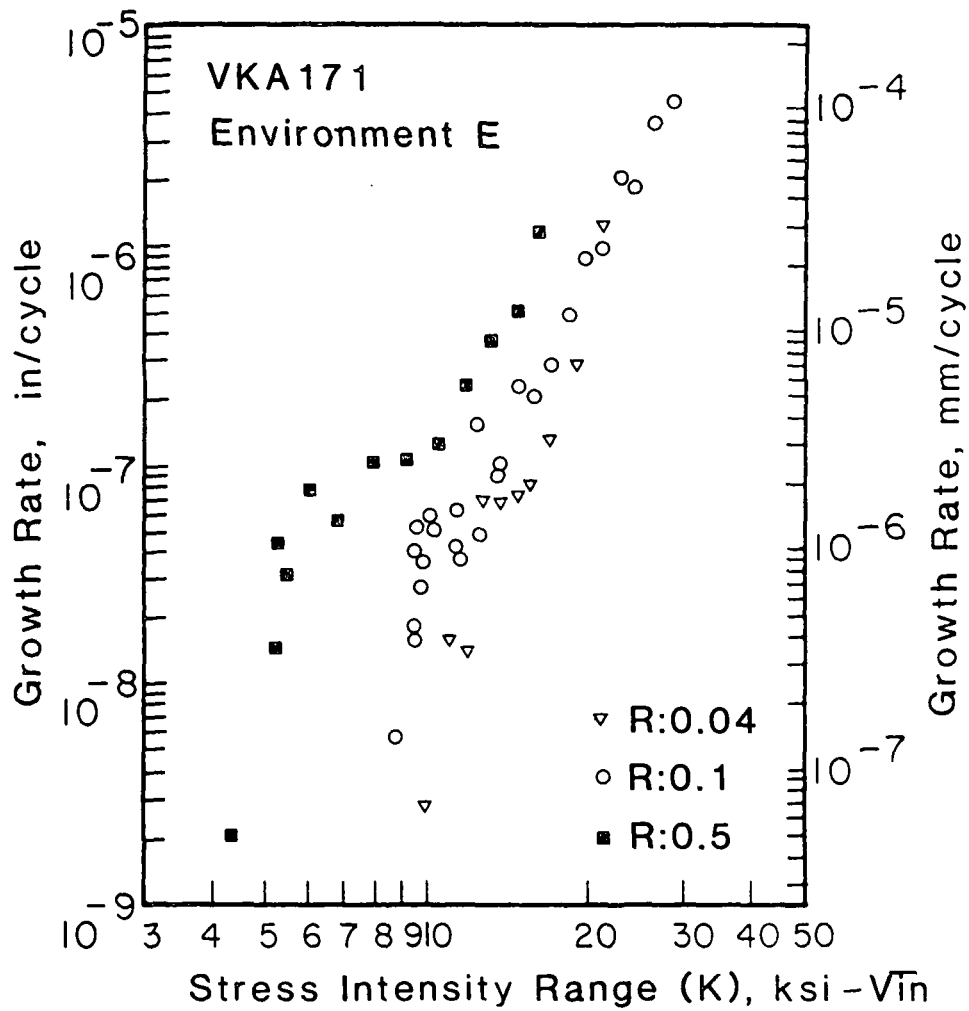


Figure 7. Near-threshold fatigue crack growth behavior for Alloy VK-A171 in a 1000 ppm Cl<sup>-</sup>, pH 3 - 3.5 environment.

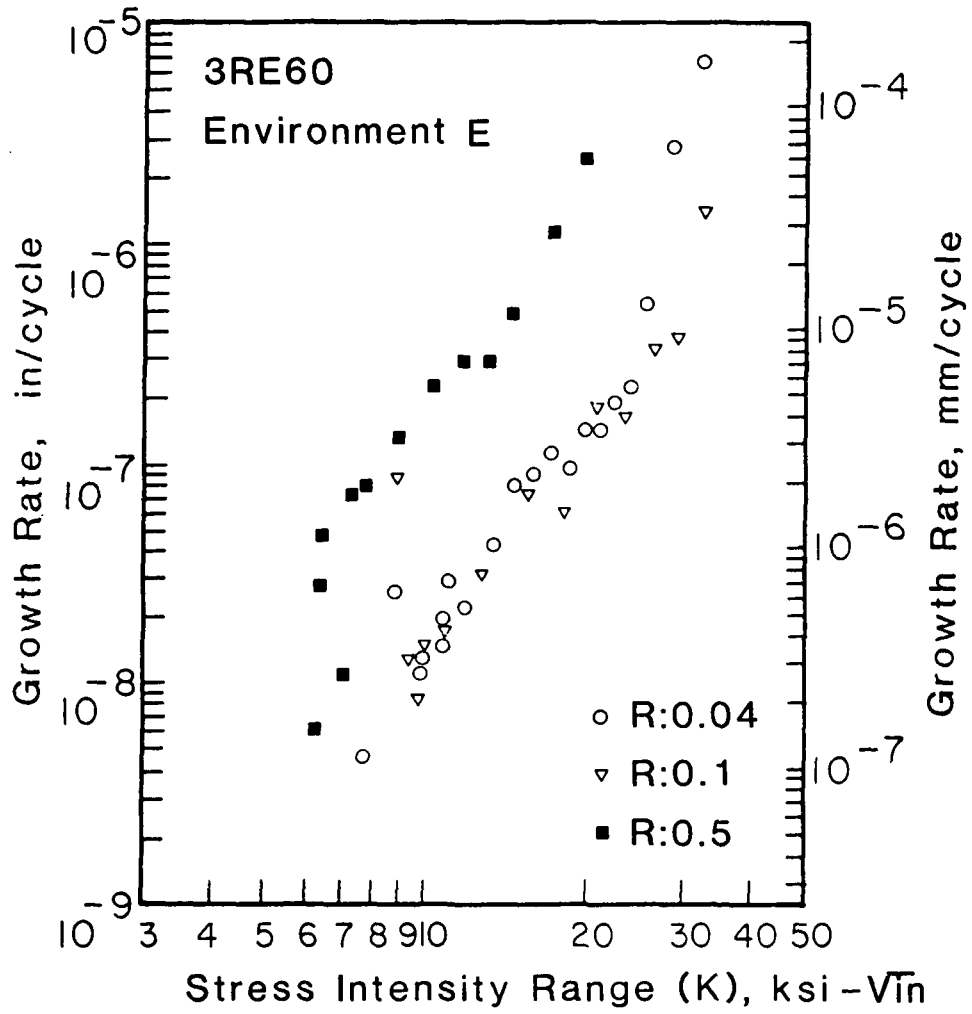


Figure 8. Near-threshold fatigue crack growth behavior for Alloy 3RE60 in a 1000 ppm Cl<sup>-</sup>, pH 3 - 3.5 environment.

3RE60, the threshold stress intensity for crack growth fell to 4-5 ksi- $\sqrt{\text{in}}$  when  $R = 0.5$ , whereas the value for A75 remained at 7 ksi- $\sqrt{\text{in}}$ . The near threshold data for the five alloys at  $R = 0.5$  are compared in Fig. 9. For some of the alloys, notably VK-A171, VK-A378, and 3RE60, the threshold value at  $R = 0.5$  was only one-half the value found when tensile mean stress was low ( $R = 0.04$ ).

The ranking of alloys based on threshold stress intensity at high mean stress values does not agree with a ranking based on service performance statistics. The good resistance of Alloy 75 agrees with the excellent cracking resistance exhibited by this alloy in service, but VK-A378, which also has good field performance, exhibited a large (50%) reduction in  $\Delta K_{\text{th}}$  at high mean stress levels. The mean stress effect therefore does not produce the desired ranking for these alloys, in and of itself.

However, the near-threshold crack growth data can be made to agree with the service performance ranking by considering the mean stresses present in suction roll alloys when they are placed in service. Two of the five alloys tested — A63 and VK-A171 — are placed in service with high tensile residual stresses as a result of the final water-quenching treatment given to rolls fabricated from these alloys. The near-threshold data presented above show that these two alloys are quite susceptible to accelerated crack growth under the influence of a high tensile residual stress. With high residual stresses in actual rolls, and a strong sensitivity to mean stress effects, it is not surprising that these two alloys have experienced severe cracking in service. Alloy VK-A378, on the other hand, is also susceptible to accelerated crack growth rates in the near-threshold regime when tensile mean stresses are present, but these rolls have a satisfactory service performance because the rolls are given a heat-treatment to remove residual stresses. Alloy 75 appears to be immune from the effects of a tensile residual stress, so the final heat

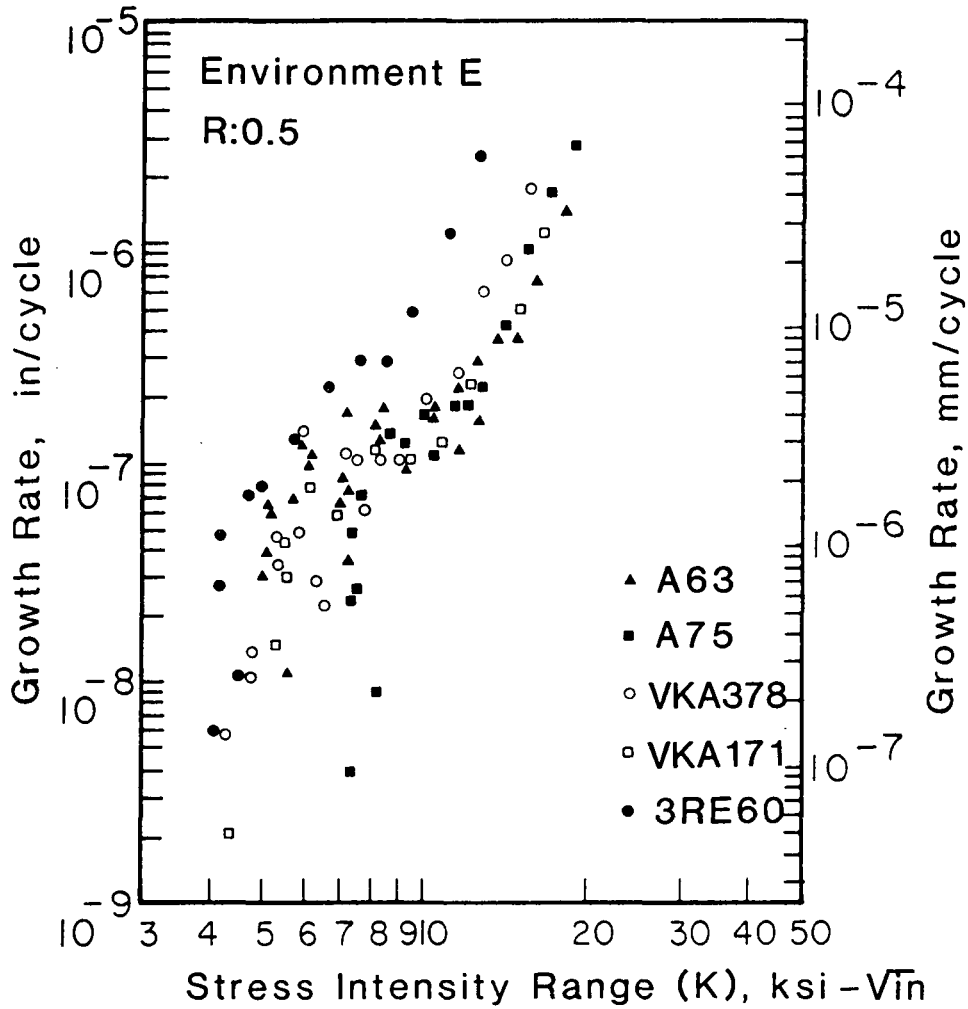


Figure 9. A comparison of crack growth rate data for five suction roll alloys tested in Environment E at R = 0.5.



treatment to reduce residual stress may not be critical to the good cracking resistance of this alloy in service. Finally, the 3RE60 alloy is found to be susceptible to accelerated crack growth when tensile mean stresses are present. When this alloy was first placed in service, high tensile residual stresses were present because of the manner of final heat treatment and several early incidents of roll failure were reported. In recent years, the problem with the final heat treating practice has been resolved, the residual stresses in actual rolls have been reduced, and the service performance of 3RE60 rolls has improved dramatically.

Thus, the effect of mean stress on near-threshold crack growth in a low pH whitewater does correlate with service performance as summarized below:

- Alloy 75 does not exhibit a significant mean stress effect on crack growth, which is reflected in good service performance.
- Alloy VK-A378 experiences accelerated crack growth when mean stresses are present, but roll performance has been good because mean stresses in actual rolls are low.
- Alloys 63 and VK-A171 are susceptible to mean stress effects on growth rates and perform poorly in service because these suction rolls have large tensile residual stresses.
- 3RE60 is susceptible to accelerated crack growth under tensile mean stresses, but modern rolls perform well because tensile residual stresses are low. Earlier rolls with higher residual stresses experienced cracking.

Thus, with this interpretation, the mean stress effect on crack growth rates in the near-threshold regime during exposure to a simulated whitewater does correlate with field performance for these five suction roll alloys.

Near-threshold crack growth rates have also been measured in a simulated whitewater containing 50 ppm thiosulfate, labelled Environment D. This whitewater was chosen to examine suction roll performance in papermaking applications where thiosulfates are present because of decomposition of hydro-sulfite brightening agents. These tests were conducted with  $R = 0.1$ , a temperature of  $50^{\circ}\text{C}$  and a pH in the range, 4.0 - 4.5. The results are summarized in Fig. 10.

Alloys A75 and VK-A171 exhibited the highest threshold stress intensities for crack growth in the thiosulfate-doped whitewater environment, followed by VK-A378, A63, and 3RE60. While the threshold stress intensities for the cast alloys ranged from 5 to  $10 \text{ ksi}\sqrt{\text{in}}$ , the threshold for the wrought 3RE60 alloy was much lower — on the order of only  $2 \text{ ksi}\sqrt{\text{in}}$ . The poor cracking resistance of the 3RE60 alloy appears to be related to the mode of crack growth through the material. In the wrought 3RE60, where the metallurgical microstructure is more homogeneous and refined, the crack path is quite straight and is apparently unaffected by the microstructure, as shown in Fig. 11. In the cast alloys, the large grain size and inhomogeneous microstructure result in a crack morphology with frequent branching on a fine scale and a torturous path through the structure. Crack branching and deviations from planarity are commonly associated with low crack growth rates. In this case, the uniform microstructure of the 3RE60 alloy is an apparent disadvantage.

The resistance to cracking of the alloys tested in the thiosulfate-doped whitewater did not correlate with corrosion resistance, as suggested by

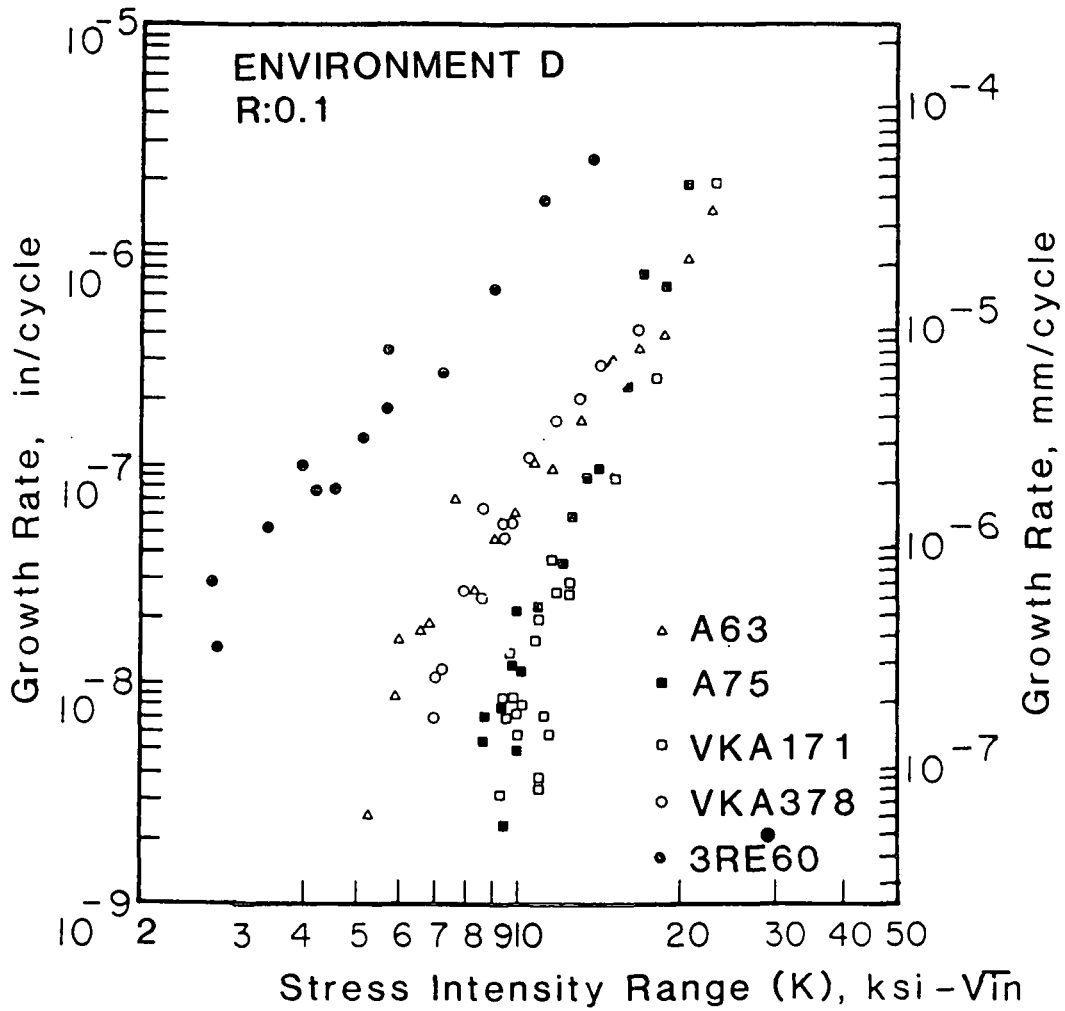
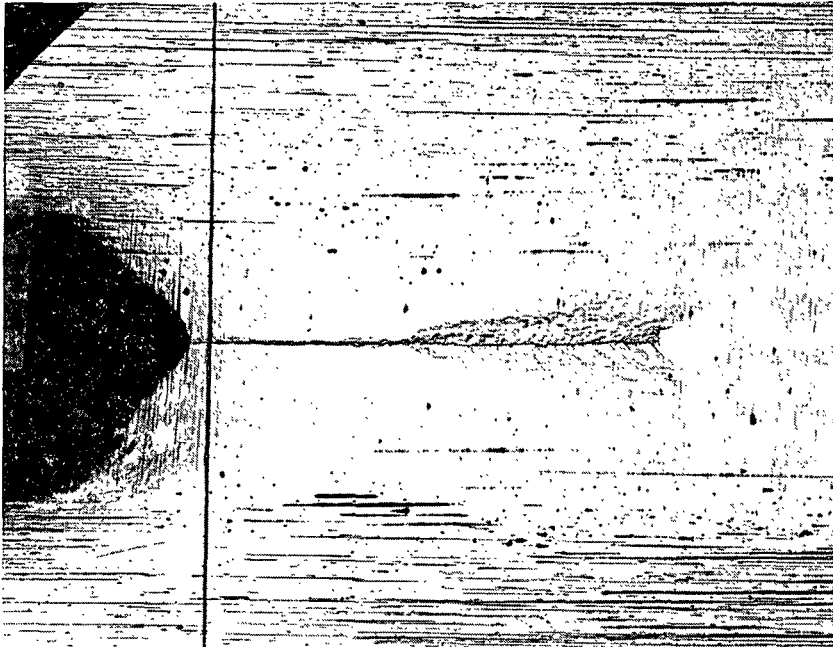
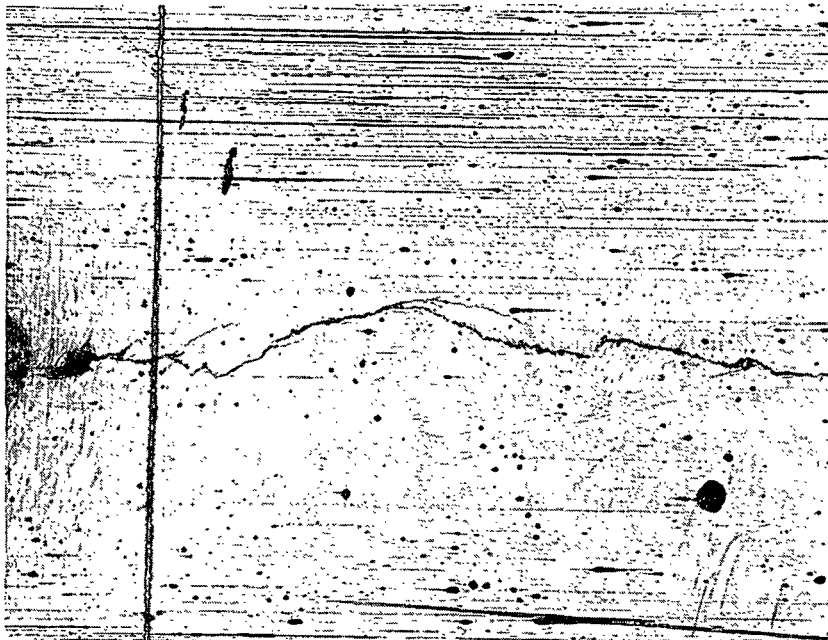


Figure 10. Fatigue crack growth rate behavior for suction roll alloys tested in Environment D containing 50 ppm S<sub>2</sub>O<sub>3</sub><sup>2-</sup>.



3RE60



A75

Figure 11. A comparison of crack growth morphologies in cast and wrought suction roll material.

corrosion data generated by Bowers under this project. Alloy 75 exhibited extensive corrosion in the thiosulfated whitewater, as shown in Fig. 12, yet this alloy exhibited superior resistance to crack growth in this environment. Other alloys with far better corrosion resistance (e.g., A63 shown in Fig. 12) exhibited inferior resistance to crack growth in this whitewater environment.

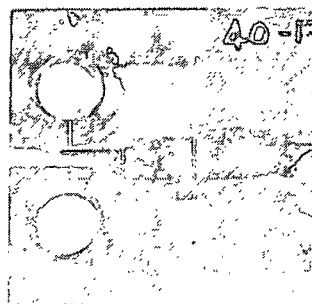
Near-threshold crack growth tests were also conducted on the five suction roll alloys in air to examine the environmental effect attributed to whitewater exposure. The differences among the threshold stress intensities of the various alloys were smaller for exposures in air, as shown in Fig. 13. The ranking of the threshold stress intensities for these alloys in these air tests was as follows: A75 > VK-A171 = VK-A378 = A63 > 3RE60.

The electrochemical behavior of suction roll alloys has been examined during near-threshold fatigue testing by measuring the electrochemical rest potentials of test specimens during crack growth periods. The rest potentials of companion coupons were also measured at the same time. The extremes of behavior are shown in Figs. 14 & 15 for Alloy 75 and Alloy 63 tested in Environment D containing chloride, thiosulfate, and sulfate ions and a pH in the range, 4.0 - 4.5. The rest potentials are shown versus crack growth rate for the fatigue test specimen.

The electrochemical potentials reflected the overall corrosion behavior of the alloys, and there was only a slight effect of crack growth on the measured potentials. The active corrosion of Alloy 75 in Environment D is clearly indicated by the relatively low (i.e., active) potentials exhibited by this alloy. The potential of the compact tension specimen experiencing crack growth was even more active than the uncracked coupon, apparently because of the exposure of bare metal at the freshly cracked surface. However, the difference



ALLOY 75



ALLOY 63

Figure 12. Appearance of Alloys 75 and 63 following testing in a thiosulfate-doped whitewater.

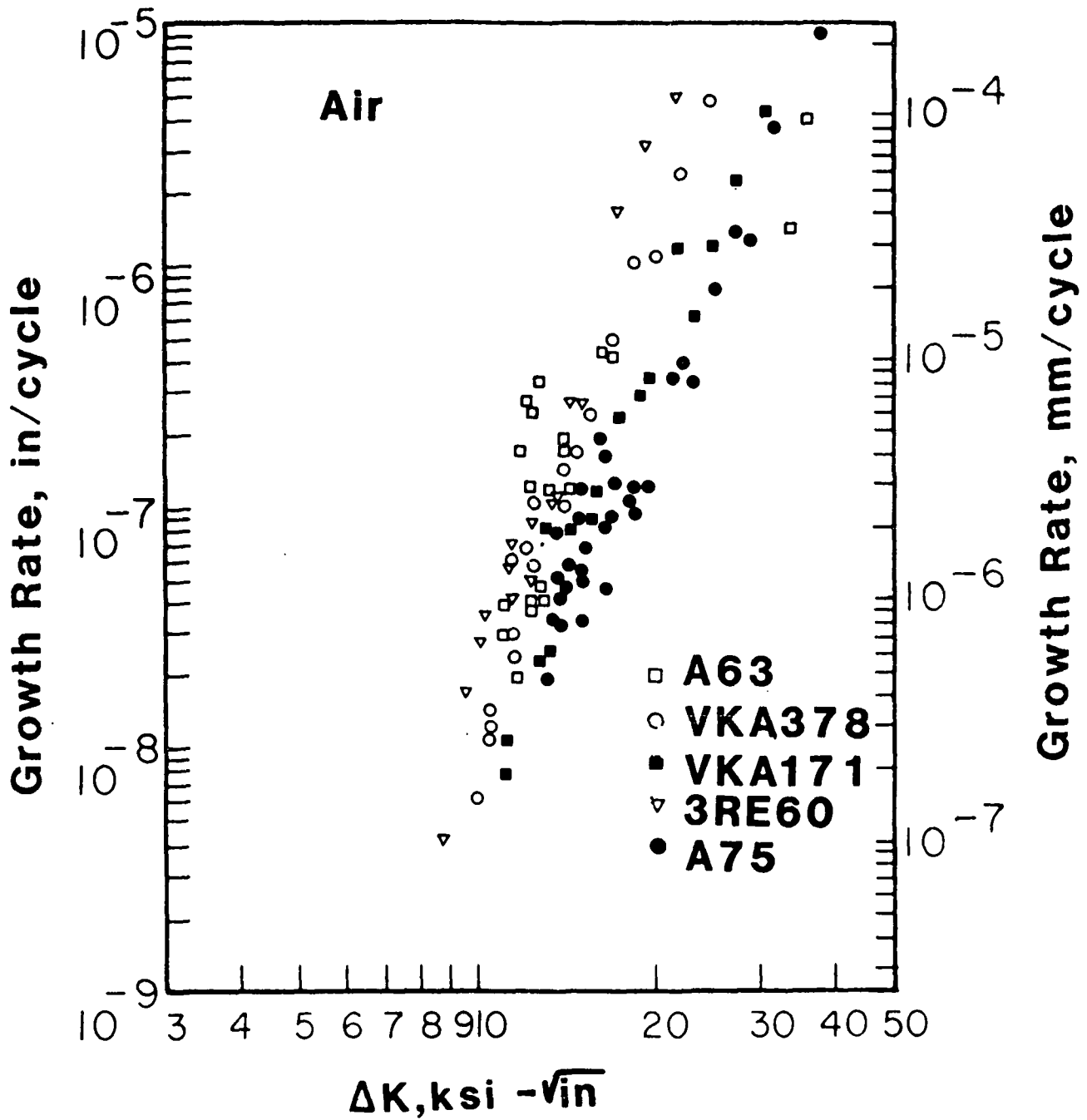


Figure 13. Near-threshold crack growth rate data for tests in air.

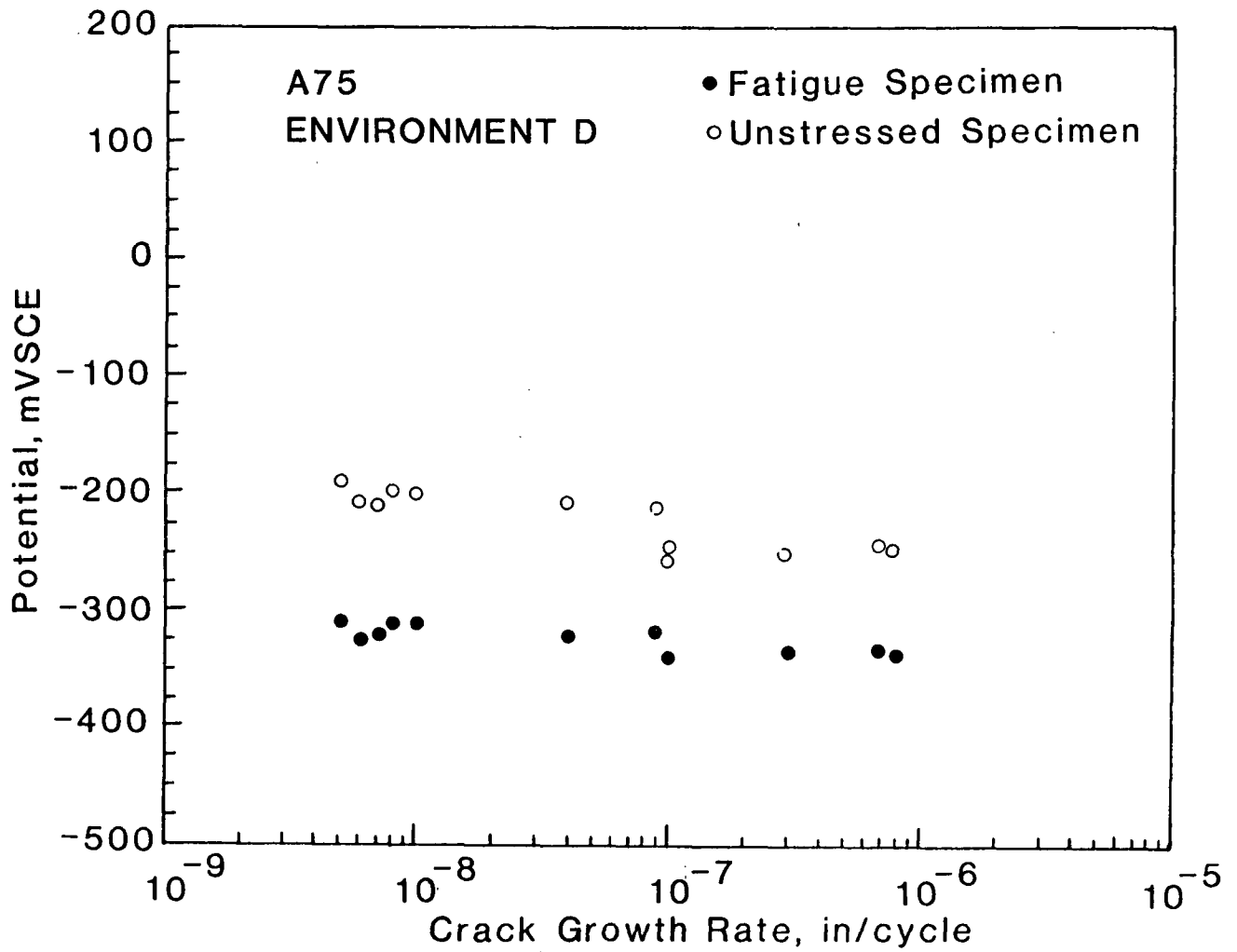


Figure 14. Comparison of rest potentials for cracking and dummy coupons of Alloy 75 in Environment D.



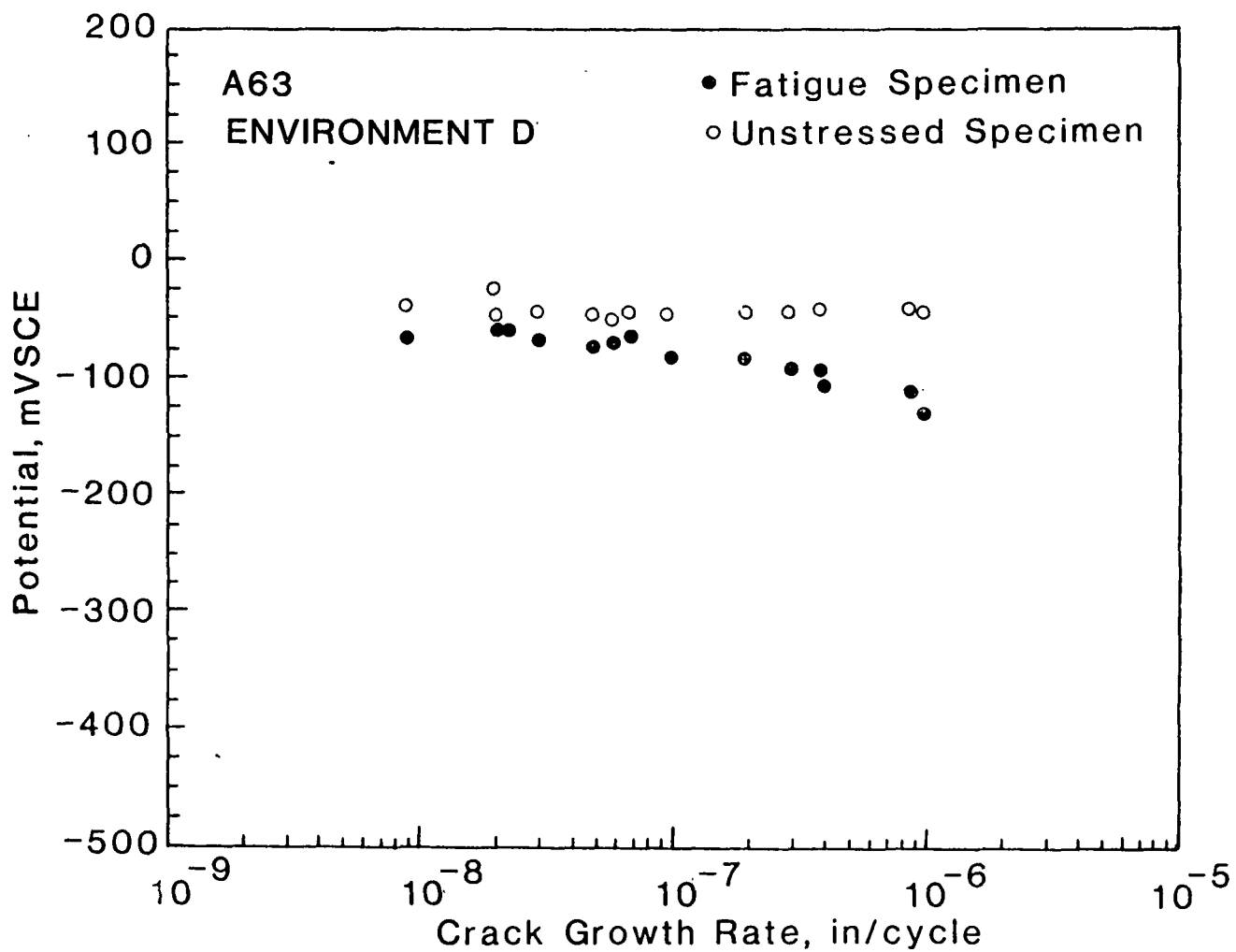


Figure 15. Comparison of rest potentials for cracking and dummy coupons of Alloy A63 in Environment D.

in potential between the cracked and uncracked specimens was about the same, regardless of the growth rate (i.e., the rate of production of bare metal surface). The good corrosion resistance of Alloy 63 in Environment D was evident in its high (i.e., passive) rest potentials relative to those of Alloy 75. The high potential attests to the effectiveness of a passivating film that forms spontaneously on this alloy during exposure to simulated whitewaters. The difference between potentials of cracked and uncracked specimens was relatively small when growth rates were low, but the cracked coupons became more active as the rate of crack growth increased and the rate of bare metal exposure increased.

The electrochemical behavior of roll alloys tested in Environment E was similar, but the potentials achieved were somewhat higher in this acid-chloride whitewater, compared to the thiosulfate-doped whitewater.

In general, the potentials measured in these tests reflected the extent of corrosion on the specimens, either on the exposed side surfaces or on the crack faces created by crack growth, but there was no correlation between crack growth resistance and potential. In most cases, the potentials measured on specimens with propagating cracks decreased as the rate of crack growth increased, which is consistent with the anticipated effect of creation of fresh metal surfaces due to crack advance. Specimens with little evidence of active corrosion maintained high potentials consistent with passivity. In the critical near-threshold regime, where little crack advance occurs, the effect of crack growth on electrochemical potential was negligible. Active corrosion on the fatigue test specimen — as revealed by low corrosion potentials — did not result in accelerated cracking. In fact, Alloy 75 exhibited the greatest resistance to crack growth in the near-threshold regime, yet clearly exhibited the poorest corrosion resistance of the alloys considered.

Crack Initiation Studies — S-N Curves

High cycle fatigue tests are being used to examine the resistance of suction roll alloys to crack initiation. S-N curves are being generated for the suction roll alloys in air and in simulated whitewater environments, with the endurance limit at a run-out of  $10^8$  cycles taken as the measure of crack initiation resistance. The effects of notches and loading morphology are being examined by conducting rotating bending (i.e., R.R. Moore) tests on smooth specimens and alternating bending (i.e., Tatnal Krause) tests on specimens containing a drilled hole.

Although additional data are needed in the long lifetime regime, the endurance limits in an air environment for the five suction roll materials in the test program have been approximately determined. The S-N data for the rotating bending tests are shown in Fig. 16. The apparent  $10^8$  cycle endurance limits for the five alloys tested in air, subject to further testing, are as follows:

Alloy	Endurance Limit ( $10^8$ cycles)
3RE60	56 ksi
VK-A378	49 ksi
VK-A171	42 ksi
A63	34 ksi
A75	30 ksi

There is little apparent correlation between the endurance limit in air and the resistance of an alloy to cracking in service. Alloy 75, one of the most resistant suction roll alloys in service, exhibits the lowest fatigue strength at  $10^8$  cycles. In an interesting reversal, the 3RE60 alloy,

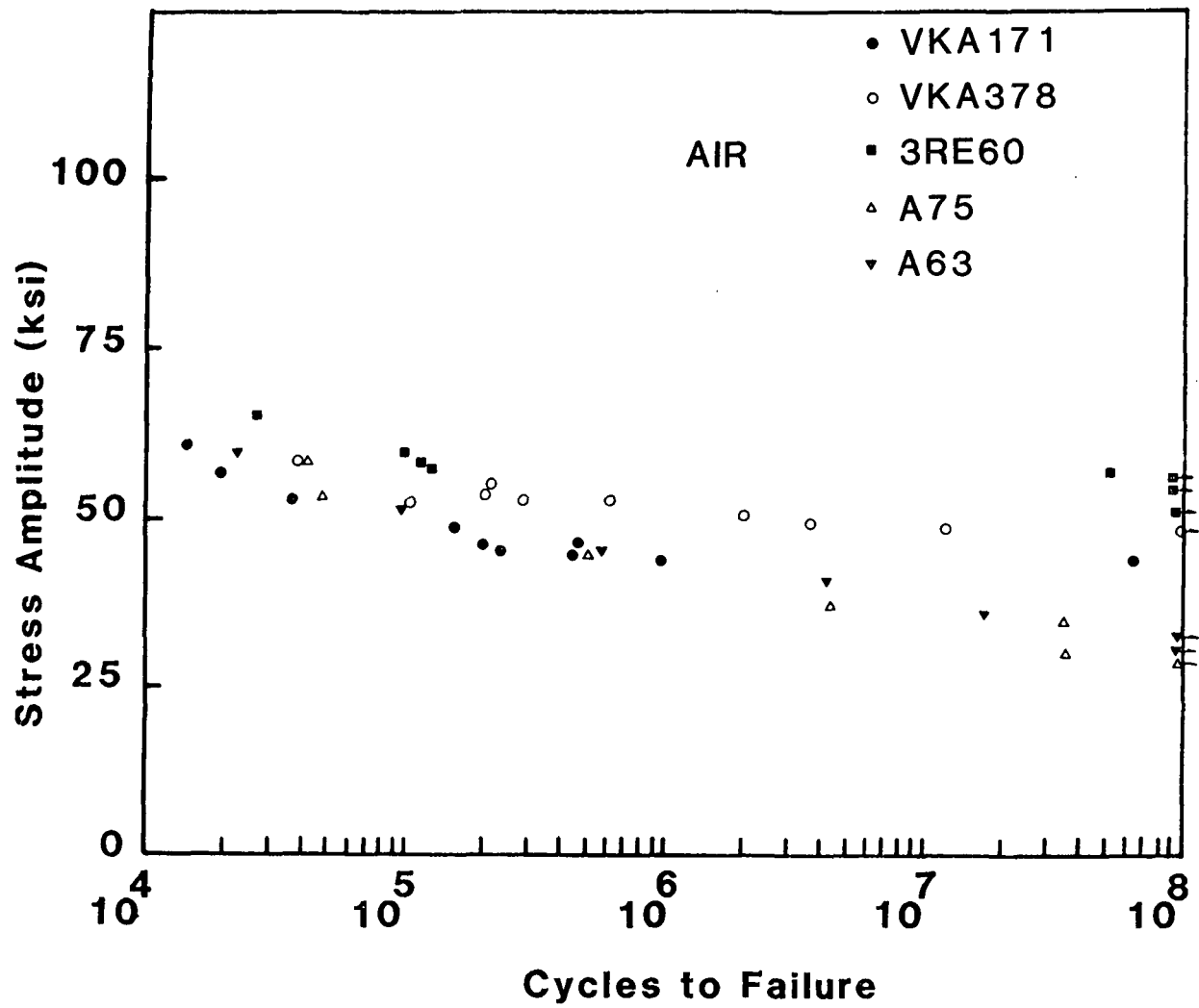


Figure 16. S-N data for suction roll alloys tested by rotating bending in air.

which had exhibited inferior resistance to near-threshold crack growth in air and other environments, exhibits very good resistance to crack initiation in these high-cycle fatigue tests.

Rotating bending S-N data has also been obtained for two of the five alloys in Environment E containing 1000 ppm  $\text{Cl}^-$  and a pH of 3.0-3.5, as shown in Fig. 17. For both A63 and A75, their  $10^8$  cycle endurance limits in this simulated whitewater are approximately the same — 24 ksi. Since these two alloys occupy the opposite ends of the spectrum of suction roll performance in service, the rotating bending test in this simulated whitewater does not correlate with service performance and further testing in this whitewater is being abandoned. It is interesting to note that exposure to the whitewater solution during fatigue testing reduced the endurance limit significantly for both alloys — on the order of 7 to 10 ksi, compared with tests conducted in air.

Alternating bending S-N curves for notched specimens have also been generated for A75 material in two simulated whitenwaters, as shown in Fig. 18. The endurance limit in either test environment is approximately 30 ksi at  $10^8$  cycles, and there is little effect of differences in simulated whitenwaters on crack initiation behavior. It is interesting to note that this alloy is relatively immune to notch effects introduced by the presence of a drilled hole in the test specimen. The alternating bending endurance limit in Environment E is approximately 10 ksi higher (in the presence of a notch), compared to rotating bending data on smooth specimens shown in Fig. 17.

To date, there is no correlation between fatigue crack initiation behavior, as represented by high cycle fatigue tests on smooth and notched specimens, and service performance ranking. A significant environmental effect

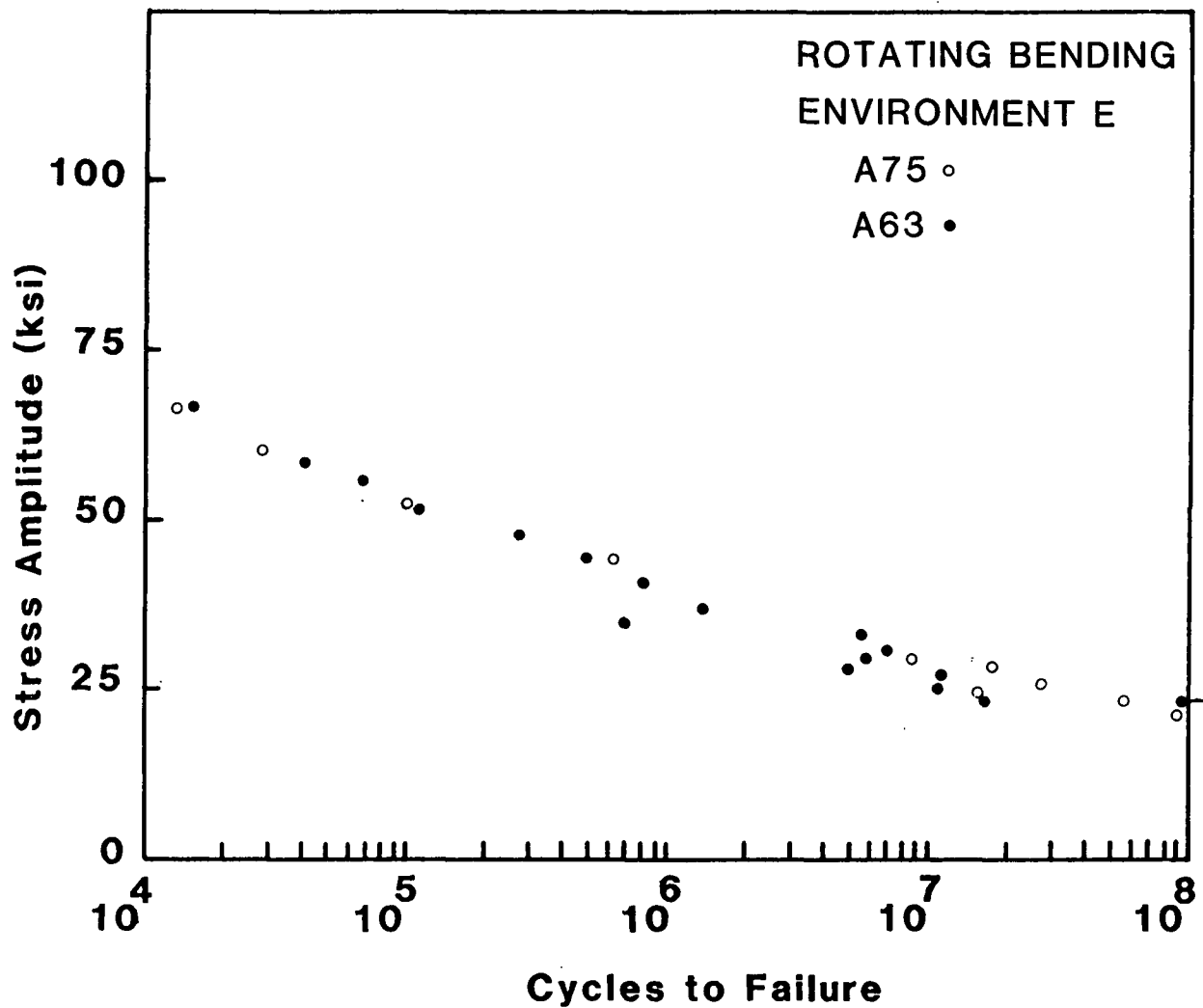


Figure 17. S-N data for Alloys 63 and 75 in Environment E.

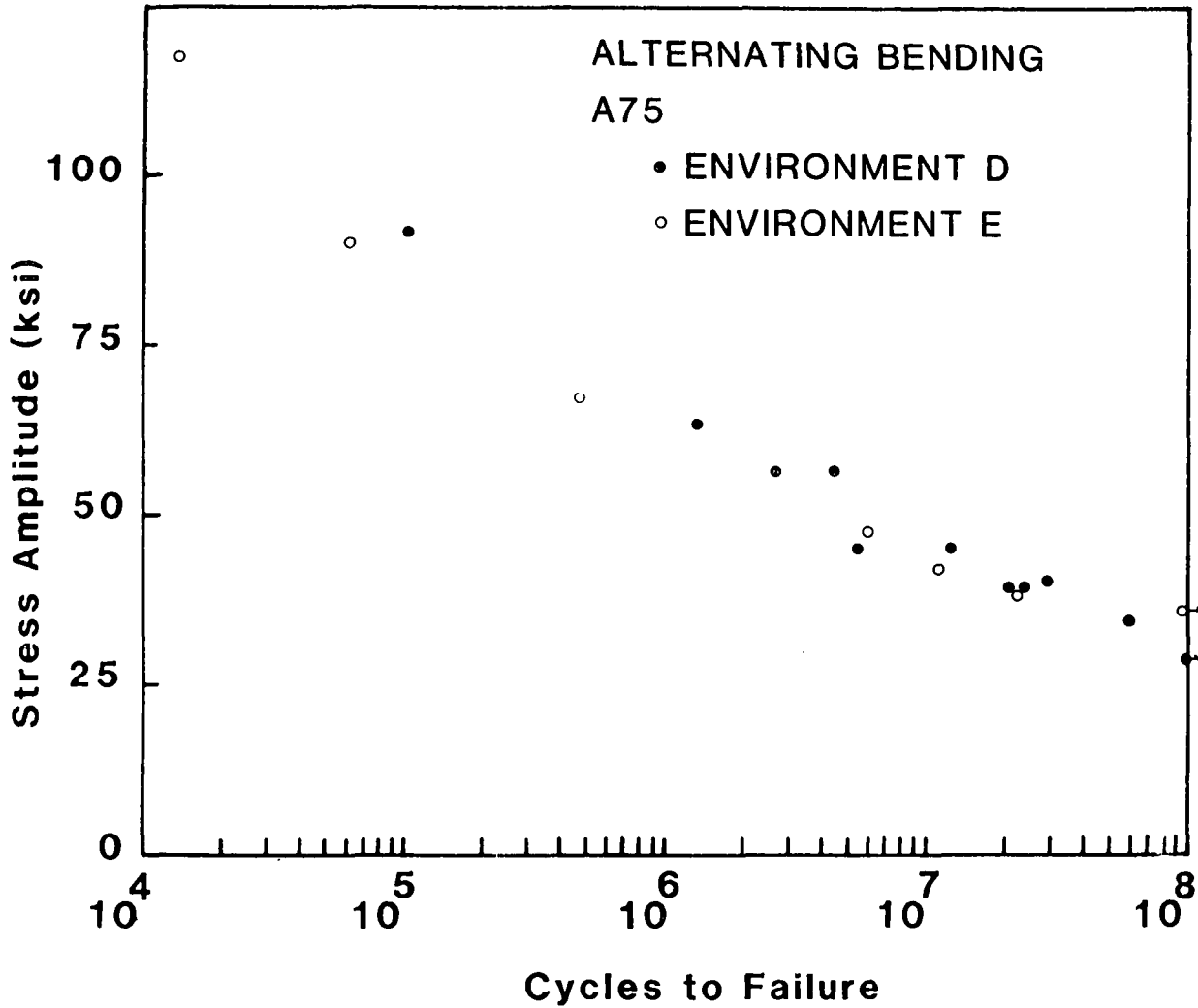


Figure 18. S-N data for Alloy 75 (alternating bending) in Environments D and E.

is seen in tests in simulated whitewaters, but this effect does not differentiate between alloys with superior and inferior performances as suction rolls. In one alloy (A75), there is no apparent notch sensitivity due to the presence of a drilled hole similar to those found in actual suction rolls.

#### Stress Corrosion Cracking Testing

Although stress corrosion cracking is seldom identified as a primary mode of suction roll failure, some of the alloys are placed in service with high tensile residual stresses which have the potential for promoting crack growth in paper machine whitewaters. Furthermore, weld repairs are frequently made subsequent to the final heat treatment and high tensile residual stresses are present in the vicinity of these cosmetic weld repairs. Failure at weld repairs is a possibility in suction roll alloys, although there is little direct evidence for such a mode of failure.

Stress corrosion cracking susceptibility is being determined by conducting slow strain rate tests on the suction roll materials in simulated whitewaters. To date, all five alloys have been tested in two thiosulfate-doped whitewaters. Some additional tests have been conducted in Environment E containing 1000 ppm Cl<sup>-</sup>. The results of tests in simulated whitewaters are being compared with tests conducted in an inert silicone oil.

Of the alloys tested, only A75 has exhibited any evidence of the secondary cracking associated with stress corrosion crack growth. The remaining four alloys were immune to stress corrosion cracking indications. This, of course, is in direct contradiction with the ranking of service performance of suction roll alloys, since A75 has been immune from cracking in service. These results do raise a question regarding the wisdom of weld repairs made in A75 alloy, and further tests to address this issue are underway.



Given the apparent sensitivity of at least one suction roll alloy to stress corrosion cracking in simulated whitewaters, tests are underway: 1) to examine the magnitude of residual stresses in the vicinity of simulated weld repairs, and 2) to determine whether stress corrosion cracking will occur in the vicinity of these simulated weld repairs. The magnitude of residual stresses is being determined by a standard hole drilling technique, wherein strain gages are used to measure the relaxation that occurs when residual stresses are relieved by drilling a hole in the stressed material. In the first such measurement, large tensile residual stresses were found in the vicinity of the simulated weld repair — on the order of 45 ksi. Further determinations of residual stress levels in other alloys are planned. Also planned are exposures of coupons with simulated weld repairs to whitewaters in order to determine whether cracking will occur as a result of the existence of high residual stresses.

#### PLANS FOR NEXT PERIOD

In the next reporting period, near-threshold fatigue testing will be completed in more aggressive environments whose compositions simulate the acidic conditions that develop in pits and crevices. The composition of test solutions will have a lower pH and a higher concentration of chloride and thiosulfate anions than have been used in the preceding tests. Tests will also be conducted on a new Sandusky alloy that has been made available, to attempt to predict the service performance of this alloy based on its resistance to crack growth in the near-threshold regime. In response to requests from the PAC committee, some near-threshold fatigue crack growth tests will be conducted using CA-15 stainless steel and several bronze alloys now in use as commercial suction roll alloys.

Crack initiation behavior will be examined via high cycle fatigue tests to determine the S-N behavior in simulated whitewaters. Tests planned for the next period will involve more aggressive whitewaters which better simulate the acidic conditions that develop in the electrolytes in pits and crevices. Tests will focus on the behavior of Alloys 63 and 75, in order to screen the value of this test method for predicting service performance, without testing all five of the alloys in the program.

The effort to characterize any degradation in stress corrosion cracking resistance caused by cosmetic weld repairs will also be continued in the next reporting period. The residual stresses in the vicinity of weld repairs will be determined for all five of the alloys in test using the hole drilling technique described above. The extent of relaxation of residual stresses near welds, by imposition of a post-weld heat treatment, will also be examined. Welded coupons will be exposed to simulated whitewaters to determine if cracking occurs under the static stresses present in welds that have (or have not) been stress relieved.

#### SIGNIFICANCE TO THE INDUSTRY

The ultimate objective of this effort is to encourage development of improved suction roll alloys by identifying microstructures and alloy compositions with greater resistance to corrosion-assisted cracking. A significant test program is underway to determine the characteristics of suction roll alloys with improved resistance to corrosion-assisted cracking in service. Attempts to identify laboratory tests which can be used to predict eventual service performance of new alloys have met with some success in near-threshold crack growth testing, but this effort is continuing.

REFERENCES

1. Garner, A. Suction roll failures in Canada. Proceedings from the 70th Annual Meeting of the Canadian Pulp and Paper Association, Paper A209 (1984).
2. Bowers, D. Corrosion and corrosion fatigue of paper machine suction roll alloys. Report 2, Project 3309, December, 1984.

THE INSTITUTE OF PAPER CHEMISTRY  
Appleton, Wisconsin

Status Report  
to the  
ENGINEERING PROJECT ADVISORY COMMITTEE

Project 3556  
FUNDAMENTALS OF KRAFT LIQUOR CORROSIVITY

October 22, 1986

## PROJECT SUMMARY FORM

DATE: September 15, 1986

PROJECT NO.: 3556 - Fundamentals of Kraft Liquor Corrosivity

PROJECT LEADER: D. C. Crowe

IPC GOAL:

Increase the useful life of equipment by proper selection of materials of construction and by identifying suitable process conditions.

OBJECTIVE:

To understand the causes of corrosion and corrosion-assisted cracking of carbon steels exposed to kraft liquor, as the basis for developing methods for reducing corrosion damage in kraft process streams.

CURRENT FISCAL BUDGET: \$130,000

SUMMARY OF RESULTS SINCE LAST REPORT: (March 1986 - September 1986)

Combinations of polysulfide and thiosulfate have been added to simulated white liquors in the laboratory to determine their effect on corrosion of mild steel. The combination of corrosive species led to lower corrosion rates than for either of the species alone.

A study using a rotating cylinder electrode to simulate velocity effects in white liquor is currently underway as a student project.

Slow strain rate tests in simulated white liquors containing organic additives have been completed through student research.

Slow strain rate tests have been performed in liquor from operating digesters to identify differences in stress corrosion behavior between mills. Liquor from three digesters has been gathered for these tests.

In-mill testing in the white liquor area has been completed at two more locations, both within the same mill. One of the tests included testing immediately after a shutdown.

A progress report has been written (No. 5) describing results of corrosion monitoring in the white liquor area at mills 5-7, development of the microprocessor-based data acquisition system and laboratory results of corrosion tests in simulated white liquor with sulfite additions.

A new electrode arrangement has been designed for mill testing. The electrode leads will be potted with epoxy to prevent shortcircuits caused by leakage of liquor into the probe. The electrode will be suspended by a hose and cable instead of a pipe arrangement for ease of installation.

## INTRODUCTION

### Approach

Corrosion monitoring methods and equipment are being developed and demonstrated for use in kraft white liquor systems in mills. A better understanding of liquor conditions that accelerate corrosion is being developed in the laboratory as a basis for interpretation of behavior in real systems.

### LABORATORY STUDY - EFFECTS OF COMBINATIONS OF POLYSULFIDE AND THIOSULFATE

Previous laboratory results have shown that white liquor corrosivity increases with higher sulfide and caustic concentrations. Thiosulfate increased the corrosion rates dramatically. Polysulfide, at moderate concentrations

(<2.5 g/L), caused a short-term increase in corrosion rate, but in longer tests it stimulated passivation (1). Sulfite additions were found to increase corrosion rates only in liquors containing more than about 20 g/L Na<sub>2</sub>S (2).

The objective of the present work has been to determine the effect of combinations of polysulfide and thiosulfate on the long-term corrosion rate of steel in a range of NaOH + Na<sub>2</sub>S solutions. The polarization behavior was also investigated as part of this work. This work completes the study of the effects of various white liquor constituents on corrosion of mild steel.

#### Experimental Procedure

Corrosion rates were investigated in the present work by exposing 1018 carbon steel weight loss coupons to liquors at 90 C containing NaOH (80 & 120 g/L), Na<sub>2</sub>S (20 & 40 g/L), Na<sub>2</sub>S<sub>2</sub>O<sub>3</sub> (2.5, 5.0 & 25 g/L) and S (0.5, 1.0, 1.5 & 5 g/L) for 2, 4, 6 and 8 weeks.

As described previously (1,3), experiments were performed in 180 mL fluoroethylenepolymer (FEP) beakers with screw-top lids. The cylindrical electrodes were 3/8 inch diameter with a surface area of 9 cm<sup>2</sup>, tapped at one end, polished to 120 grit and degreased. The composition of the 1018 steel has been listed previously (3). The electrode holders were constructed of polytetrafluoroethylene (PTFE). The electrode was isolated from the holder by a Hypalon gasket. Each cell contained four electrodes to be removed at two week intervals and a silver-silver sulfide reference electrode. After the test, the electrodes were carefully blasted clean before weighing. Solutions were changed at 2 week intervals under a nitrogen atmosphere in a glove bag to prevent oxidation by air. The corrosion potentials (open circuit) of the specimens were recorded and plotted versus time. Anodic and cathodic polarization curves were

obtained for steel and gold in each liquor composition at 90 C. Potential was scanned at 1 mV/s using a Princeton Applied Research Model 350 corrosion measurement system. All measured potentials have been quoted with respect to the silver/silver sulfide electrode, V(SSSE) in the liquor at temperature.

### Results and Discussion

Corrosion rates have been tabulated in Table 1. Values for 0 g/L S and 0 g/L Na<sub>2</sub>S<sub>2</sub>O<sub>3</sub> were taken from previous results (1) and tabulated for comparison. Corrosion potential was monitored throughout the exposures. After a period of exposure the corrosion potential of the steel moved upward from the active range to the passive range where lower corrosion rates would be expected. The time for the electrodes to passivate is indicated in Table 1 by the letter following each corrosion rate measurement. A sample plot of corrosion potential vs time is shown in Figure 1. The electrodes passivated immediately in solutions containing 5 g/L S. A period of about six days was a common time to passivation in solutions containing 1.0 and 1.5 g/L S. Passivation was often faster in the weaker solutions containing 80 g/L NaOH + 20 g/L Na<sub>2</sub>S. Solutions containing 0.5 g/L S usually took the longest time to passivate.

Table 1. White liquor studies - Effect of combinations of thiosulfate and polysulfide.

NaOH g/L	Na <sub>2</sub> S g/L	Na <sub>2</sub> S <sub>2</sub> O <sub>3</sub> g/L	S, g/L				
			0.0	0.5	1.0	1.5	5.0
			After 2 weeks, mpy				
80	20	0	5.5	7.6	8.8	12.4	1.7
		2.5	10.5	0.9a	0.5a	20.8b	1.1a
		5.0	14.7	26.6b	1.1a	1.0a	1.1a
		25.0	22.6	8.5b	1.0a	1.1a	1.0a
80	40	0	4.5	15.7	14.2	17.1	4.8
		2.5	11.9	15.4b	53.0c	24.0b	9.5a
		5.0	20.9	38.0c	20.8b	23.0b	13.9a
		25.0	27.8	26.2b	19.9b	18.7b	11.0a



Table 1.- Continued.

NaOH g/L	Na <sub>2</sub> S g/L	Na <sub>2</sub> S <sub>2</sub> O <sub>3</sub> g/L	S, g/L				
			0.0	0.5	1.0	1.5	5.0
After 2 weeks, mpy (continued)							
120	20	0	5.1	15.6	9.5	14.0	5.9
		2.5	15.0	30.1c	-	13.0b	4.4a
		5.0	24.7	8.8b	13.4b	19.1b	8.9a
		25.0	39.9	13.1b	18.1b	22.1b	2.8a
120	40	0	5.5	19.9	39.0	16.8	16.6
		2.5	16.0	36.4c	20.2b	21.3b	15.2a
		5.0	45.5	20.5b	21.1b	25.0b	11.3a
		25.0	43.8	26.9b	32.3b	27.8b	11.1a
After 4 weeks, mpy							
80	20	0	3.6	4.0	4.5	6.7	2.1
		2.5	11.6	0.7a	6.6b	13.1b	1.1a
		5.0	8.5	0.6a	1.1a	1.0a	1.0a
		25.0	24.6	4.4b	0.9a	0.8a	1.2a
80	40	0	5.4	18.0	7.1	10.2	6.7
		2.5	13.4	8.7b	25.4c	10.8b	7.2a
		5.0	16.5	41.2c	12.3b	12.5b	6.8a
		25.0	30.6	12.3b	9.9b	9.2b	1.6a
120	20	0	5.9	10.8	4.9	7.3	5.1
		2.5	11.8	24.3c	15.8b	7.1b	4.4a
		5.0	13.8	7.0b	8.6b	12.0b	5.0a
		25.0	46.6	9.1b	11.0b	12.8b	2.7a
120	40	0	5.1	19.3	34.6	8.6	6.6
		2.5	14.4	18.9c	9.8b	10.7b	5.9a
		5.0	37.9	8.8b	10.8b	11.9b	5.0a
		25.0	41.5	12.8b	15.6b	13.3b	5.5a
After 6 weeks, mph							
80	20	0	6.0	3.0	3.6	4.3	2.0
		2.5	8.6	7.3b	4.8b	0.6a	0.7a
		5.0	7.0	0.3a	0.9a	0.5a	0.8a
		25.0	26.6	3.1b	0.7a	0.8a	0.6a
80	40	0	4.1	13.6	4.4	6.8	4.6
		2.5	17.1	5.7b	17.1c	7.3b	4.8a
		5.0	11.8	14.3c	9.4b	7.7b	4.2a
		25.0	36.0	8.7b	6.7b	6.1b	5.2a
120	20	0	13.6	8.0	3.4	4.7	6.6
		2.5	9.0	17.3c	10.6b	6.6b	5.0a
		5.0	12.3	4.5b	7.4b	9.8b	4.6a
		25.0	54.7	7.1b	9.1b	10.9b	5.0a
120	40	0	5.5	24.5	31.8	5.0	3.0
		2.5	23.4	11.7c	6.3b	7.6b	3.5a
		5.0	40.3	6.4b	7.2b	8.1b	3.5a
		25.0	40.4	8.7b	11.0b	9.6b	3.7a

Table 1 - Continued.

NaOH g/L	Na <sub>2</sub> S g/L	Na <sub>2</sub> S <sub>2</sub> O <sub>3</sub> g/L	S, g/L				
			0.0	0.5	1.0	1.5	5.0
After 8 weeks, mpy (continued)							
80	20	0	6.5	2.2	2.6	3.9	1.4
		2.5	7.1	0.7a	3.71b	0.6a	0.7a
		5.0	7.0	0.5a	0.7a	0.7a	0.7a
		25.0	27.8	2.5b	0.6a	0.5a	0.6a
80	40	0	4.8	10.6	3.7	6.2	3.2
		2.5	5.5	4.2b	9.2c	5.7b	4.1a
		5.0	19.6	11.0c	7.0b	5.7b	2.9a
		25.0	43.2	24.4c	5.1b	4.8b	3.6a
120	20	0	6.9	6.9	3.0	4.0	4.5
		2.5	7.5	13.0c	8.1b	3.8b	4.4a
		5.0	17.1	3.6b	6.1b	7.2b	2.5a
		25.0	61.5	6.0b	7.0b	8.3b	4.2a
120	40	0	5.8	11.1	34.2	3.8	3.5
		2.5	26.4	7.9c	4.2b	5.0b	1.8a
		5.0	44.0	3.7b	4.6b	5.1b	1.8a
		25.0	35.0	5.2b	6.4b	5.4b	2.0a

Key a - immediate passivation.  
 b - passivation in < 200 h.  
 c - passivation after > 200 h.

Comparison of the corrosion rates in these solutions with solutions containing no thiosulfate showed that in general, solutions with more thiosulfate had higher corrosion rates. In comparison with solutions containing no sulfur additions, it can be seen that solutions with sulfur additions had lower corrosion rates. This was most true in short exposure tests in stronger liquor (due to faster passivation).

The polarization curves for steel were obtained and are illustrated in Appendix 1. A wide active/passive peak was observed in most of these solutions. A detailed analysis of these curves has not been completed at this time.

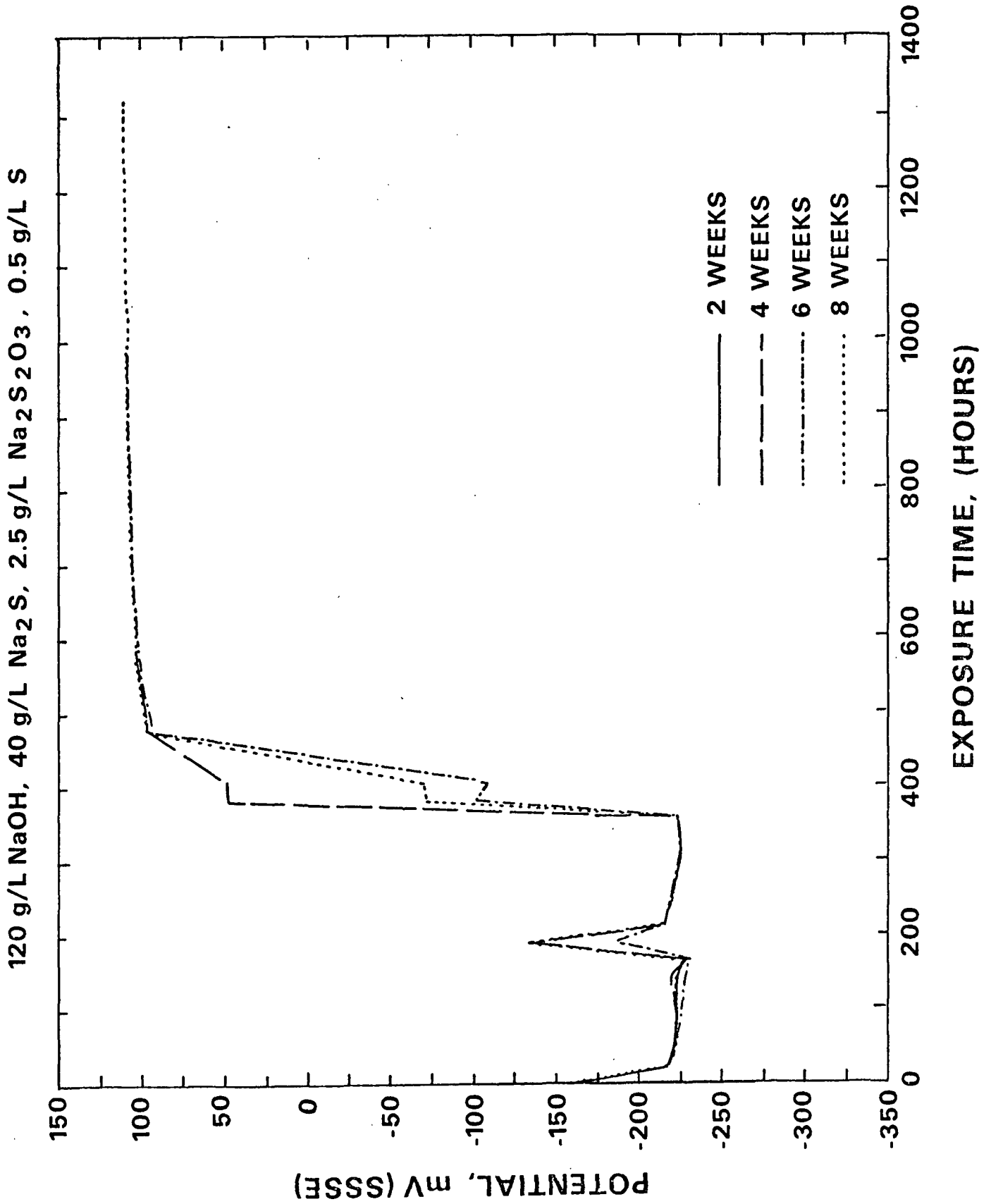


Figure 1. Corrosion potential vs. time of 1018 steel in 120 g/L NaOH + 40 g/L Na<sub>2</sub>S + 2.5 g/L Na<sub>2</sub>S<sub>2</sub>O<sub>3</sub> + 0.5 g/L S.

## Conclusions

1. Combinations of thiosulfate and polysulfide have lower corrosion rates than if either species is present by itself. Small amounts of sulfur were especially effective in reducing the effect of thiosulfate. In long tests in weak liquor, thiosulfate additions may have decreased corrosion rates.

2. Trends become somewhat unclear in this more complex liquor. This may account for the wide variations in corrosion rate observed in the mill exposures where liquor composition is continuously fluctuating.

## DIGESTER STRESS CORROSION CRACKING

Mill Liquor. Stress corrosion cracking of continuous kraft digesters has been a costly problem to the pulp industry. A puzzling feature of the cracking problem has been that some digesters are more prone to cracking than others. The objective of this study is to cast some light on the reasons for these differences. Liquor samples have been obtained from three operating continuous digesters. This liquor is being used in tests to determine the susceptibility of steel to stress corrosion cracking. Specimens of steel are being pulled very slowly to failure in the liquors at digester temperature. These tests are known as slow strain rate tests. If the steel is susceptible to cracking, failure will occur sooner in the test and cracking will be observed on the specimen. The results of these tests will indicate whether there are differences between mills which correlate with differences in their susceptibility to stress corrosion cracking.

Table 2. Digester liquor analysis.

Mill	Composition, g/L							
	NaOH	Na <sub>2</sub> S	Na <sub>2</sub> SO <sub>3</sub>	Na <sub>2</sub> S <sub>2</sub> O <sub>3</sub>	Na <sub>2</sub> SO <sub>3</sub>	Na <sub>2</sub> SO <sub>4</sub>	NaCl	Na <sub>2</sub> S <sub>x</sub>
M5	14.13	11.1	30.7	2.54	1.32	3.42	1.17	0.67

Slow strain rate tests have been completed using liquor from the top circulation line at Mill M5. The tests have been performed at 260 F (127 C) in a 316 stainless steel test cell. Potentials of the test specimens were controlled with respect to a silver/silver sulfide reference electrode (SSSE) in the cell at test temperature. Open circuit potential was 55 mV(SSSE). The specimens were pulled at a slow strain rate of  $2 \times 10^{-6}$  sec<sup>-1</sup>. After failure, the specimens were sectioned, polished and examined for cracking. Maximum cracking depth occurred at -80 mV(SSSE). The shortest time to failure and lowest percent reduction of diameter (two other measures of stress corrosion susceptibility) were at -40 mV(SSSE). This indicates that the maximum susceptibility to stress corrosion occurs in the range from -40 to -80 mV(SSSE).

Simulated liquor with organic additives. Slow stain rate tests have been completed in simulated white liquor solutions (NaOH + Na<sub>2</sub>S) containing additions of tannic acid, quebracho tannin, catechol and pyrogallol to determine the effects of organic species on the susceptibility to stress corrosion. These tests are being performed by Jack Hayford III as part of his master's degree research.

#### IN-MILL CORROSION MONITORING IN THE WHITE LIQUOR AREA

##### Previous Work

In previous work, the linear polarization resistance and electrical resistance techniques were evaluated for use in kraft white liquor. The electrical resistance technique gave good agreement with weight loss results, and the linear polarization resistance method agreed well when a correction factor was applied. These methods were used in testing at four mills in white liquor tanks and clarifiers. A microprocessor-based data acquisition system significantly improved the effectiveness of the testing and prevented the loss of data due to chart recorder failures.

Corrosion rates in mills were found to depend on white liquor compositions; mills with higher sulfidity, causticity and thiosulfate concentration experienced higher corrosion rates. Liquor velocity was also a factor in mill corrosion. The corrosion rate was found to vary significantly during the exposure, but this variability did not depend on liquor composition. The four carbon steels used in the study were ranked in order of decreasing corrosion rate: 1018, A285C, A283, A285C Special. Corrosion rates increased dramatically when the liquor level was lowered below the electrodes and then raised.

The present work is a continuation of the testing in the white liquor area. The effects of a shutdown and startup on corrosion rate were investigated. Thorough liquor analyses performed on-site by the member mill assisted in determining sources of thiosulfate and polysulfide which increase corrosion rates.

#### Mills E-8 and E-9

The results for "Mills" E-8 and E-9 are from the same mill. "Mill E-8" is the swing tank located after pressure filters. The white liquor storage tank is downstream of the swing tank and is designated "Mill E-9".

Polarization curves were obtained for the test steels: 1018, A285C, 283 and 285 Special, and for platinum. These are illustrated in Figs. 2-6. No polarization curves were obtained in the white liquor storage tank. Polarization curves are not significantly different from mill to mill and any differences are difficult to interpret, so it was decided that there was little to be gained by repeating polarization curves for this tank which was just downstream of the swing tank tested. No significant differences in behavior between the steels were observed. The polarization curve for the platinum shows

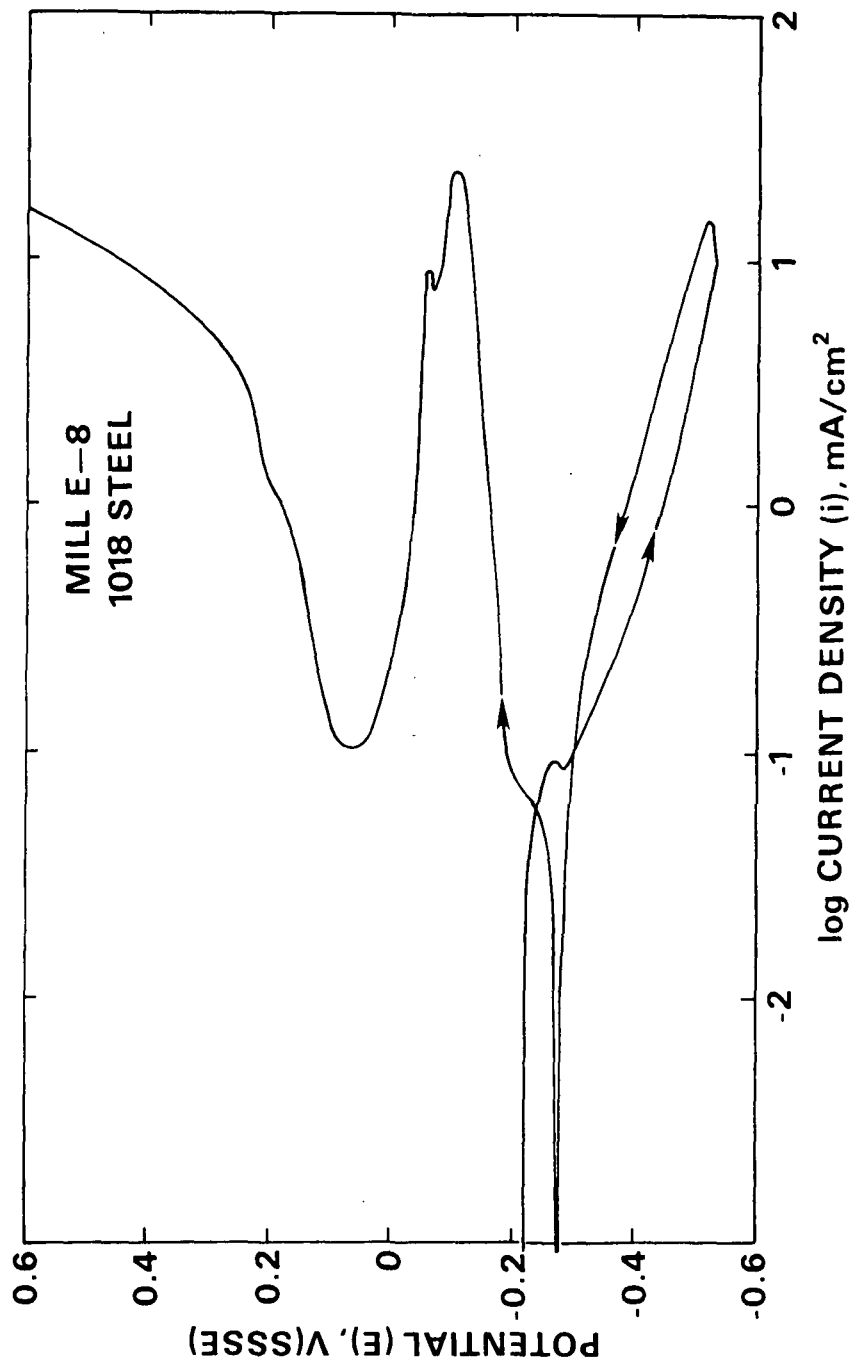


Figure 2. Polarization curve of 1018 steel at Mill E8.

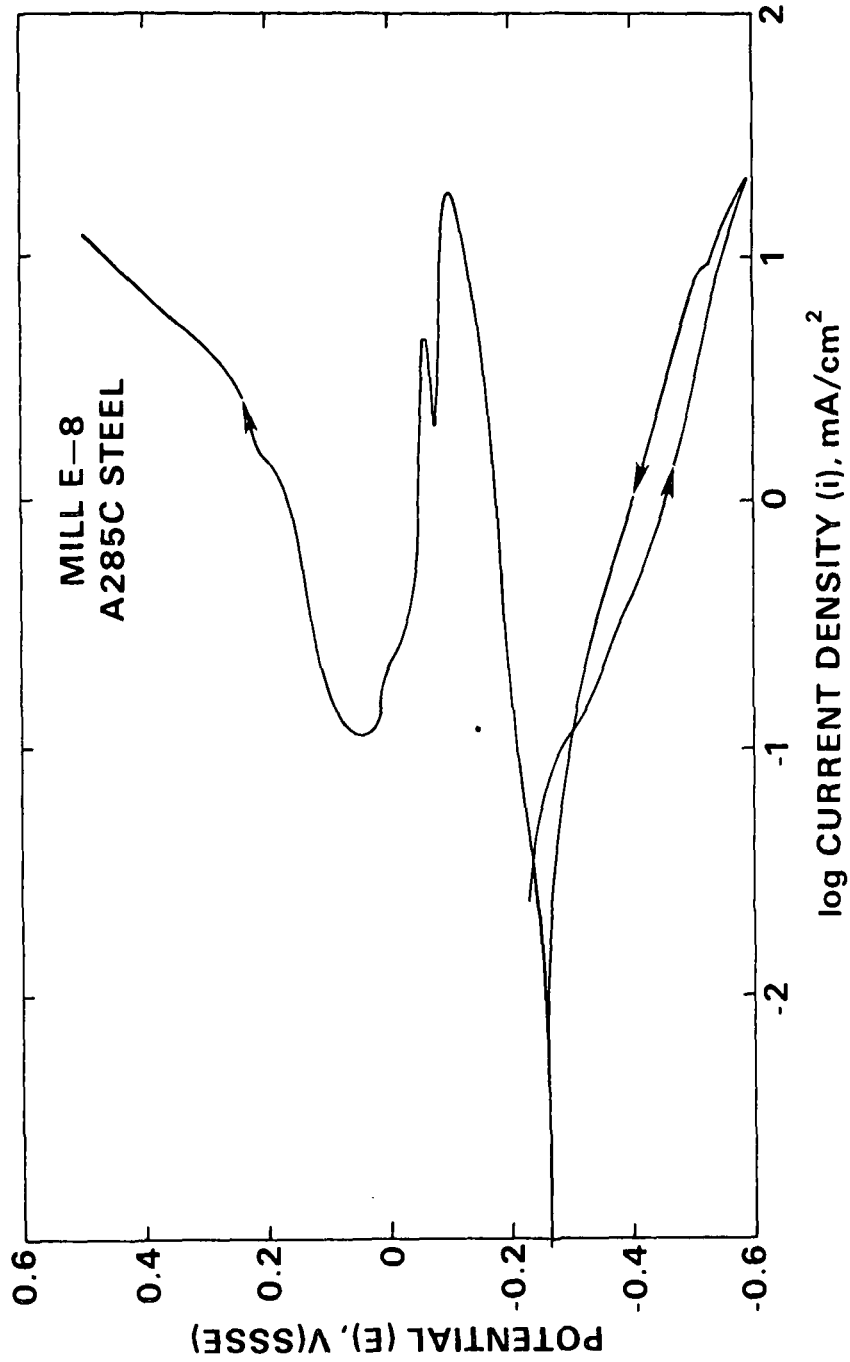


Figure 3. Polarization curve of A285C steel at Mill E8.



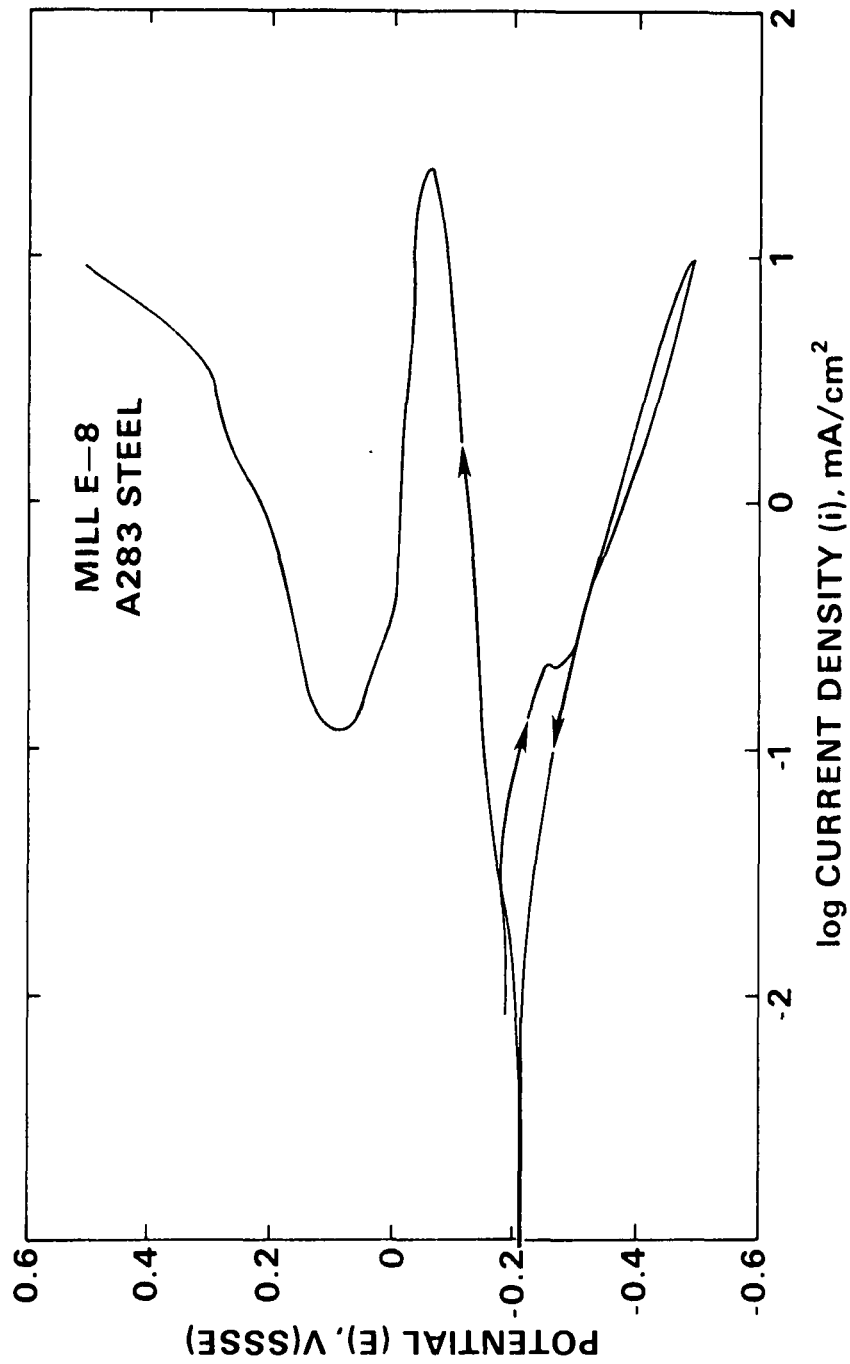


Figure 4. Polarization curve of A283 steel at Mill E8.

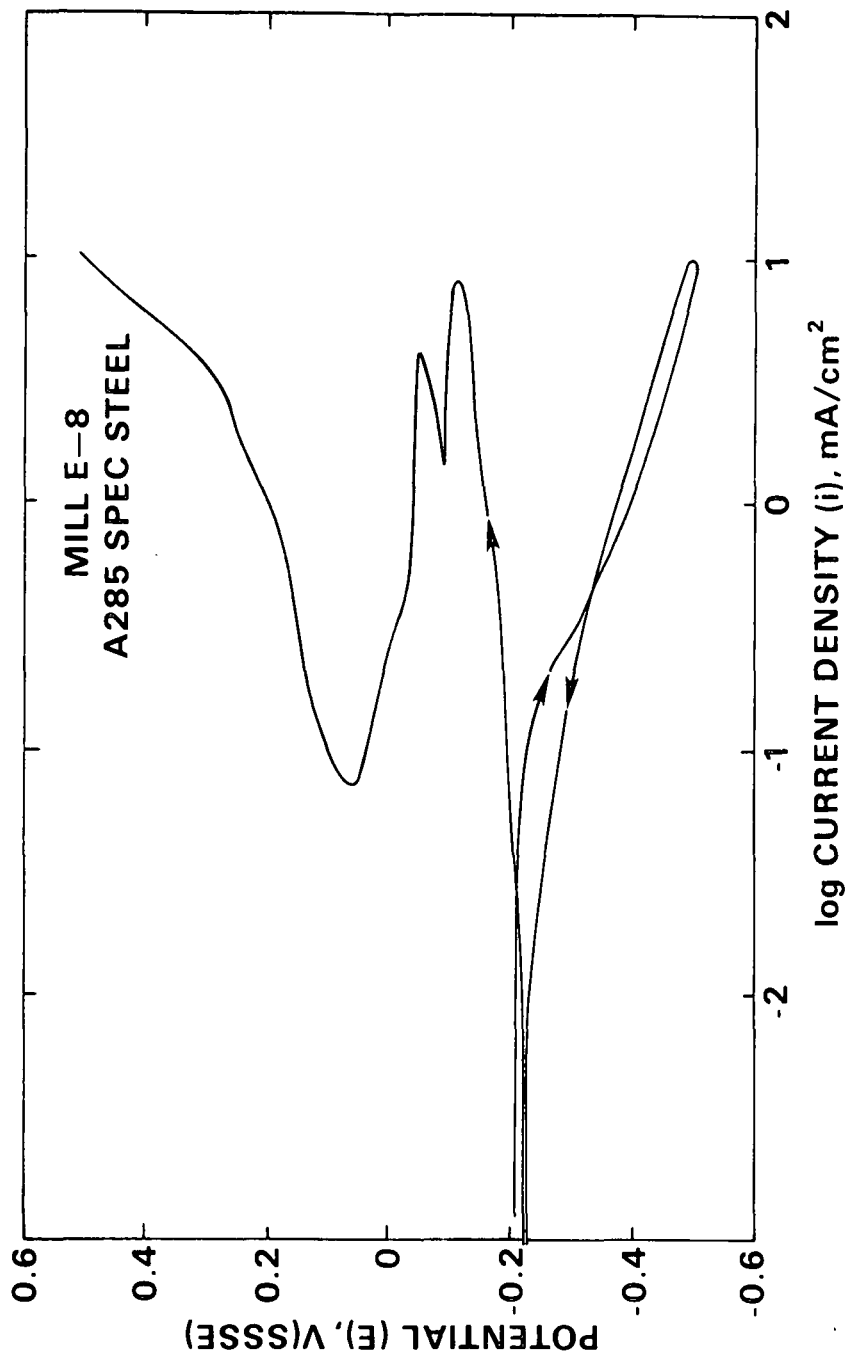


Figure 5. Polarization curve of A285-Special steel at Mill E8.

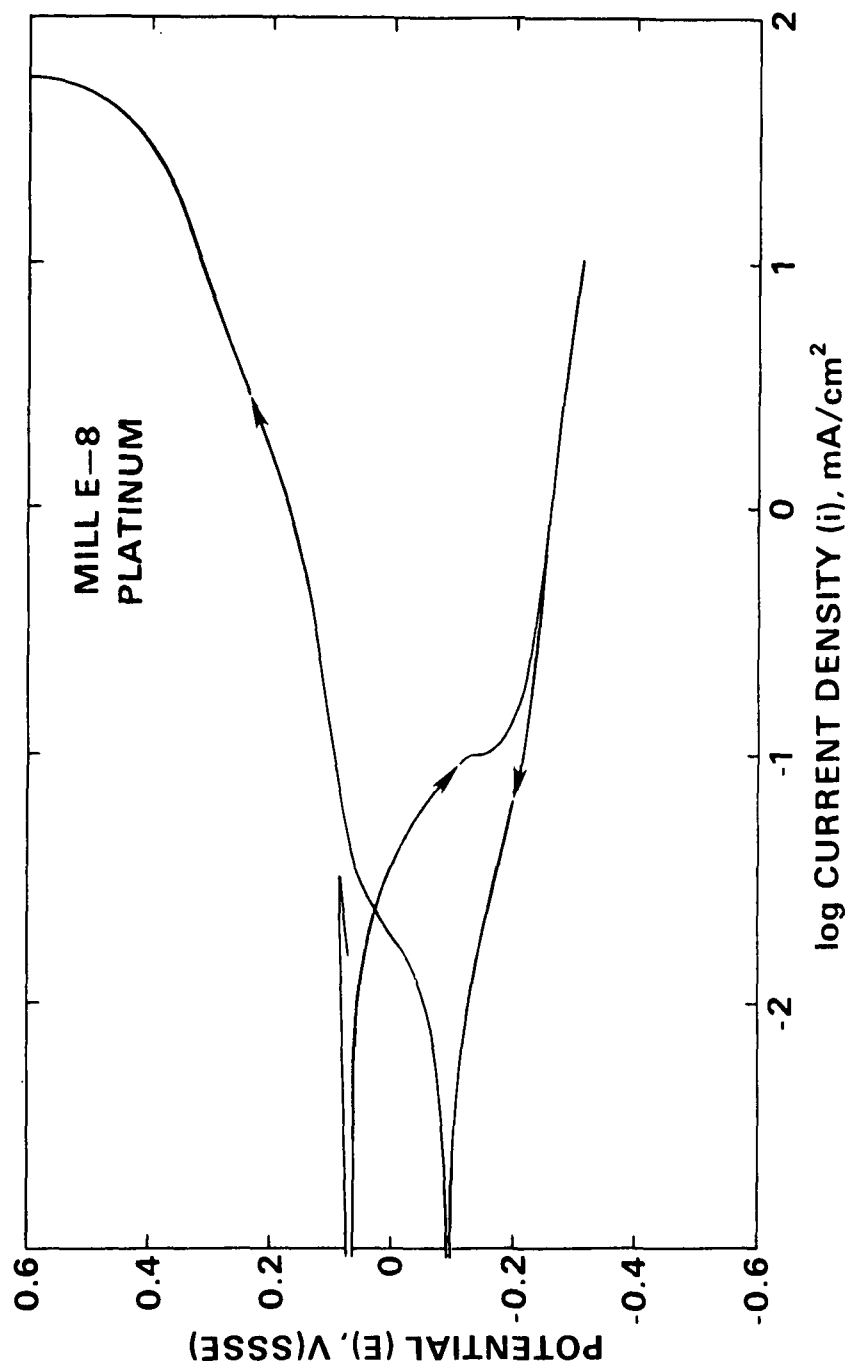


Figure 6. Polarization curve of platinum at Mill E8.

which features of the polarization curve are due to redox reactions for the liquor, not involving the steel. The platinum is inert and provides a non-reactive substrate on which the liquor redox reactions can take place. Redox reactions on the platinum would include oxidation of sulfide to polysulfide and thiosulfate at potentials above 0.1 V(SSSE). Tafel slopes were not measured from the polarization curves for use in correcting linear polarization resistance measurements of the corrosion rate because, as described in Progress Report 5, there is no improvement by calculating correction factors for individual materials or mills.

The liquor level in the swing tank was continuously monitored and is plotted versus time in Figure 7. The probe with the sample electrodes was located at about the 6 - 7 foot level. The liquor level was constant in the white liquor storage tank (Mill E9).

Corrosion rate and potential were monitored continuously and are plotted versus time in Appendix II. Data were lost from 167 to 220 hours due to a computer error. Due to low liquor level, the electrodes were not submerged during the 49-102, 355-556 and 616-706 hour periods.

The weight loss and LPR results are summarized in Table 3. The LPR corrosion rate (column 6 and 7) was calculated from the average LPR values measured approximately every 6 hours during the exposure period. In the table, 'x' is the average value, 's' is the standard deviation and 'n' is the number of measurements during the test for that electrode. These values are calculated from the measurements taken directly off of the Petrolite instrument and were divided by a correction factor of 1.7, determined for mills described in Progress Report 4 (2). The average of the values for the anodic and cathodic polarization measurements is more accurate because it cancels some errors inherent in each.

Swing Tank

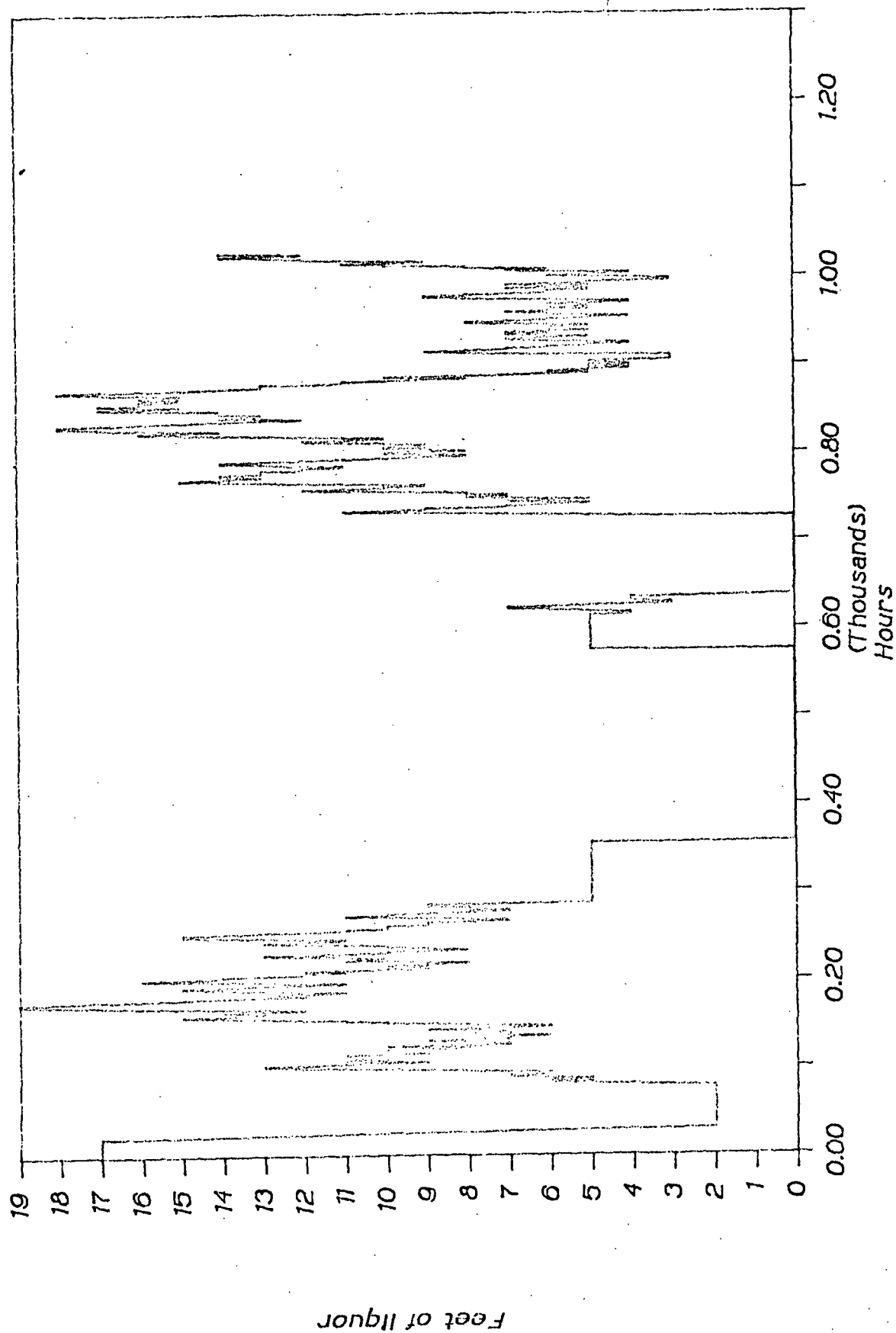


Figure 7. Liquor level in white liquor swing tank (Mill E8).

The weight loss corrosion rate for Mill E8 was calculated assuming both corrosion over the entire test period (column 4) and corrosion only during the time immersed (column 5). The true value is something between these two extremes. The value assuming corrosion over the whole test period is too low because the steel is not always in the liquor. Although some corrosion occurs while in the vapor phase above the liquor, it would be at a much lower rate. The weight loss corrosion rate calculated for immersion time only would underestimate by this amount. The LPR results were integrated to obtain measurements of the average corrosion rate during immersion time only for comparison with measured weight loss also for immersion time only. The agreement between the corrected LPR corrosion rate and the weight loss corrosion rate was good. The LPR rates for A285Special underestimated the corrosion rate as determined by the weight loss tests.

Much greater variation in corrosion rate was observed in the swing tank than in the white liquor storage tank, probably due to the fluctuations in the liquor level in the swing tank. The average corrosion rates in the swing tank for the total time of the test were not significantly different from the corrosion rates in the white liquor tank because the tank was empty for much of the test and the electrodes were in the vapor only.

Table 3. Weight loss, average corrosion rates and corrosion potentials of steels exposed at Mills E8 and E9.

Mill	No.	Mat'l.	Weight Loss, mpy		Linear Polarization Resistance					
			Total Time	Immersion Only	Anodic mpy	Cathodic mpy	Average mpy	Anodic $E_{corr}$	Cathodic $E_{corr}$	
EB	1	1018	26	59	x	58	58	58	-111	-113
					s	24	21		37	36
					n	74	71		70	67
5	1018	22	51	x	32	33	33	-98	-96	
				s	14	17		28	28	
				n	76	76		73	77	
A	1018	39	89							

Table 3 - Continued.

Mill	No.	Mat'l.	Weight Loss, mpy		Linear Polarization Resistance						
			Total Time	Immersion Only	Anodic mpy	Cathodic mpy	Average mpy	Anodic Ecorr	Cathodic Ecorr		
E9	1	1018	--	--	x	34	29	32	1	2	
					s	11	11		11	11	
					n	144	145		120	131	
	5	1018	28	--							
		A 1018	26	--							
EB	2	A285C	30	69	x	91	107	99	-105	-111	
					s	36	120		41	38	
					n	70	72		72	70	
	6	A285C	29	67	x	66	67	67	-97	-121	
					s	114	127		28	22	
					n	77	76		76	79	
	B	A285C	42	97							
E9	2	A285C	33	--							
		6	A285C	35	--	x	36	33	34	-131	-129
						s	20	16		17	16
				n	141	140	143	142			
	B	A285C	31	--							
E8	3	A283	14	32	x	42	25	34	-101	-97	
					s	64	18		43	41	
					n	45	43		46	44	
	7	A283	19	44	x	29	32	31	-115	-115	
					s	18	20		22	22	
					n	46	47		45	46	
	C	A283	25	58							
E9	3	A283	27	--							
		7	A283	31	--						
		C	A283	20	--						
E8	4	A285-Spec.	38	88	x	32	35	34	-119	-118	
					s	15	23		49	47	
					n	84	88		85	86	
	8	A285-Spec.	18	42	x	28	30	29	-102	-104	
					s	23	25		26	25	
					n	48	47		46	46	
	D	A285-Spec.	27	62							
E9	4	A285-Spec.	25	--							
		8	A285-Spec.	34	--	x	20	16	18	-132	-130
						s	18	15		18	18
				n	141	136	142	142			
	D	A285-Spec.	28	--							

The liquor analyses are listed in Table 4. These analyses were performed by the member company for Mill E8. Higher thiosulfate was observed following dry periods, one of which was a shutdown. Generally the thiosulfate levels were higher than at mills previously tested. The pressure filters did not increase the thiosulfate level and high thiosulfate levels were measured even in the green liquor so the source is located prior to this point in the process. Analysis of the liquor composition in the white liquor storage tank (Mill E9), summarized in Table 5, showed the thiosulfate level to be high there, also. The analysis of the liquor from the white liquor storage tank was performed by IPC.

Tests of the effects of liquor velocity or turbulence were performed using a probe with three specimens exposed to the flow and three protected from the flow. At mill E8, the 1018 steel electrodes exposed to flow had corrosion rates of 69, 60 and 52 mpy, assuming corrosion only when immersed. Electrodes protected from the flow had rates of 69, 64 and 59 mpy. Electrodes in mill E9 exposed to the flow had corrosion rates of 25, 21 and 24 mpy. The electrodes not exposed had corrosion rates of 22 and 21 mpy. These results indicate that the motion of the liquor in the tank had no effect on corrosion rates. They do illustrate the much greater corrosion rates found in the swing tank.

### Conclusions

1. Higher corrosion rates occur when liquor level is being cycled up and down.
2. High corrosion rates were observed at this mill and appear to be associated with the high thiosulfate levels.
3. Higher thiosulfate contents were measured following shutdown or period of low liquor level.



Table 4. Liquor analyses - Mill E8.

Sample	Time, hr	Composition, g/L						
		NaOH	Na <sub>2</sub> S	Na <sub>2</sub> CO <sub>3</sub>	Na <sub>2</sub> S <sub>2</sub> O <sub>3</sub>	Na <sub>2</sub> SO <sub>3</sub>	Na <sub>2</sub> SO <sub>4</sub>	Na <sub>2</sub> S <sub>x</sub>
1	1	--	36.97	26.08	7.87	1.72	8.61	0.15
2	6	--	36.19	26.5	7.85	1.7	8.31	0.20
3	29	--	35.34	25.13	8.11	1.21	8.38	0.17
4	49	--	36.04	25.83	8.21	1.98	9.55	0.17
5	51	--	31.98	21.16	7.77	1.67	8.71	0.09
6	52	--	36.43	26.65	7.95	1.68	8.89	0.06
7	53	--	36.04	27.77	8.35	2.17	9.55	0.19
8	96	--	34.01	24.38	9.29	0.65	8.12	0.15
9	102	--	32.76	25.86	8.31	1.44	11.06	0.12
10	104	--	32.14	20.35	8.04	1.7	12.48	0.21
11	112	--	32.76	21.31	6.97	2.05	12.63	0.16
12	119	--	31.51	23.64	6.77	1.89	12.15	0.17
13	168	--	35.1	23.11	9.07	1.77	10.48	0.16
14	173	--	33.85	22.74	8.49	1.98	11.98	0.24
15	217	--	30.96	24.17	8.03	1.75	11.08	--
16	222	--	30.11	23.11	3.75	1.15	5.55	0.13
17	265	--	35.25	25.71	7.92	0.75	9.27	0.24
18	270	--	32.76	21.62	8.07	2.09	9.76	0.27
19	553	--	63.99	4.56	11.22	1.64	10.83	0.16
20	557	--	14.82	10.07	2.41	1.08	4.71	0.10
21	601	--	33.85	29.74	12.79	1.5	6.57	0.15
22	606	--	32.76	28.62	11.73	1.35	6.23	0.17
23	673	--	32.76	28.09	11.61	1.55	6.59	0.18
24	677	--	21.84	23.85	7.16	1.21	4.27	0.12
25	722	--	34.32	29.47	10.72	2.29	8.17	0.21
26	725	--	31.98	26.5	9.7	2.16	7.84	0.15
27	745	--	34.32	27.24	8.57	2.8	11.37	0.10
28	751	--	31.98	26.82	8.71	2.66	13.17	0.13
29	841	--	36.97	23.32	8.14	3.12	9.09	0.20
30	845	--	37.91	23.11	8.42	2.88	9.14	0.20
31	889	--	33.07	24.91	8.39	3.04	18.01	0.19

Table 5. Liquor analyses - Mill E9.

Sample	Composition, g/L													
	NaOH	Na <sub>2</sub> S	Na <sub>2</sub> CO <sub>3</sub>	Na <sub>2</sub> S <sub>2</sub> O <sub>3</sub>	Na <sub>2</sub> SO <sub>3</sub>	Na <sub>2</sub> SO <sub>4</sub>	NaCl	Al	Cu	Fe	Mn	Mg	Si	V
1	111.9	27.4	18.98	9.56	6.69	13.38	2.23	0.031	0.0036	0.048	--	<0.005	0.110	0.098
2	109	30.7	22.06	10.58	4.41	10.94	2.06							

Sample 1 - White liquor storage tank  
 2 - Pressure filter feed

### Instrumentation Developments

Improvements to the data acquisition system are being made. It will incorporate the present micro-processor-based system and will replace the instrument used to perform the linear polarization resistance measurements (Petrolite 1010) which is malfunctioning due to advanced age. Some new hardware and new software (programming) will be involved to make these changes. The hardware is on order. This will complete the last phase of development of this corrosion monitoring system.

### VELOCITY EFFECTS

Corrosion in white liquor has been shown to be accelerated by velocity effects. Pipe loop testing to determine corrosion rates at different flow rates is expensive and difficult. Large quantities of liquor are required. A better test would be faster and would use a smaller amount of solution. Testing with a rotating cylinder electrode would be faster, would use less solution and would allow a larger variety of variables to be tested. Testing is underway as part of student research.

### FUTURE PLANS (1986-1987)

1. Perform testing in the white liquor area at a mill using the improved microprocessor based data acquisition system and new electrode design.
2. Trace the origin of thiosulfate and other corrosive species. This will involve sampling at a number of mills throughout the process from the recovery boiler to digester.
3. Measure corrosion rates in simulated green liquor in the laboratory.
4. Perform polarization tests and weight loss tests at various rotational speeds using the rotating electrode apparatus.

5. Perform slow strain rate tests in the laboratory using liquor collected from digesters.

6. Potentiostatic (constant potential) tests of steel in mill white liquors will be performed to assess whether the poorly understood features of the polarization curves obtained in mill liquors are due to corrosion or to some other redox phenomena (as suggested by Dr. D. Wensley, formerly of the PAC committee).

#### SIGNIFICANCE TO THE INDUSTRY

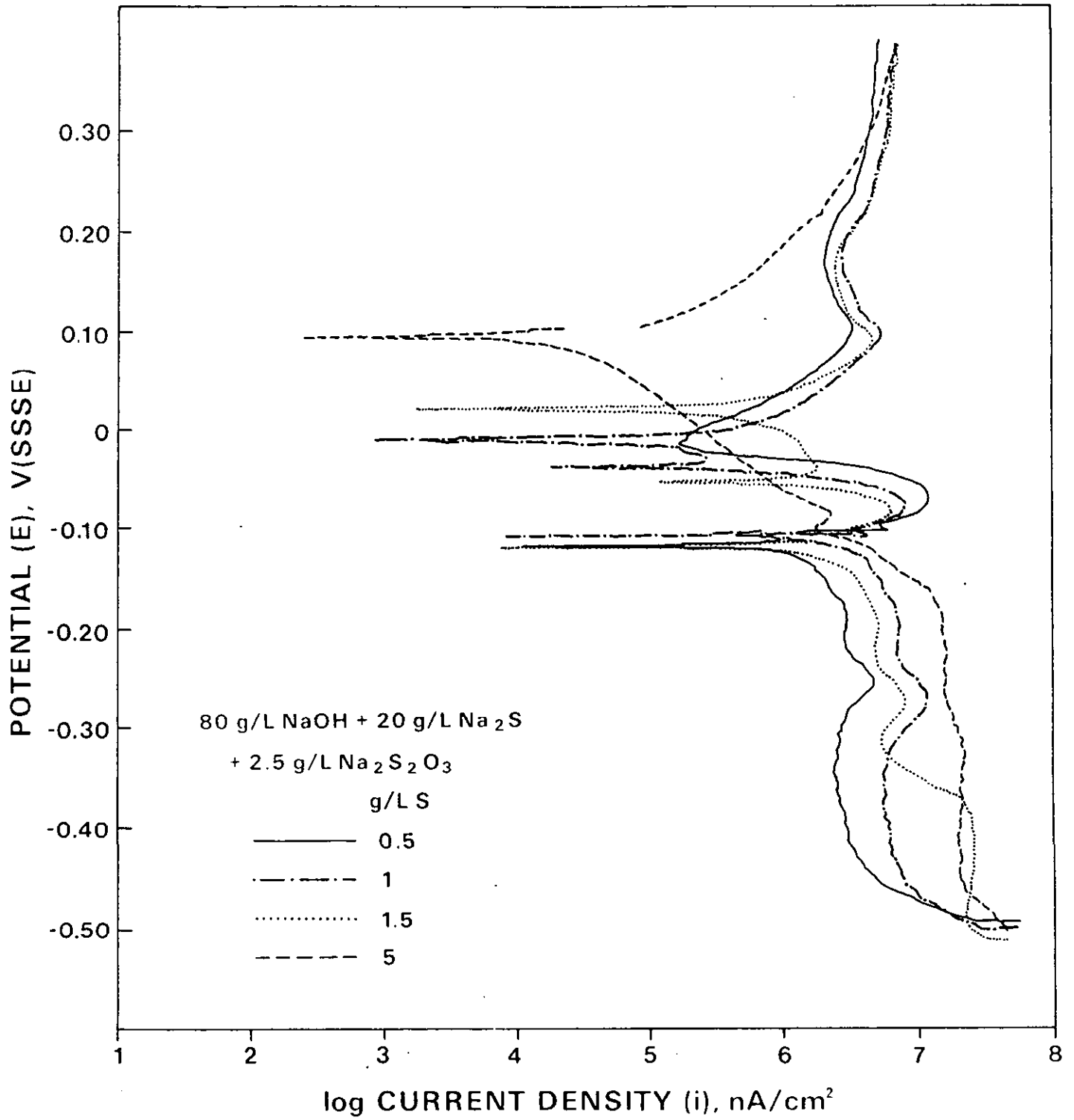
Modern corrosion measurement techniques and equipment have been developed and demonstrated for use in kraft liquor systems. Some operating parameters which increase corrosion rate have been identified. The effects of major liquor constituents on corrosivity of white liquor have been determined.

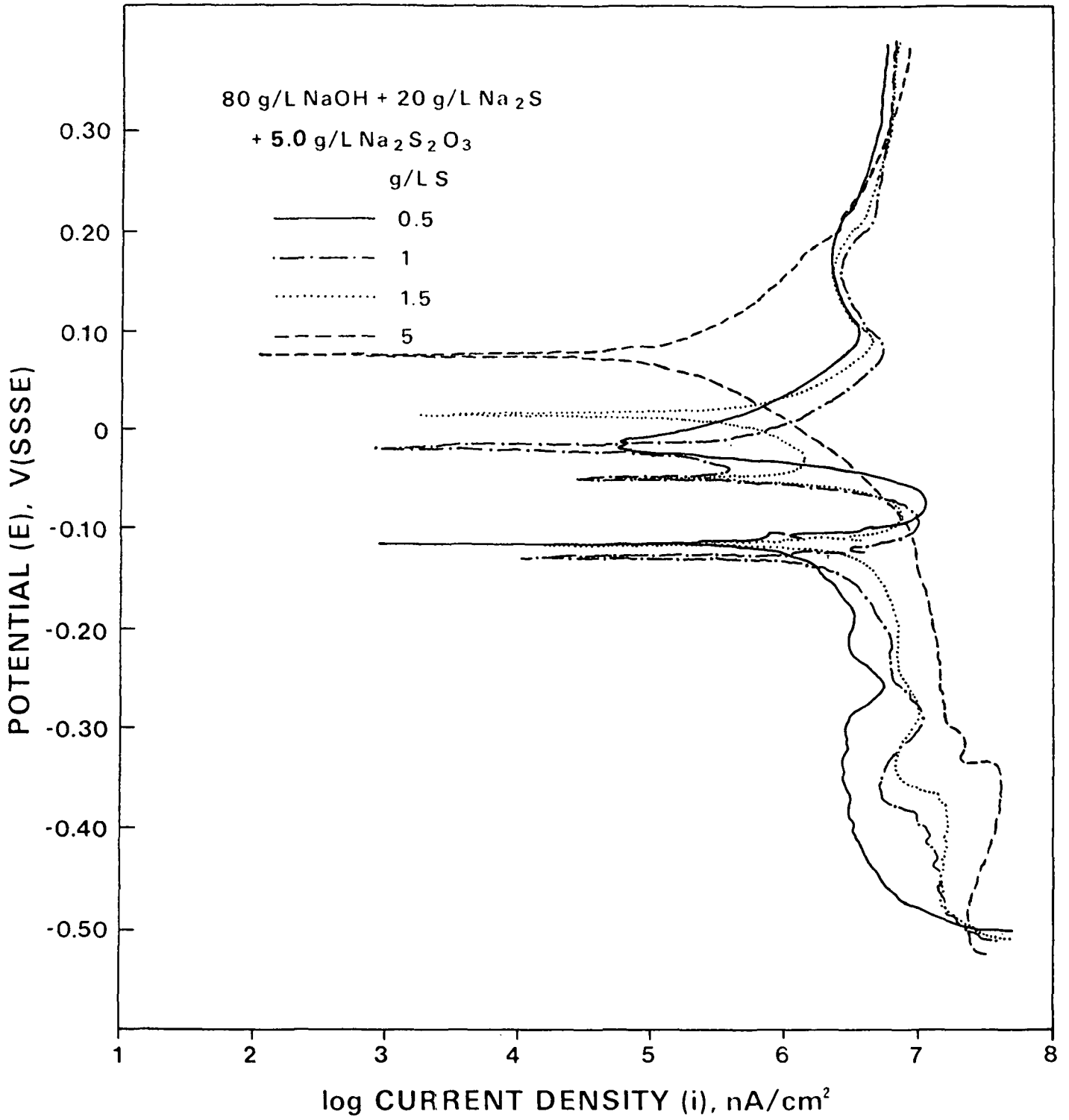
#### REFERENCES

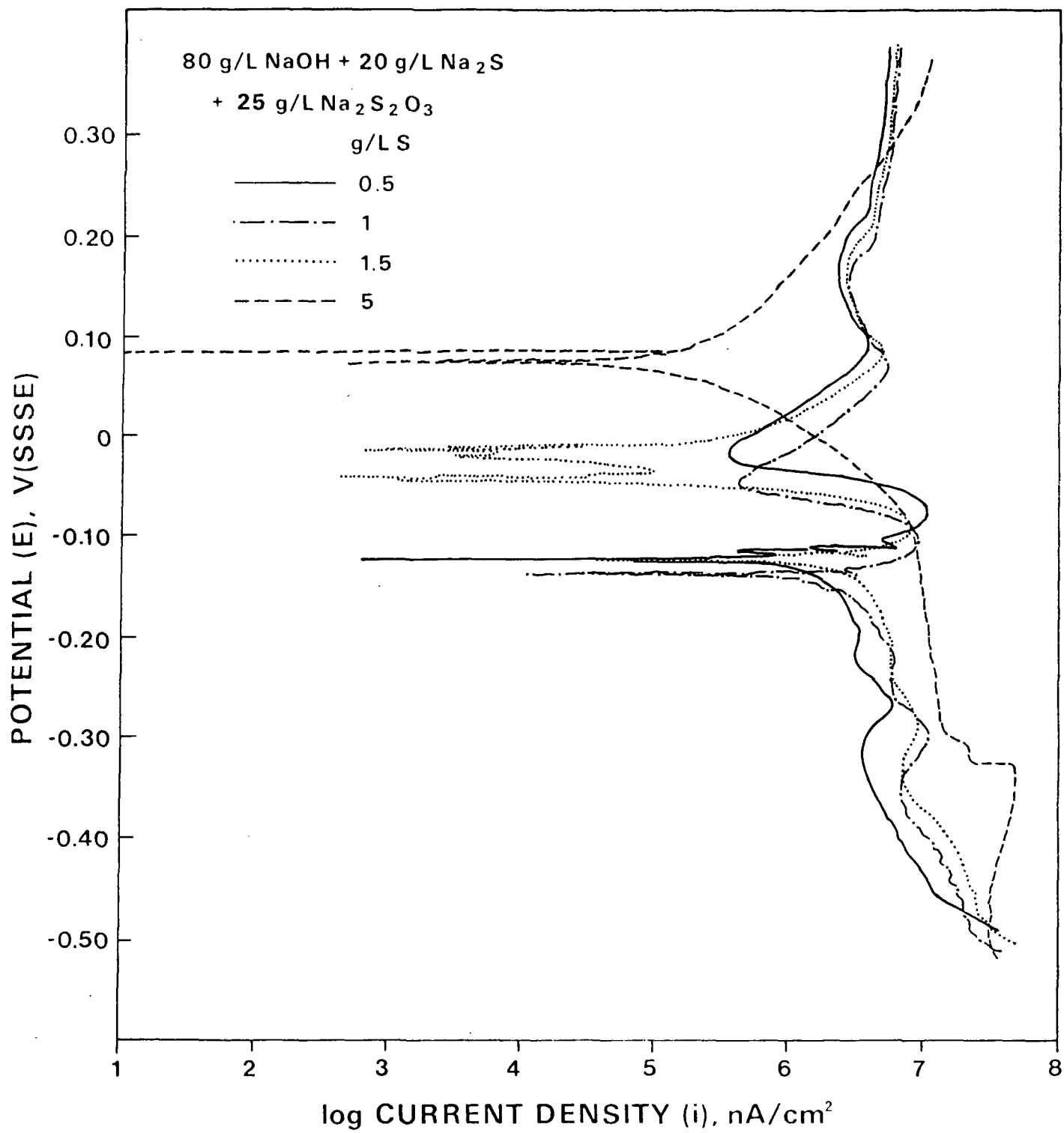
1. Crowe, D. C., Yeske, R. A. Liquor composition effects on corrosion rates in kraft white liquor, Project 3556 Progress Report Three, The Institute of Paper Chemistry, September 11, 1985.
2. Crowe, D. C., Yeske, R. A. In-mill corrosion monitoring in kraft white liquor, Project 3556 Progress Report Four, The Institute of Paper Chemistry, November 15, 1985.
3. Yeske, R. A. Corrosion rate measurements in kraft white liquor, Project 3556 Progress Report Two, The Institute of Paper Chemistry, May 21, 1984.
4. Crowe, D. C., Yeske, R. A., Project 3556 Progress Report Five, The Institute of Paper Chemistry, in preparation.

APPENDIX I

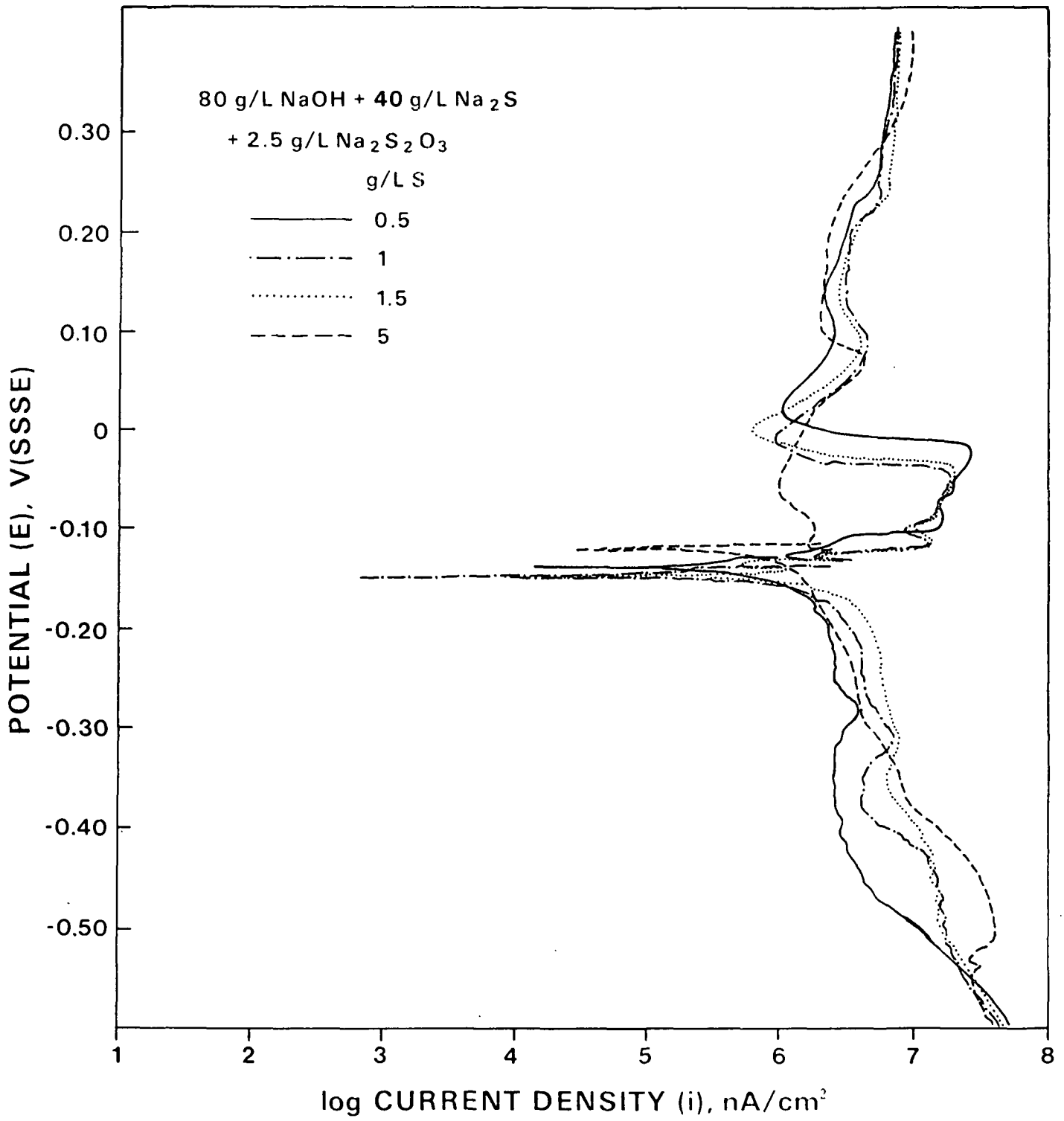
POLARIZATION CURVES FOR STEEL IN NaOH + Na<sub>2</sub>S + Na<sub>2</sub>S<sub>2</sub>O<sub>3</sub> SOLUTIONS

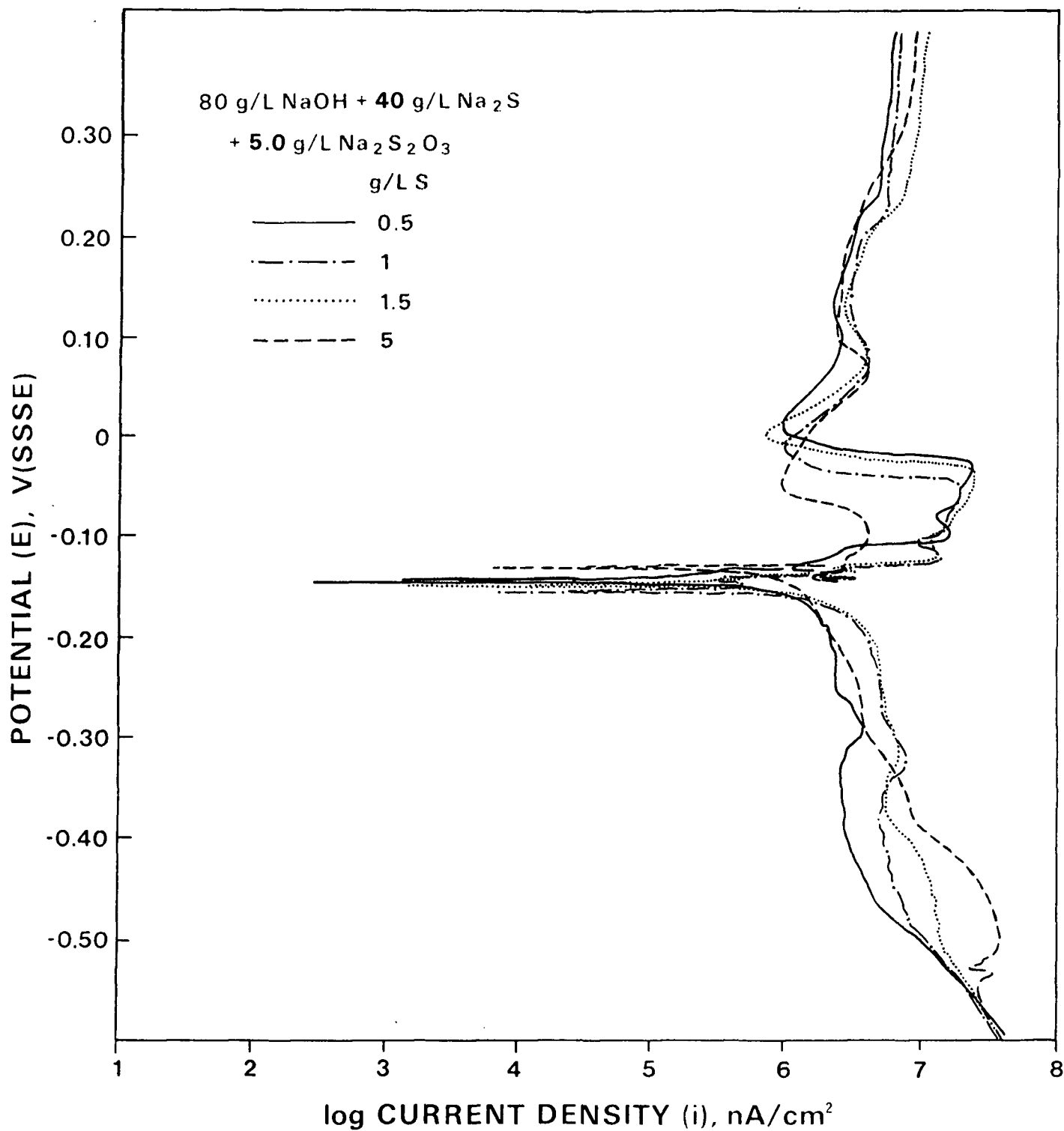


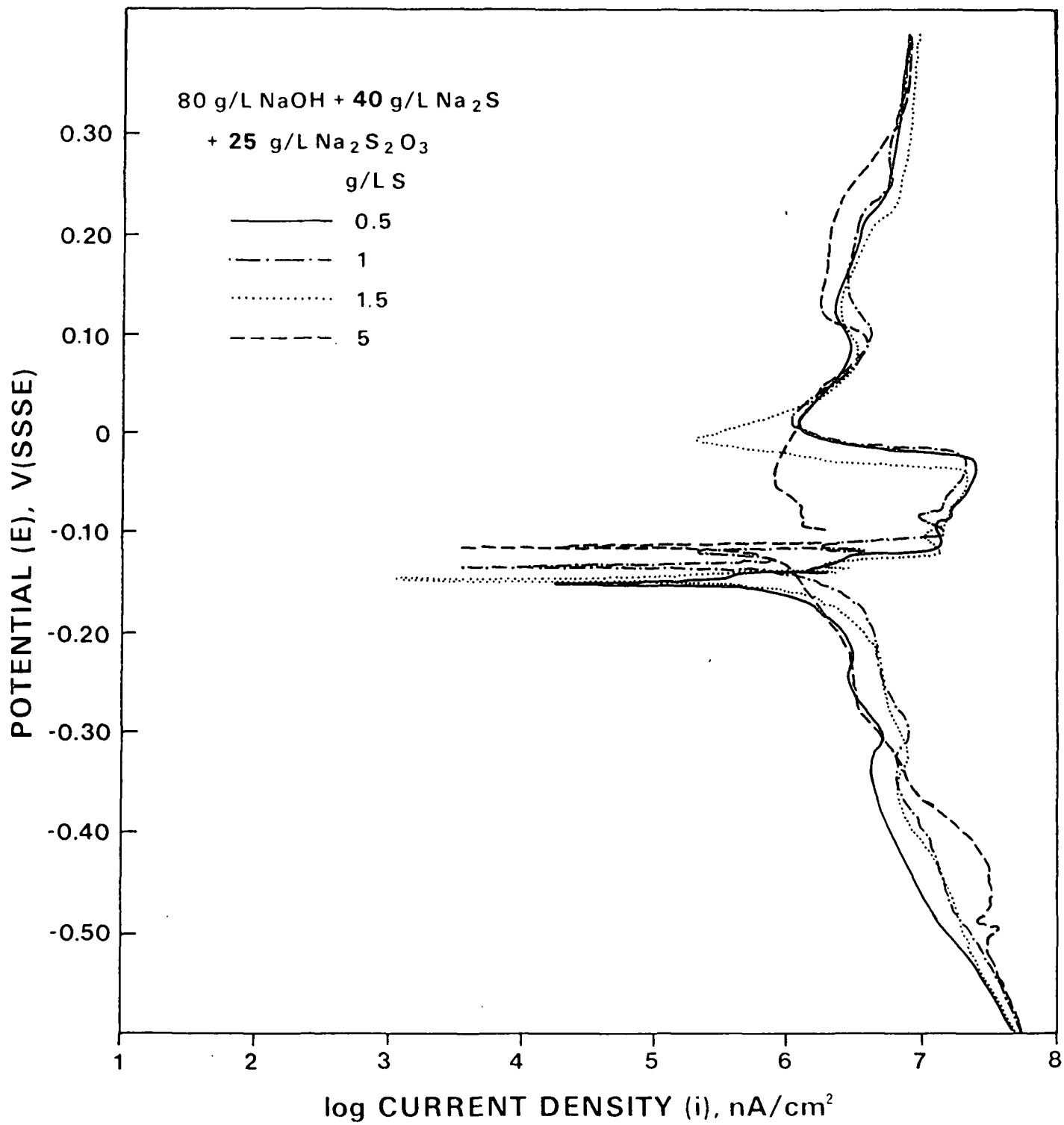


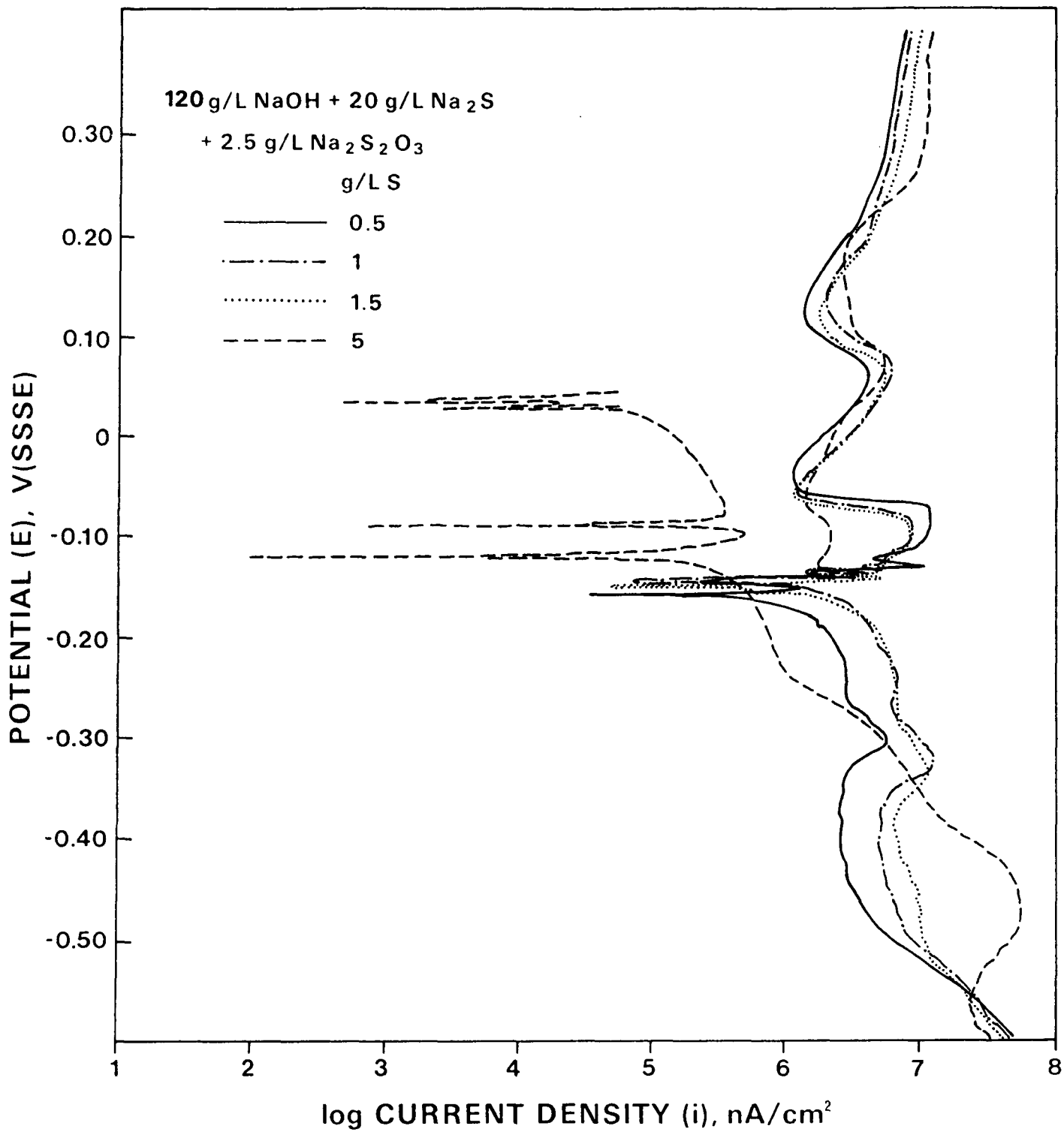


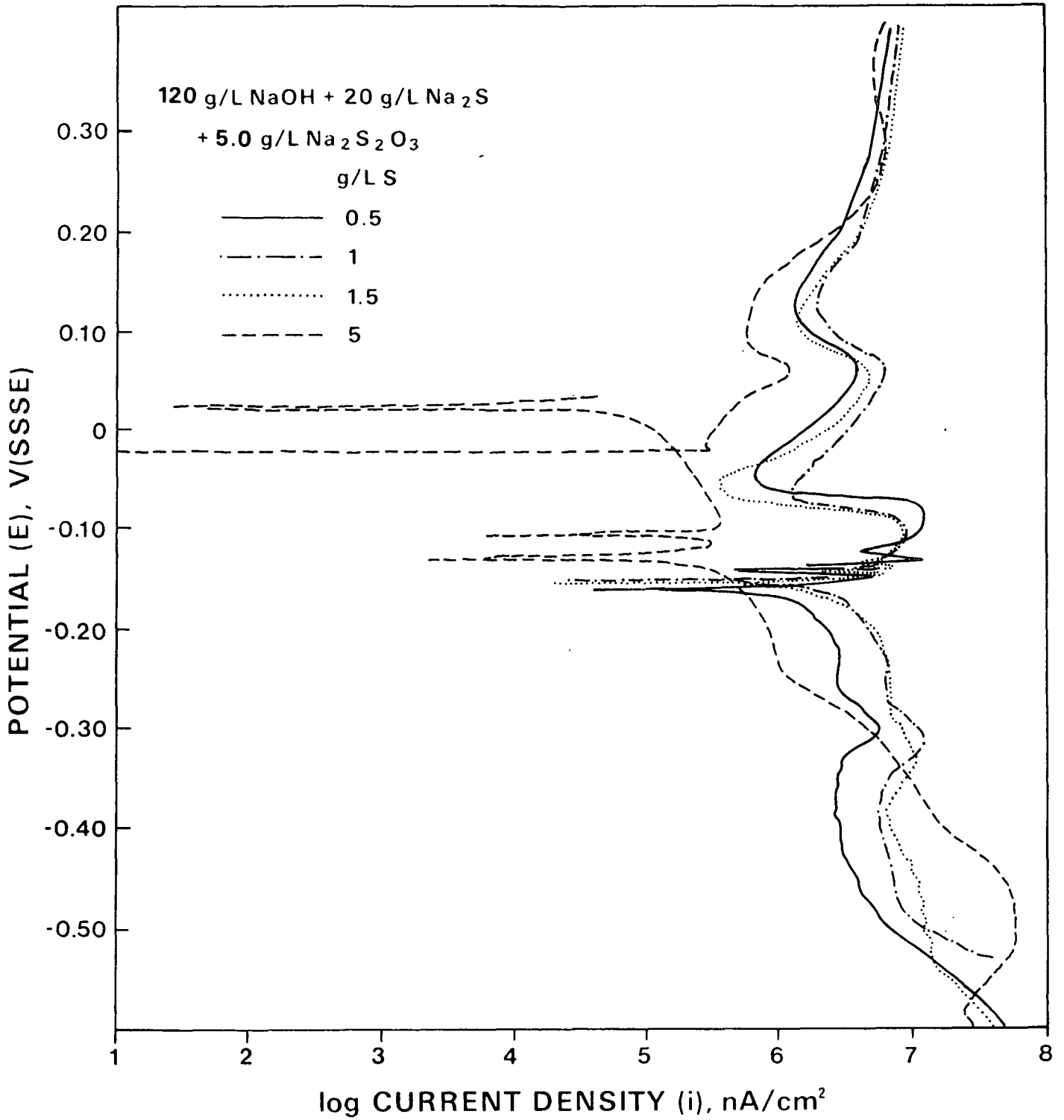


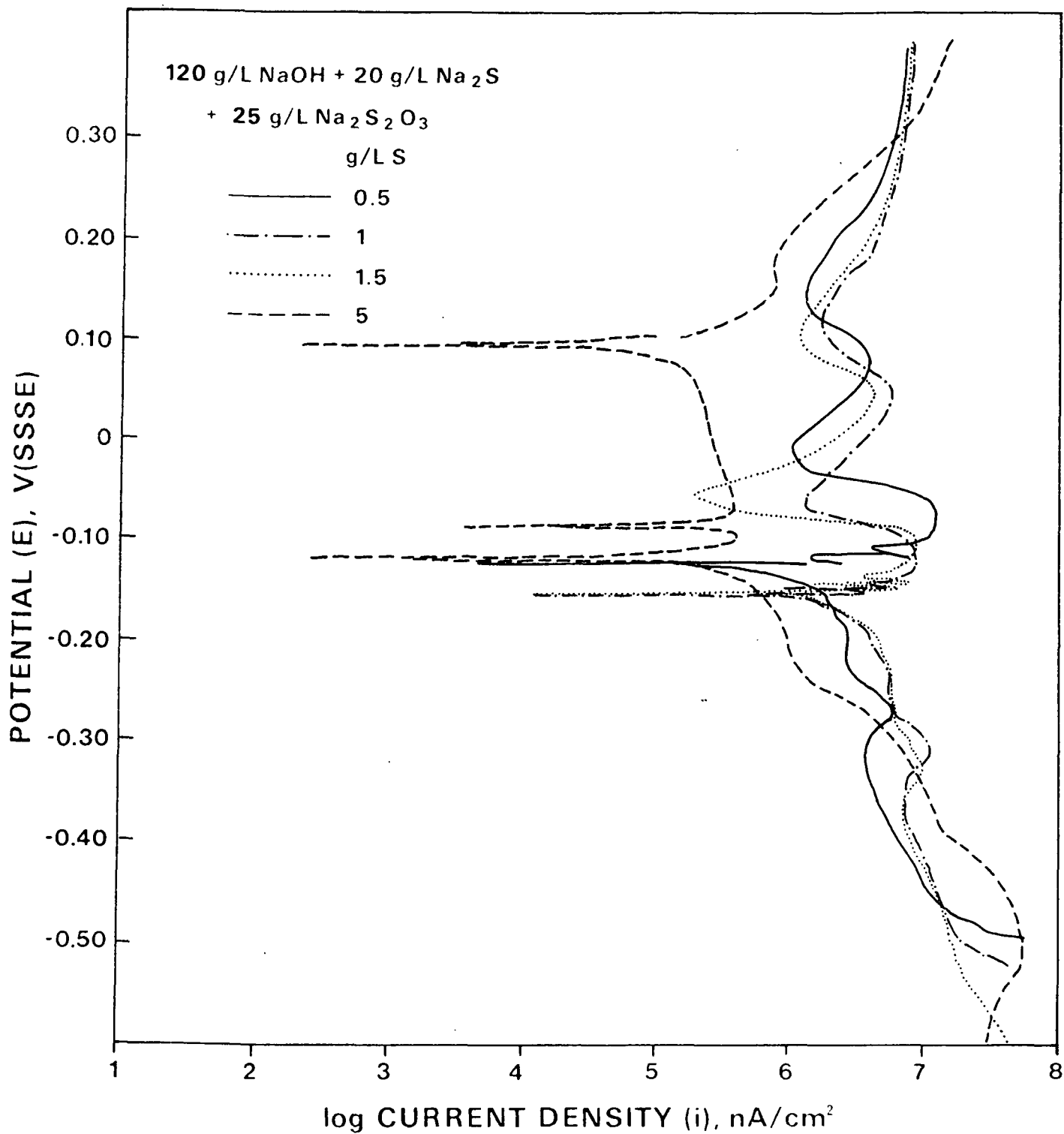


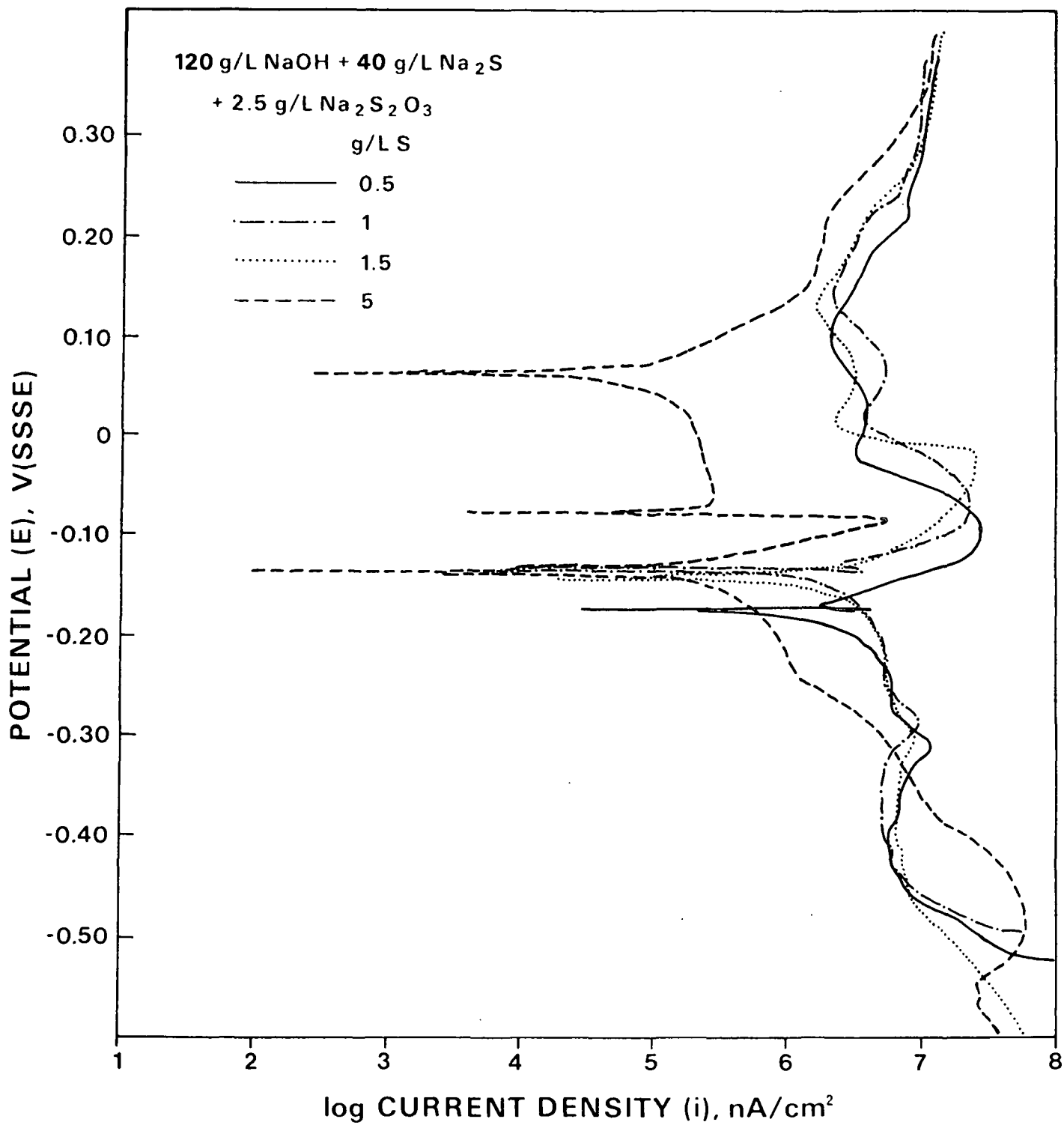


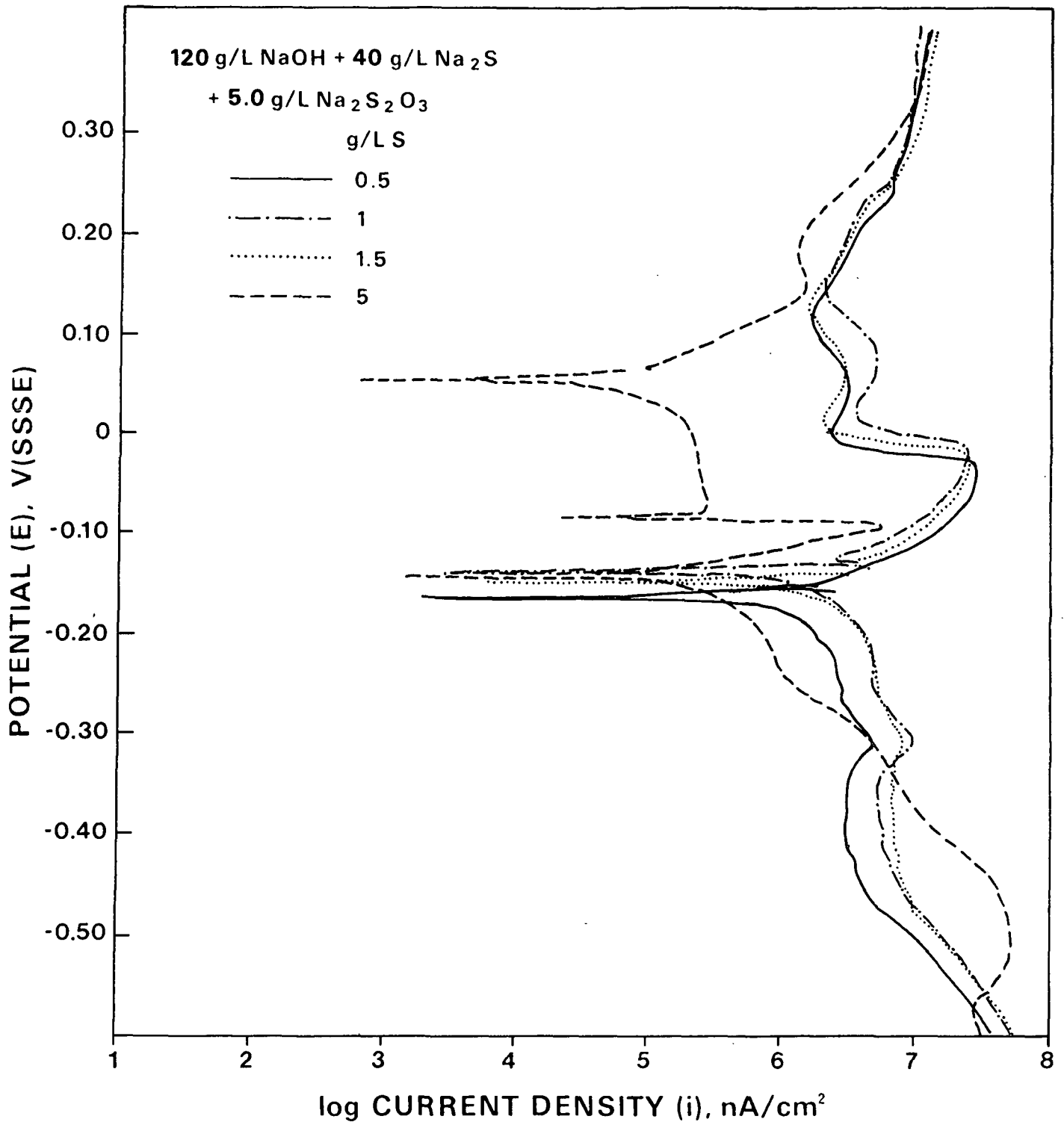




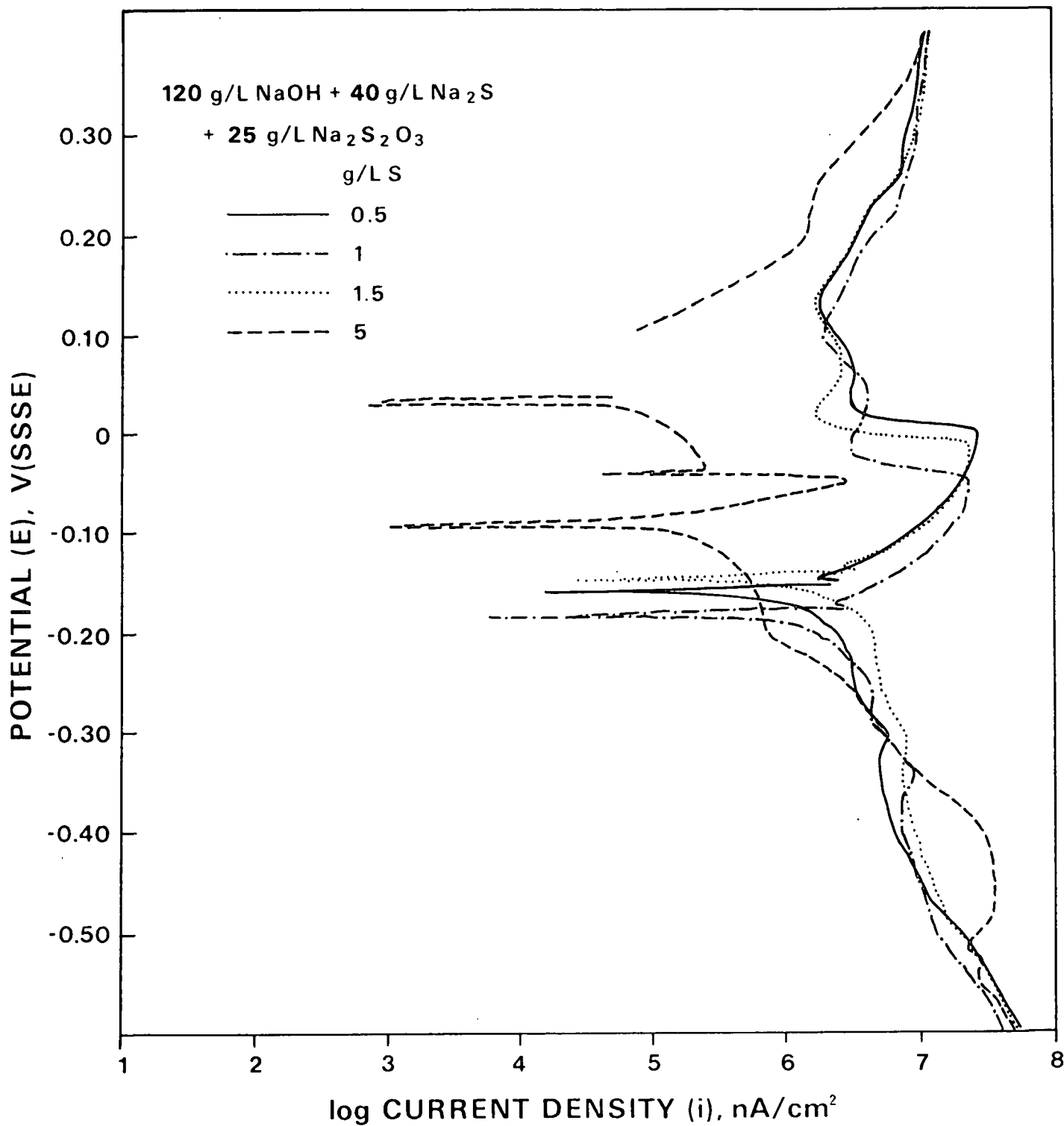








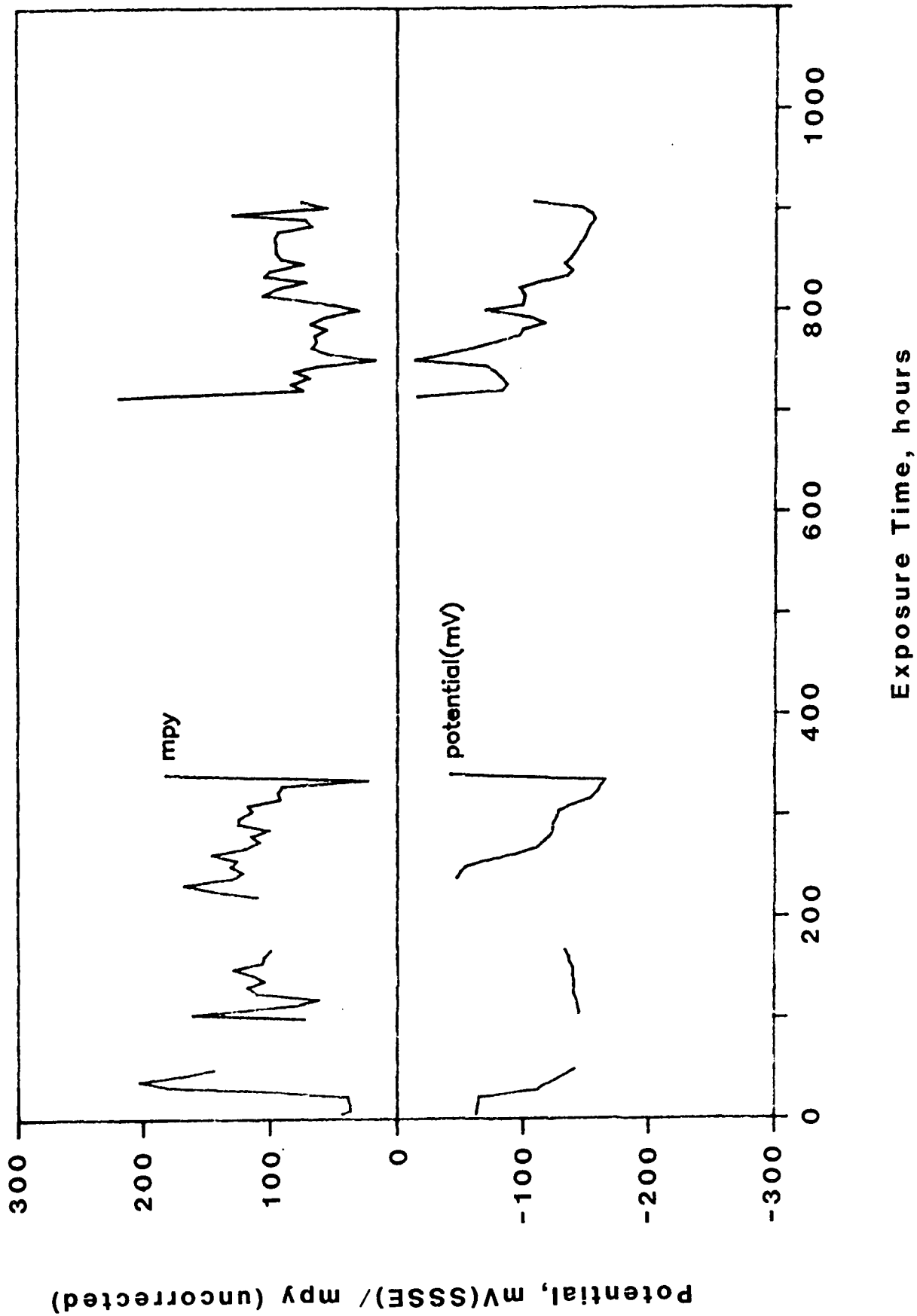




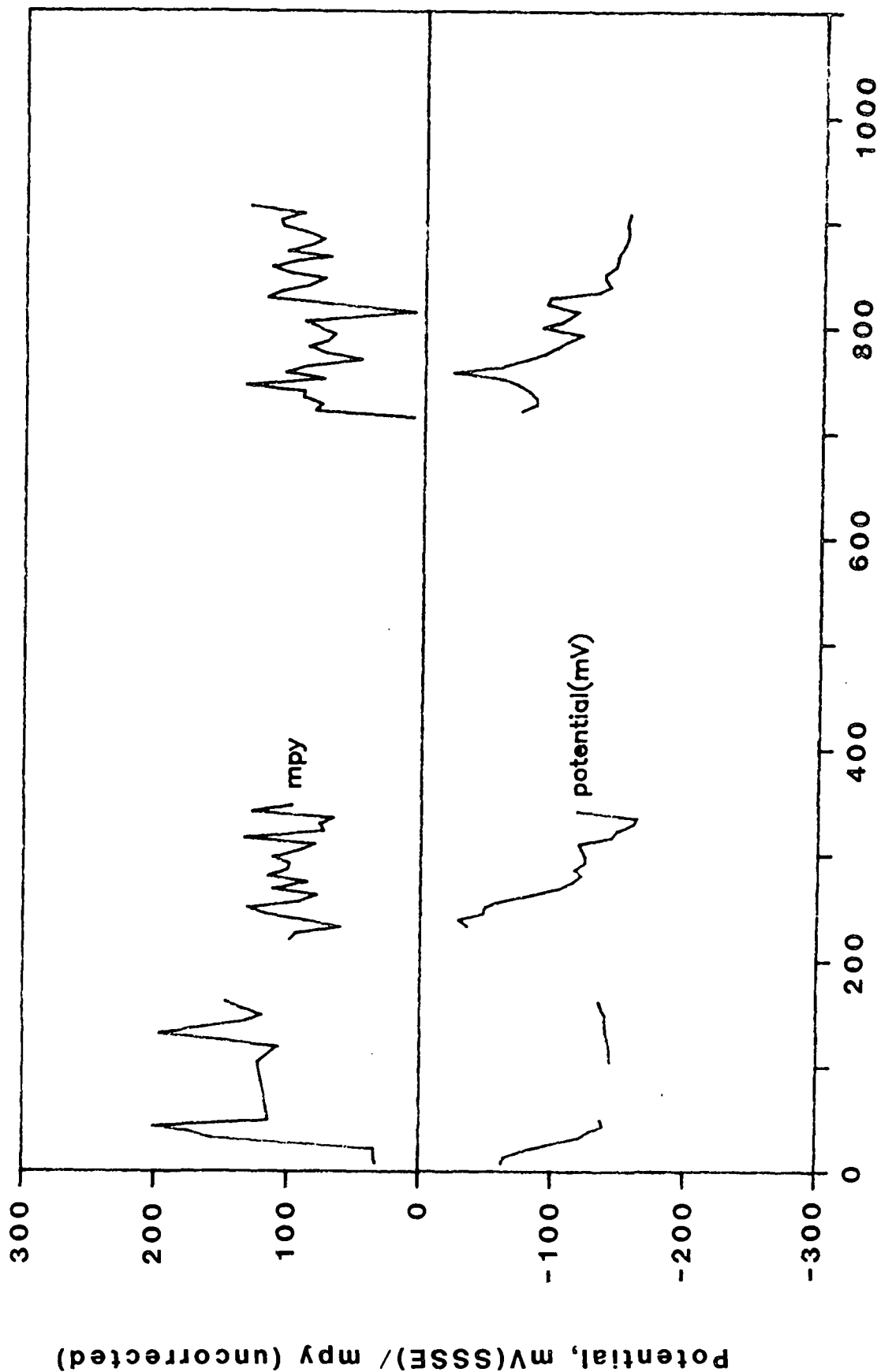
APPENDIX II

CORROSION POTENTIAL AND RATE vs. TIME AT MILLS E8 AND E9

# Mill E8 - 1018 Electrode 1 Anodic

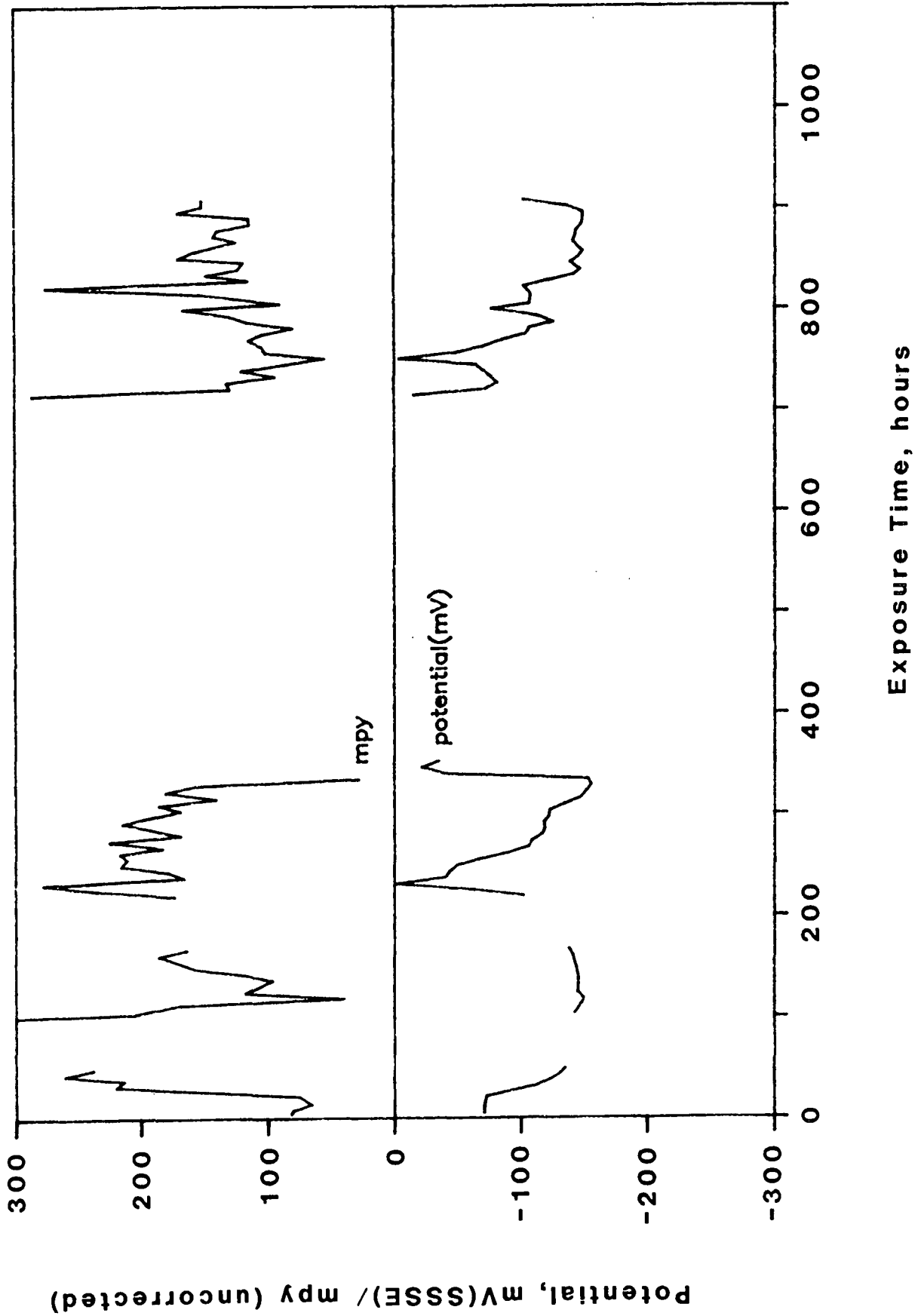


# Mill E8 - 1018 Electrode 1 Cathodic

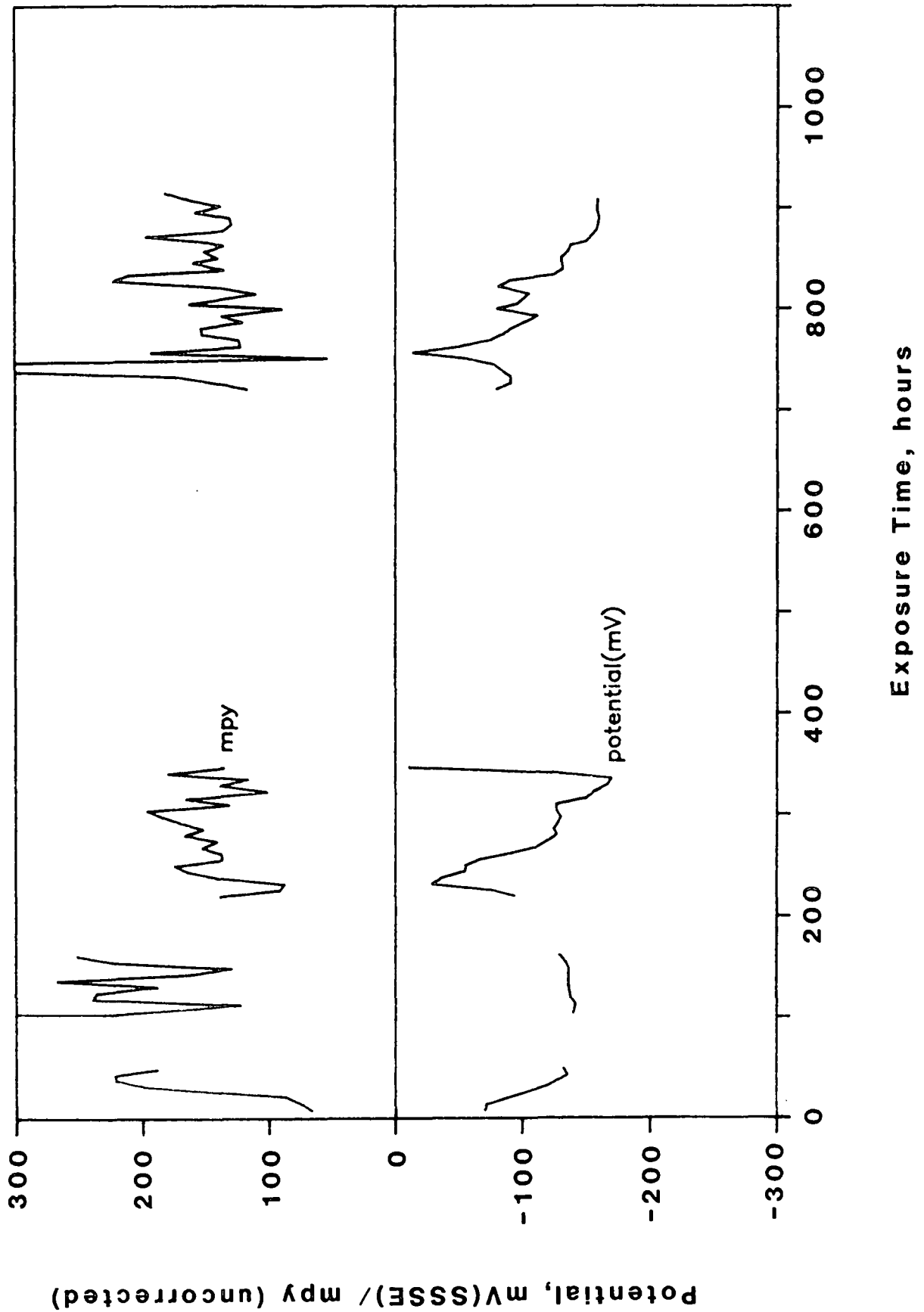


Exposure Time, hours

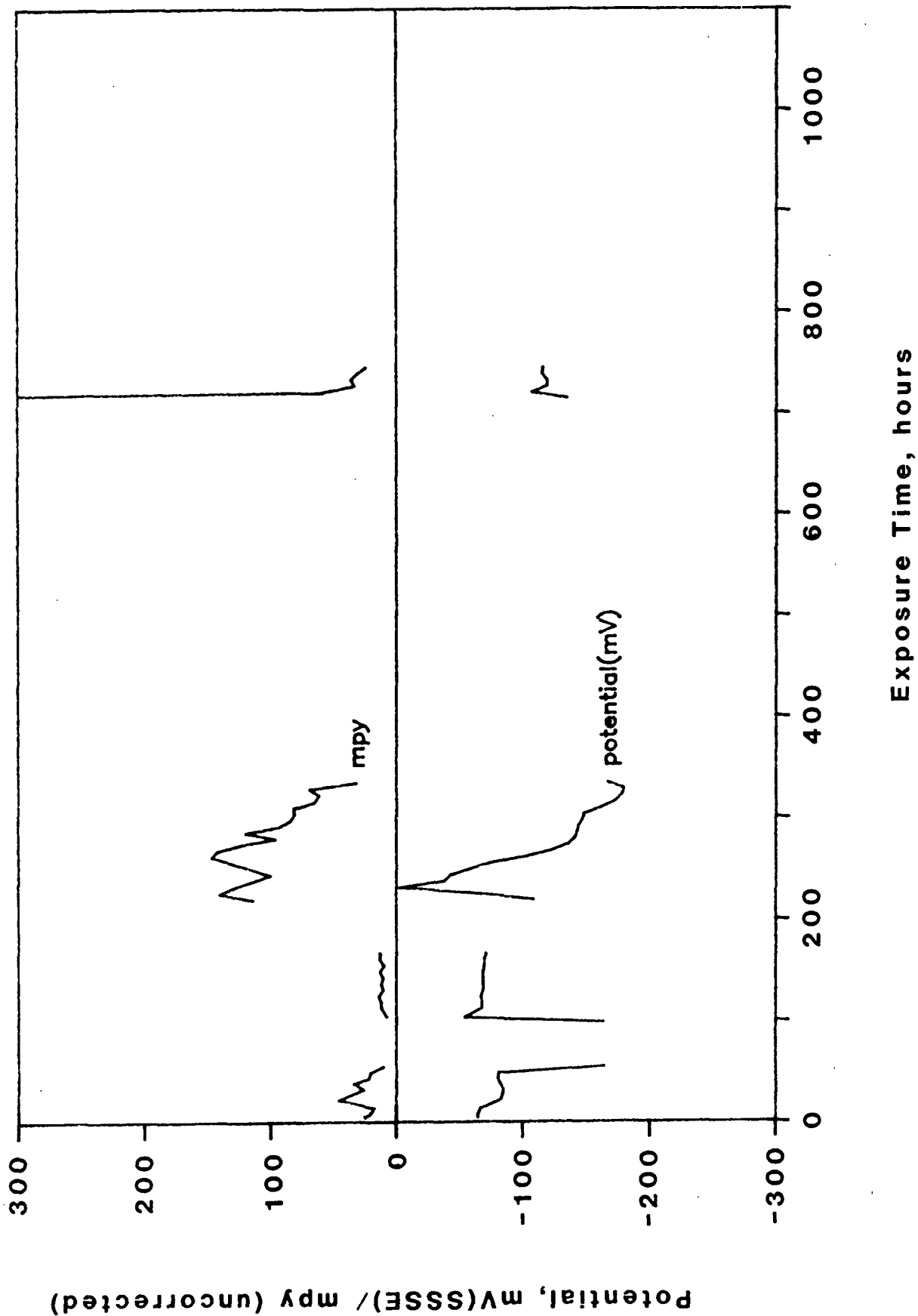
# Mill E8 - A285 Electrode 2 Anodic



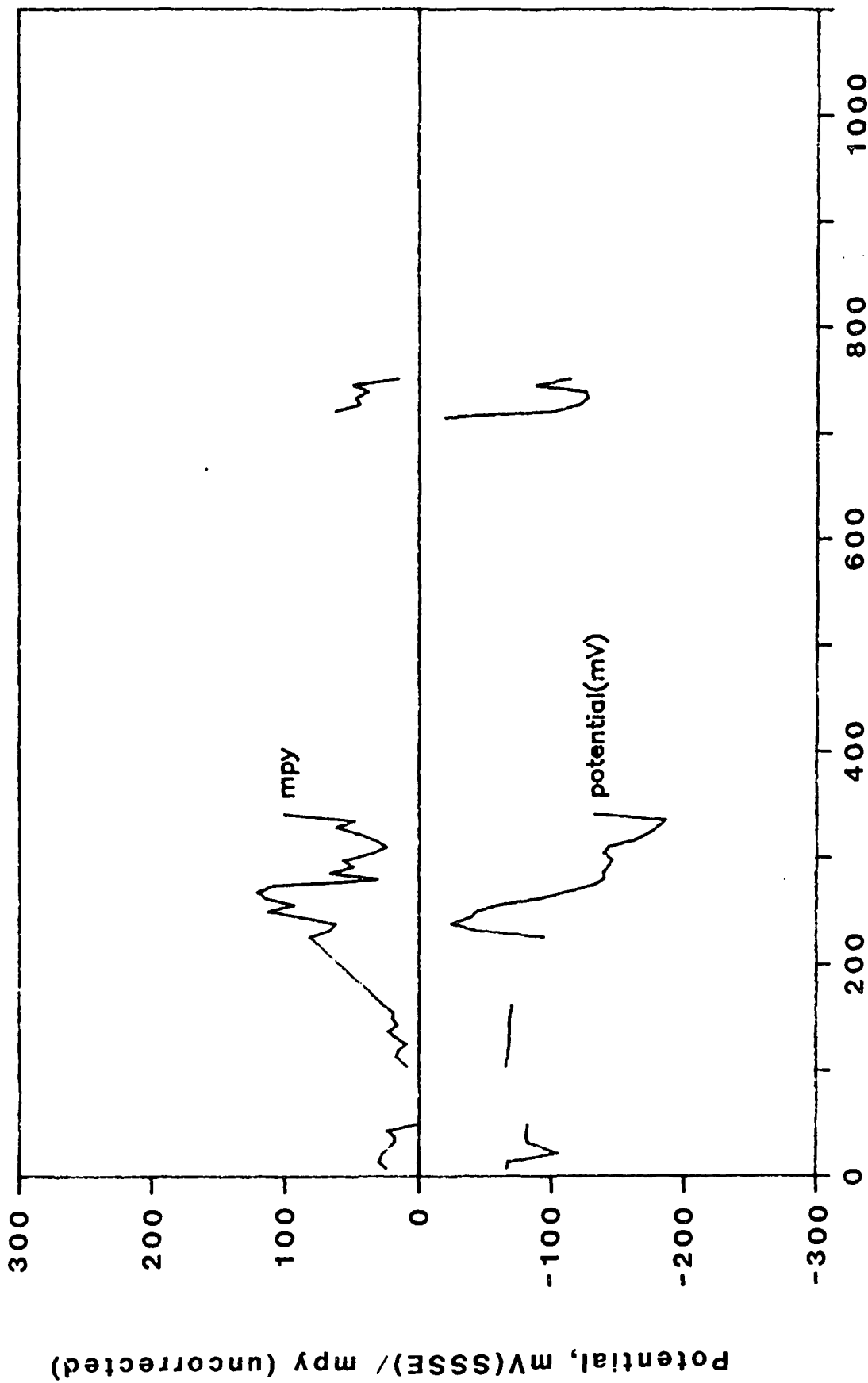
# Mill E8 - A285 Electrode 2 Cathodic



# Mill E8 - A283 Electrode 3 Anodic

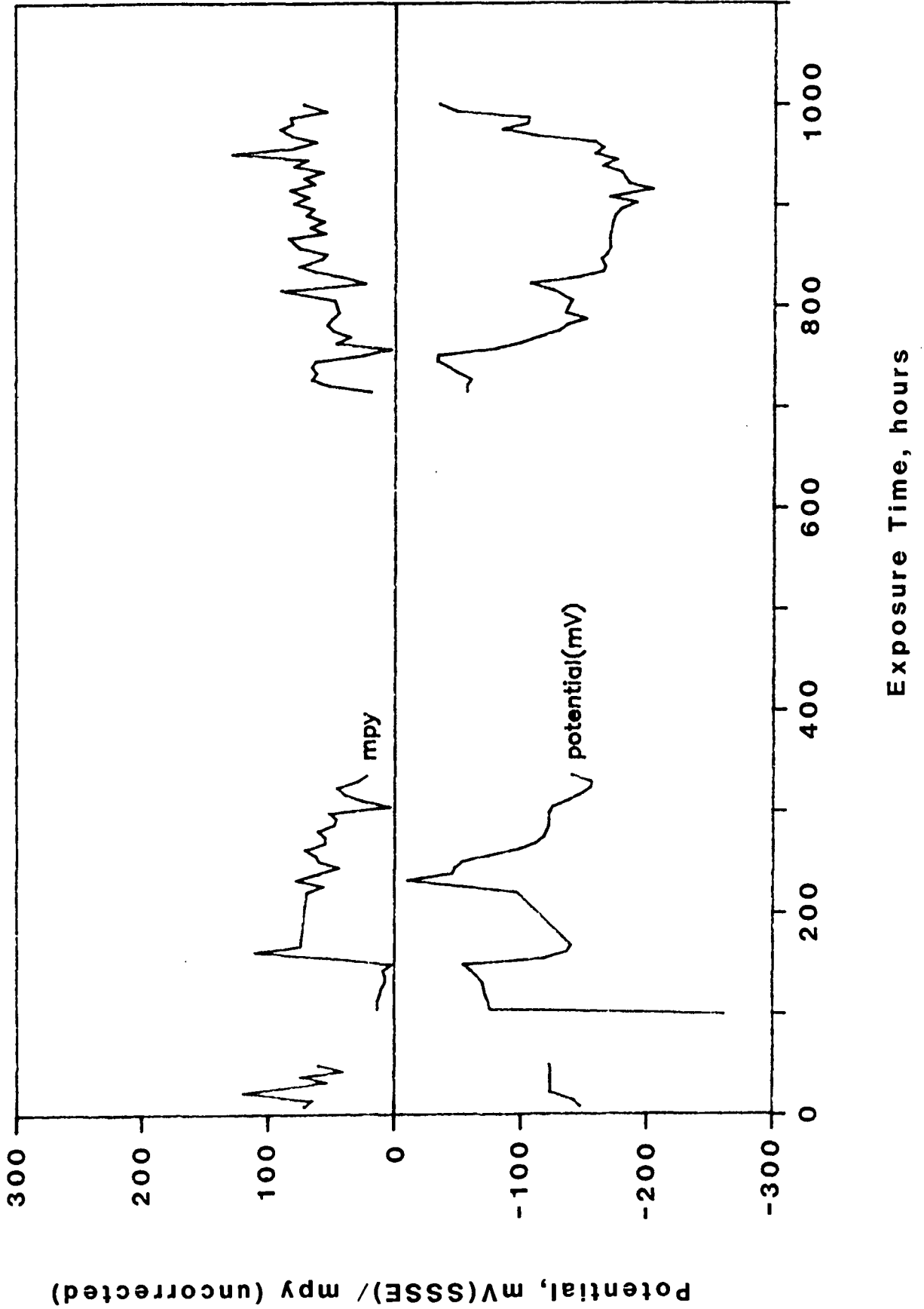


# Mill E8 - A283 Electrode 3 Cathodic

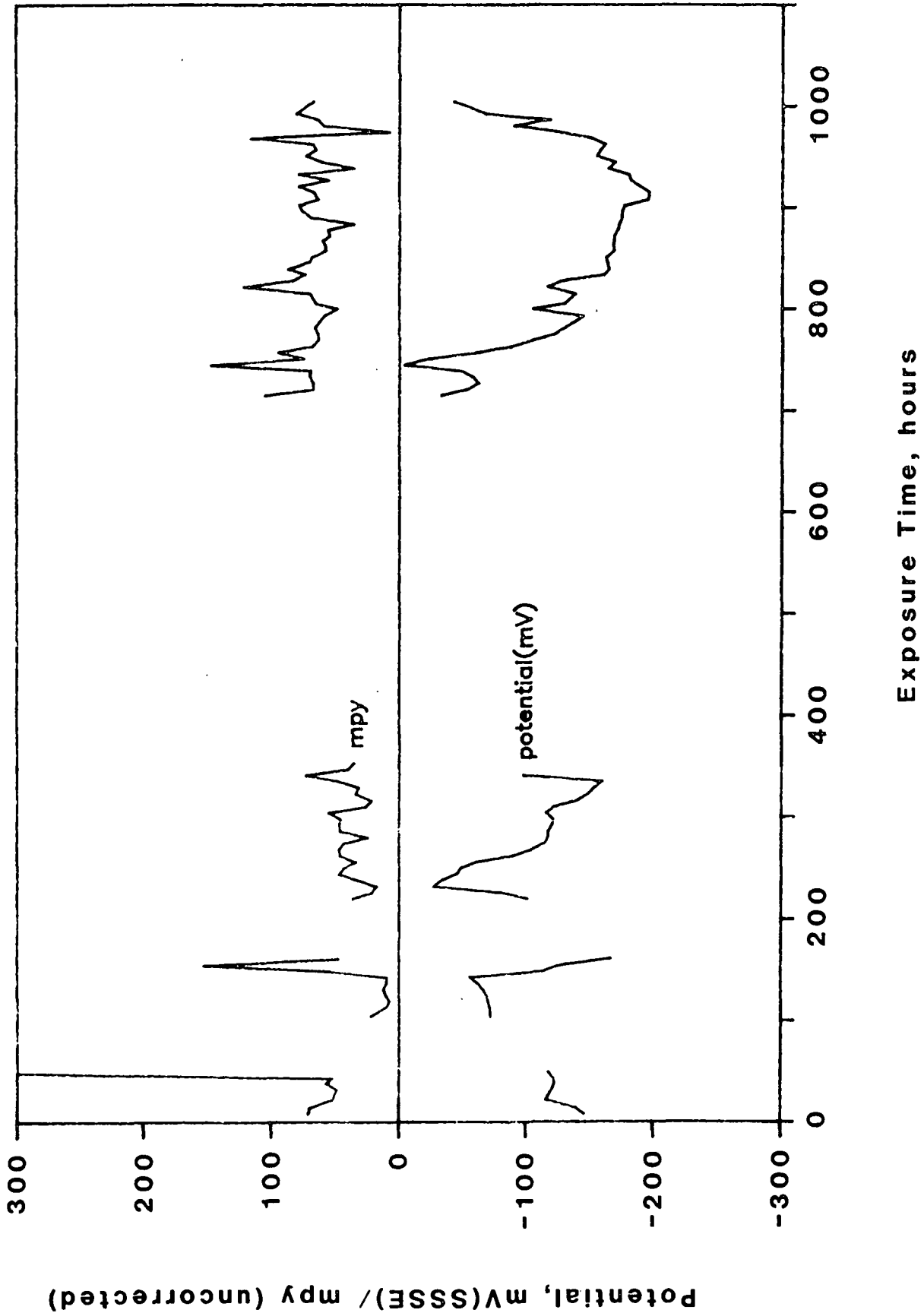




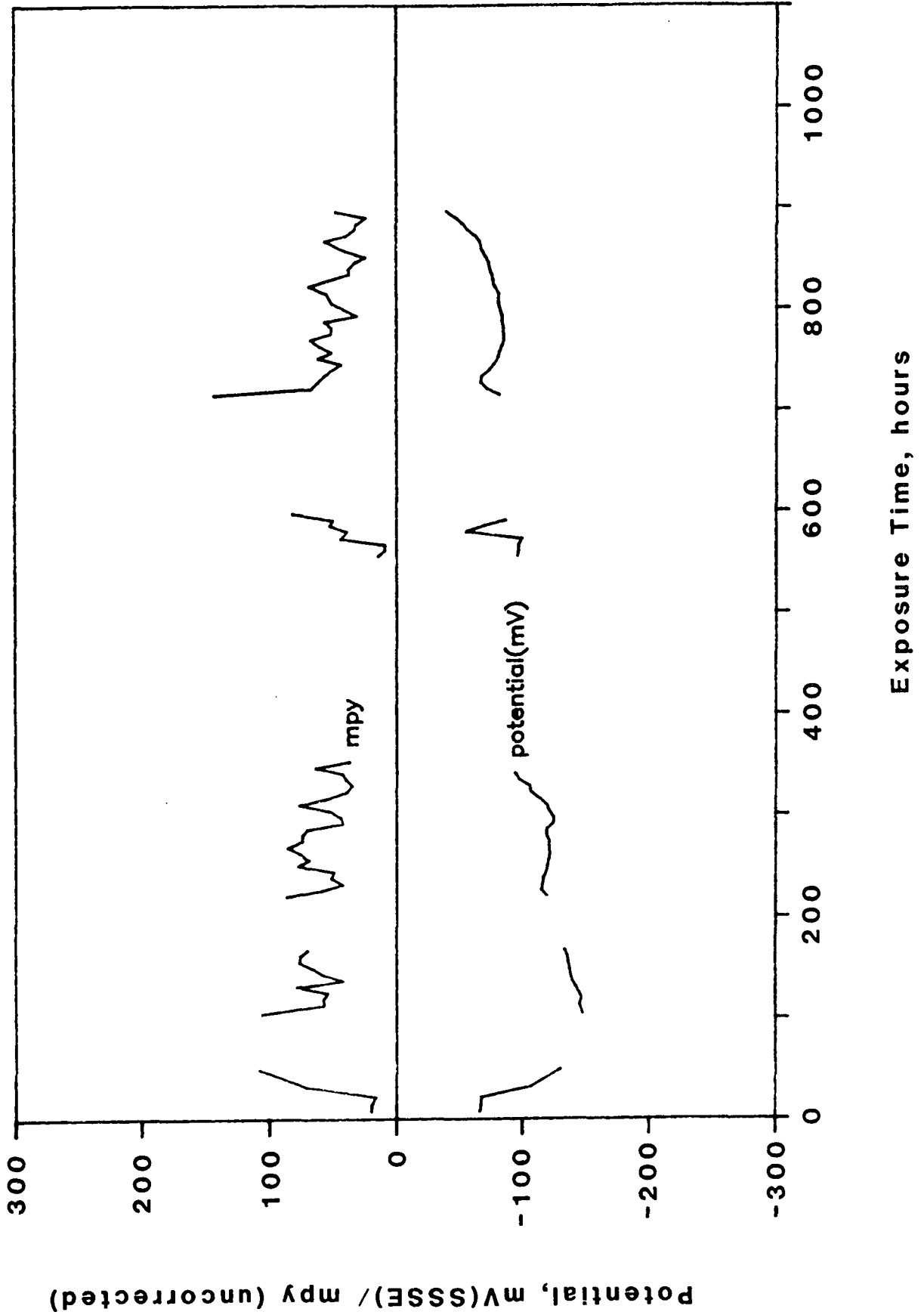
# Mill E8 - A285S Electrode 4 Anodic



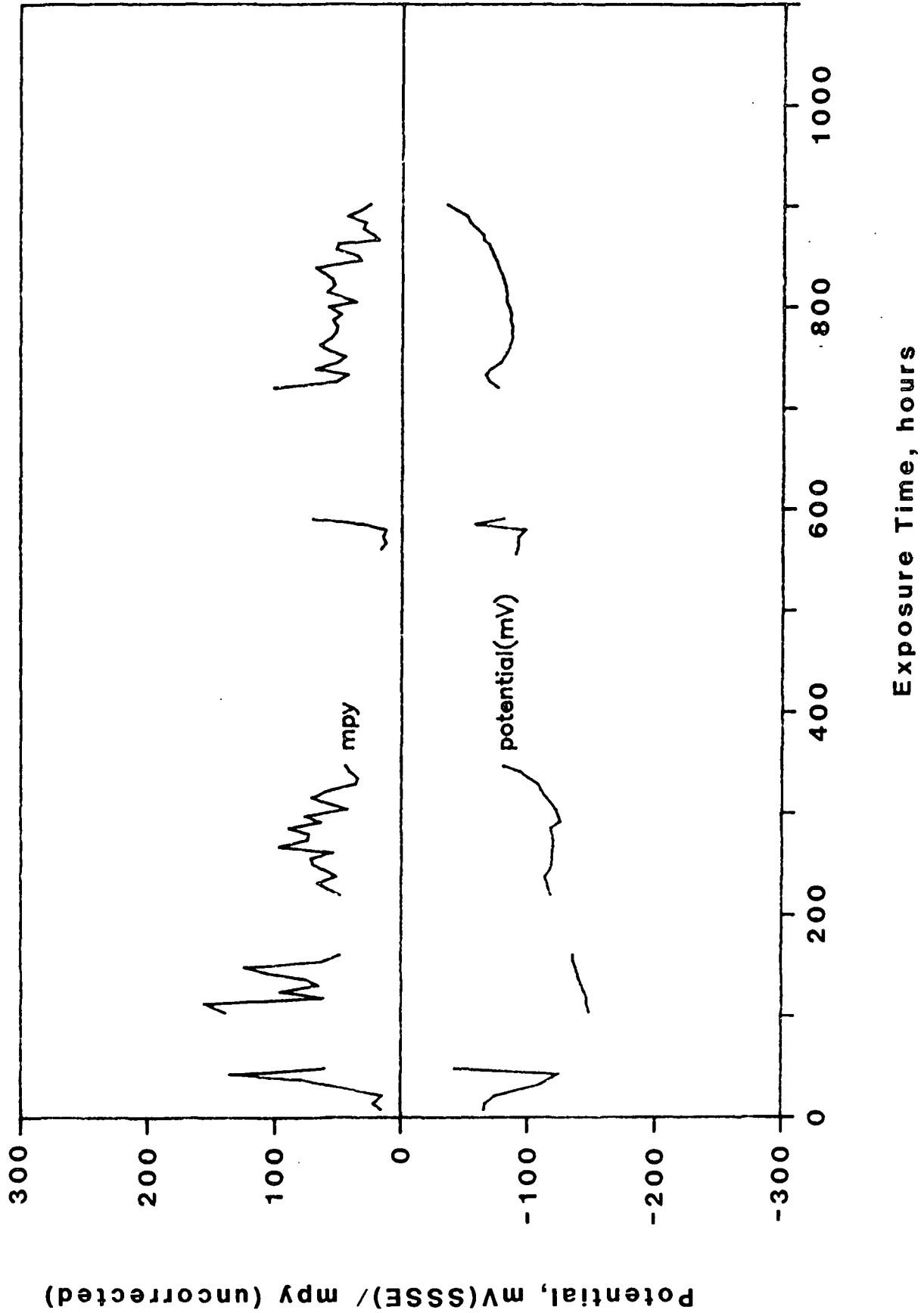
# Mill E8 - A285S Electrode 4 Cathodic



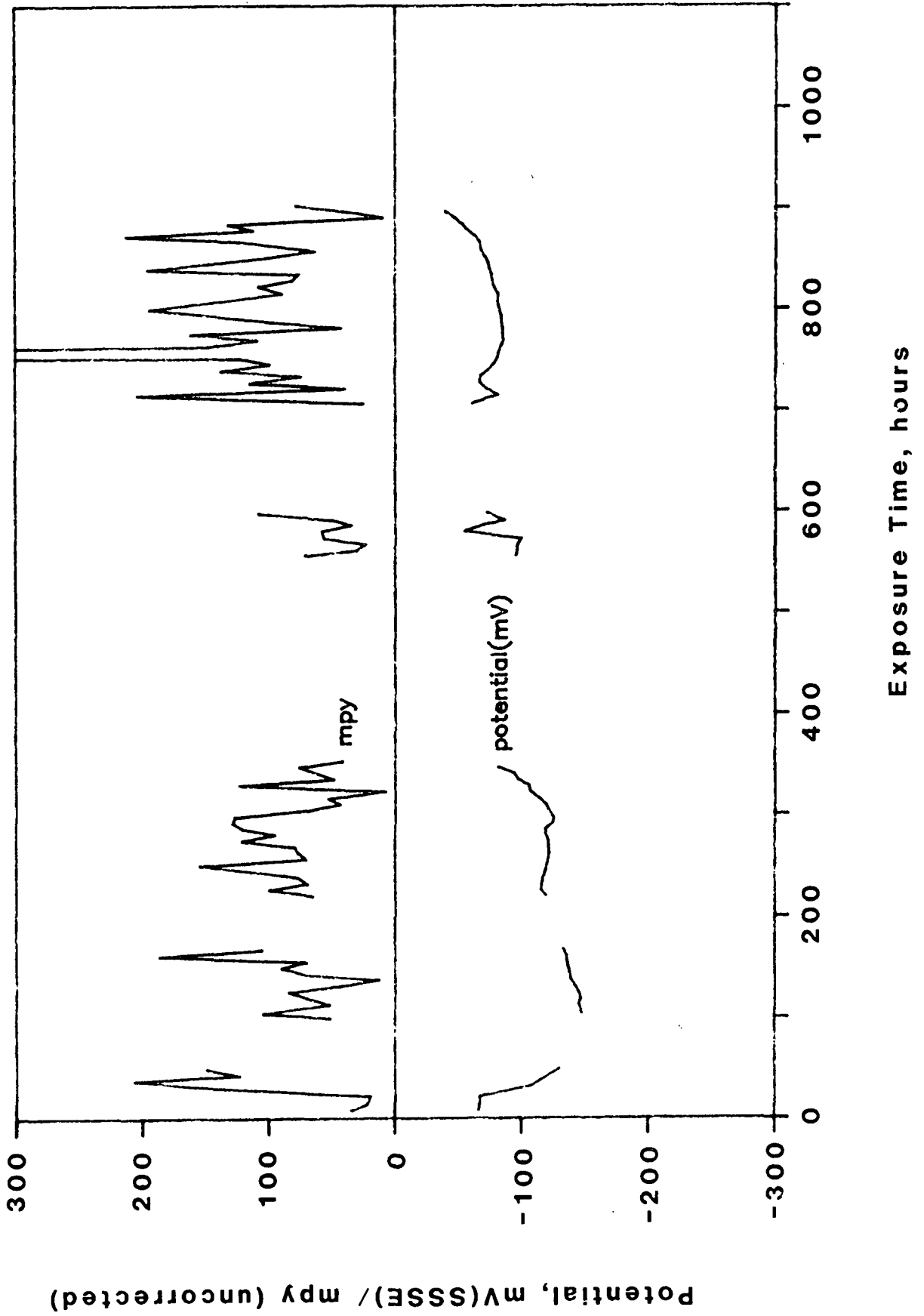
# Mill E8 - 1018 Electrode 5 Anodic



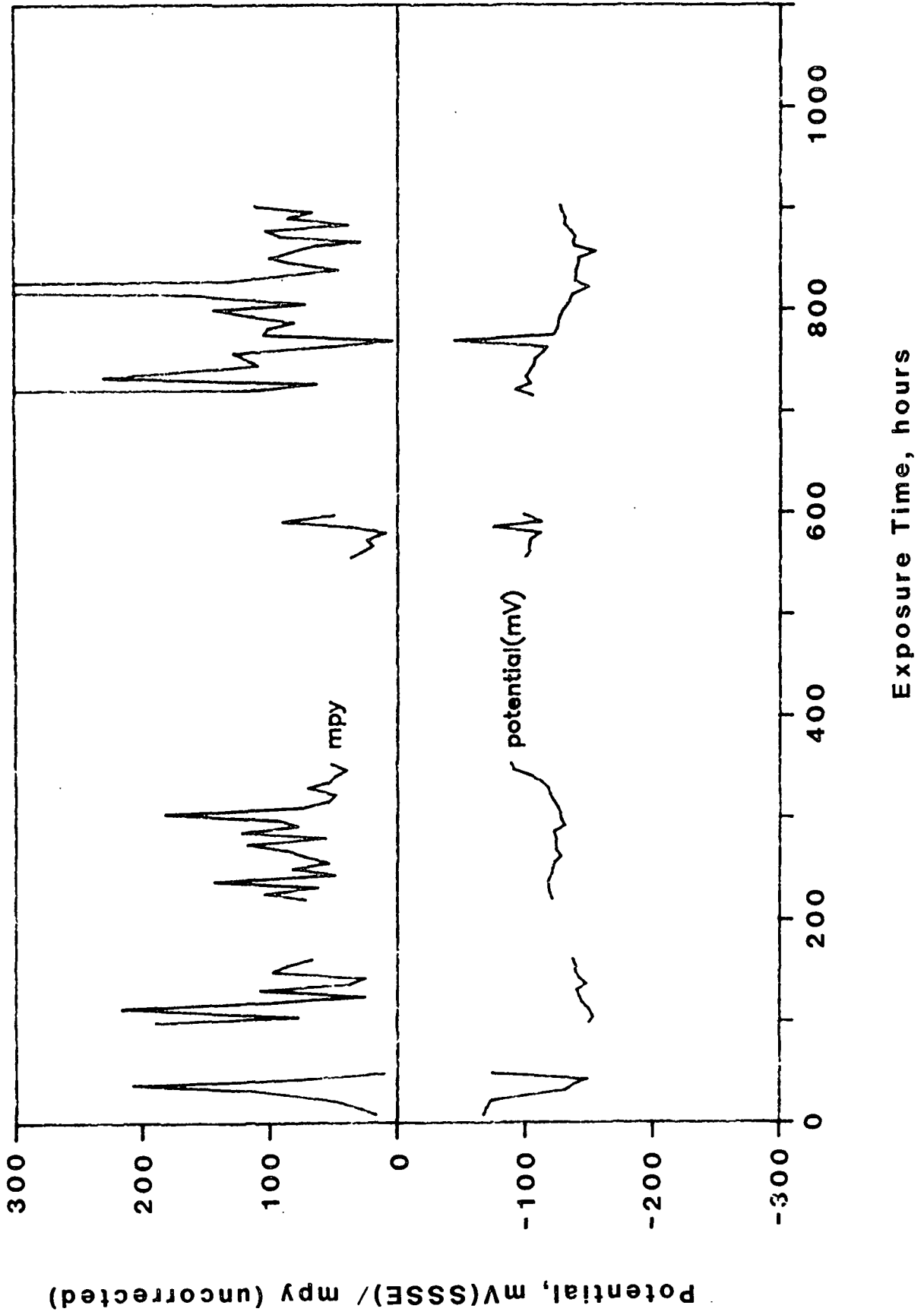
# Mill E8 - 1018 Electrode 5 Cathodic



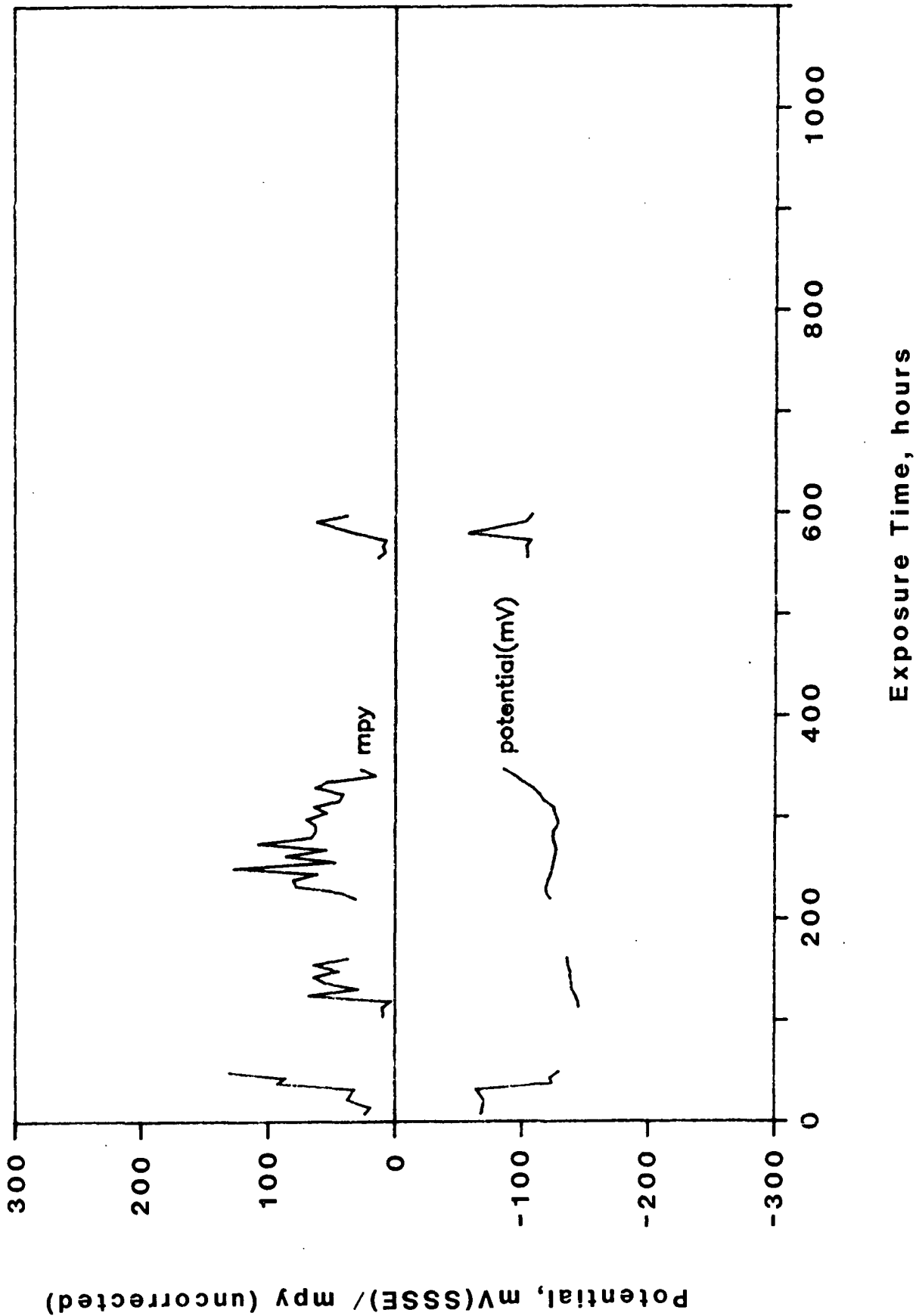
# Mill E8 - A285 Electrode 6 Anodic



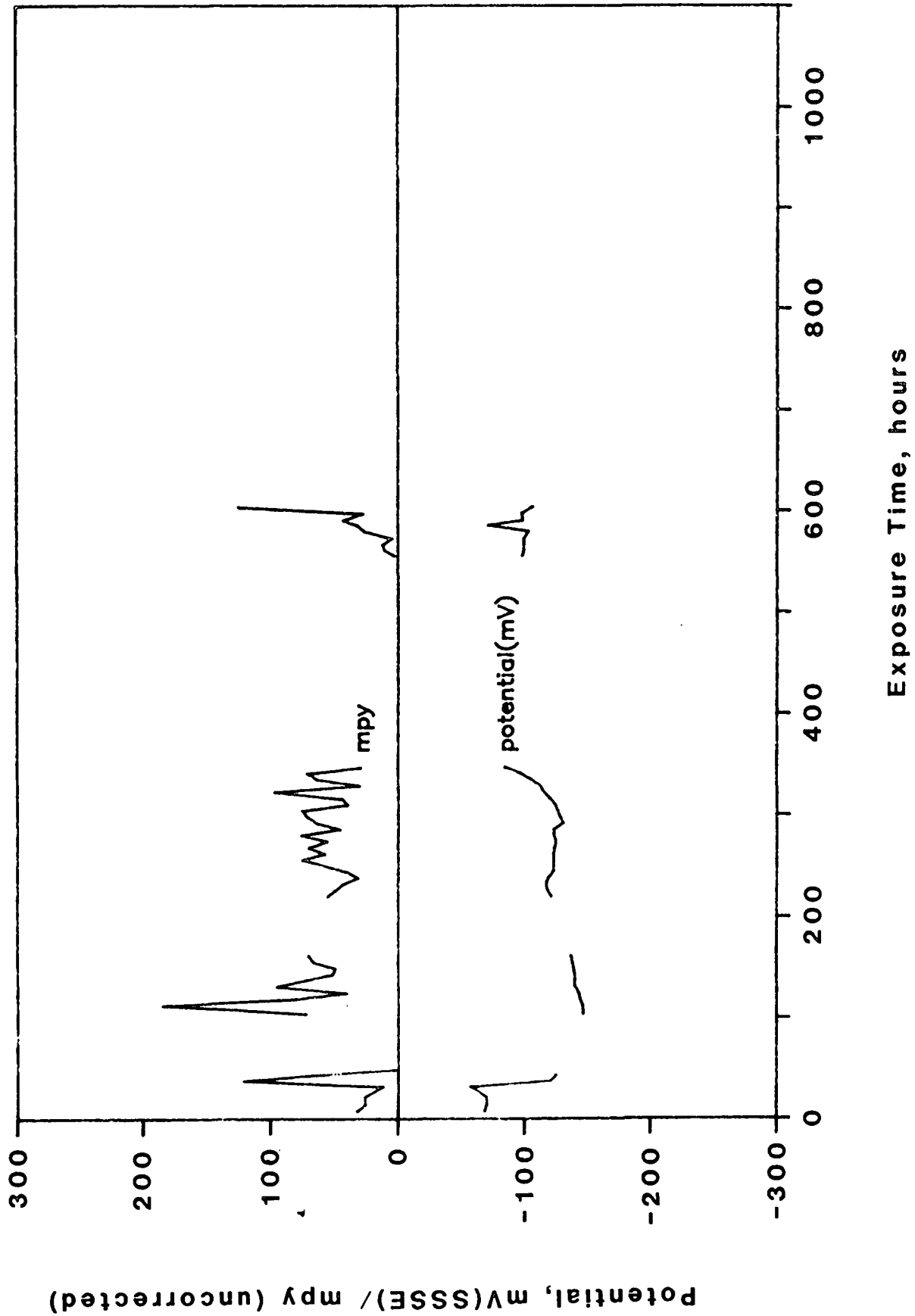
# Mill E8 - A285 Electrode 6 Cathodic



# Mill E8 - A283 Electrode 7 Anodic

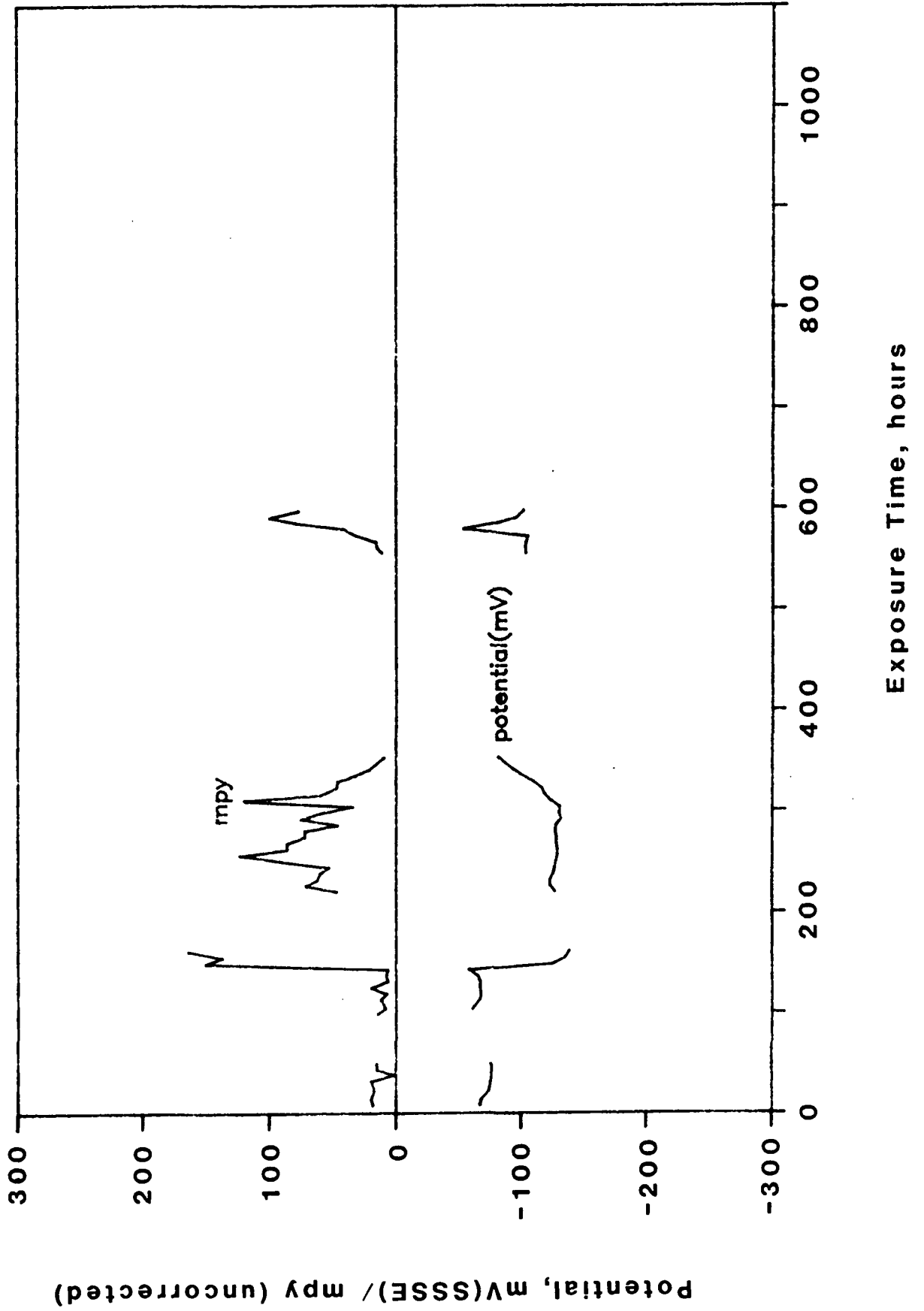


# Mill E8 - A283 Electrode 7 Cathodic

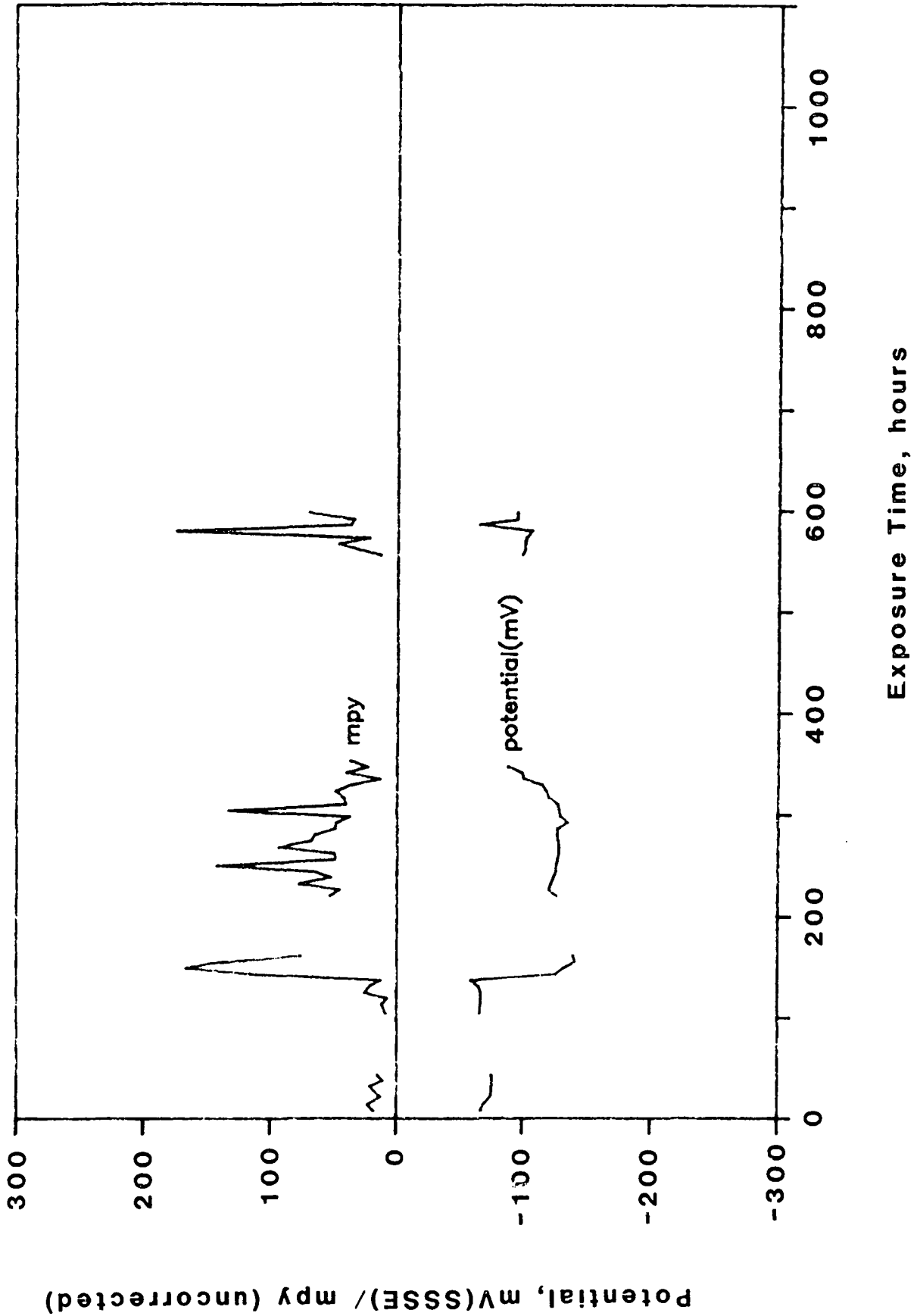




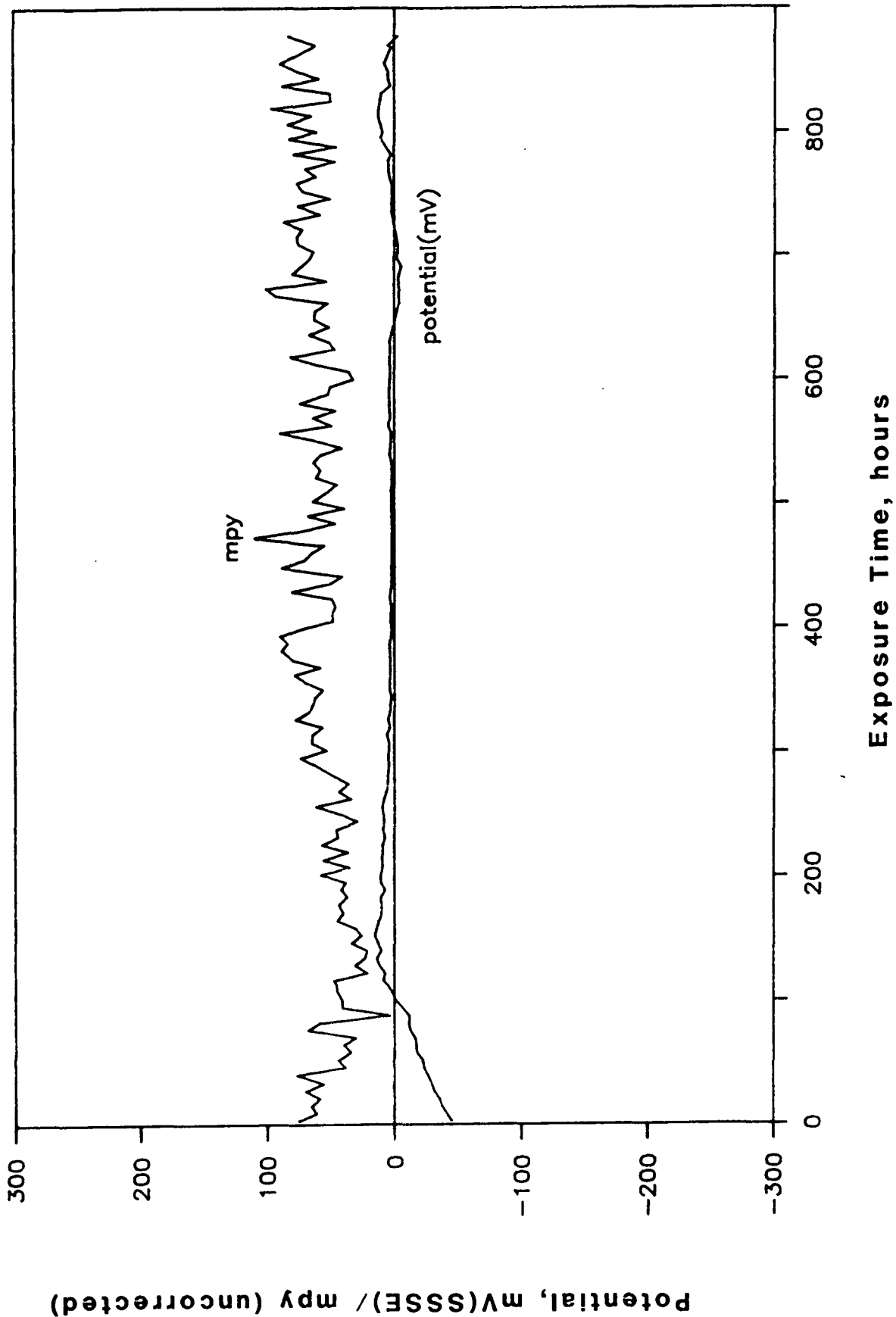
# Mill E8 - A285S Electrode 8 Anodic



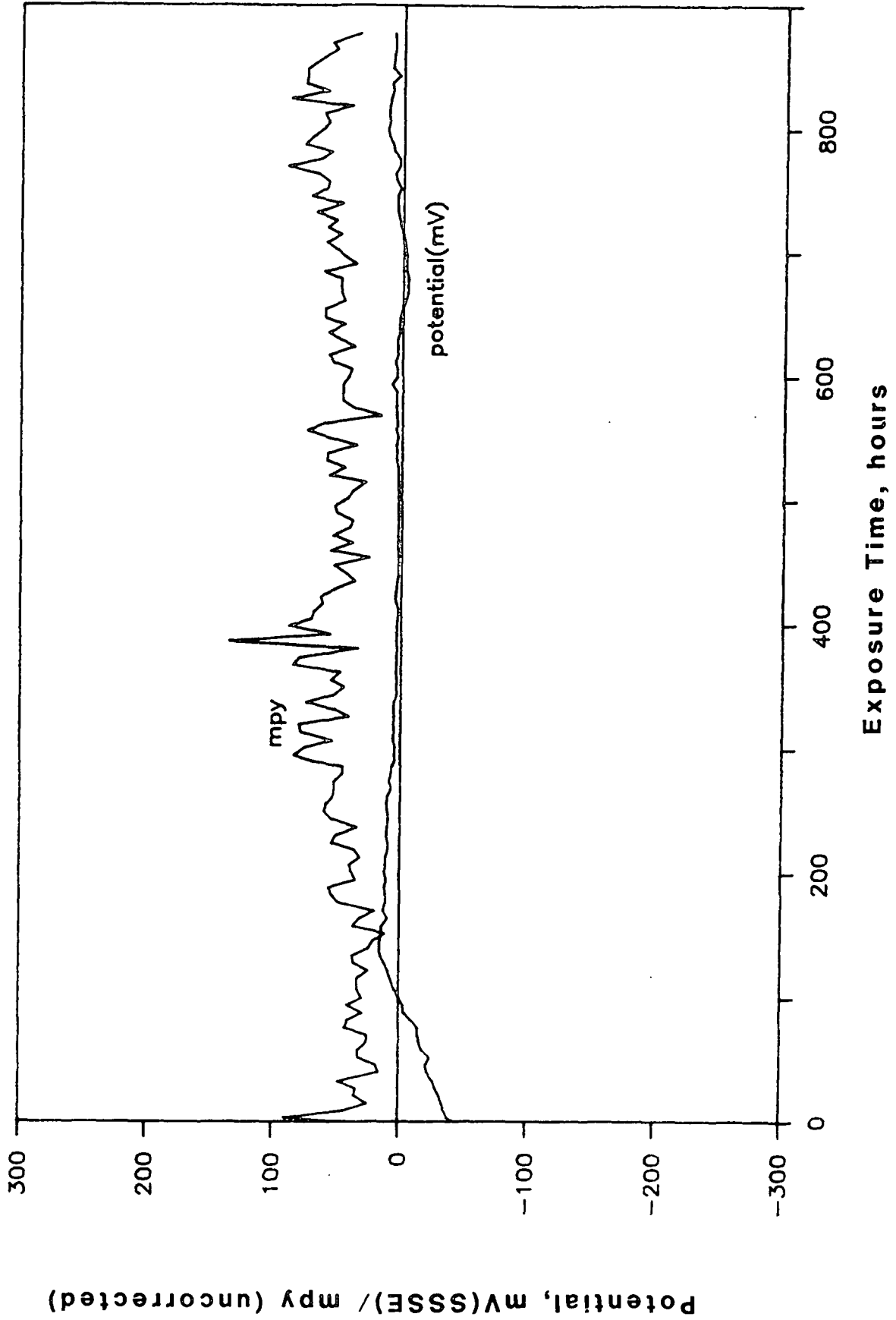
# Mill E8 - A285S Electrode 8 Cathodic



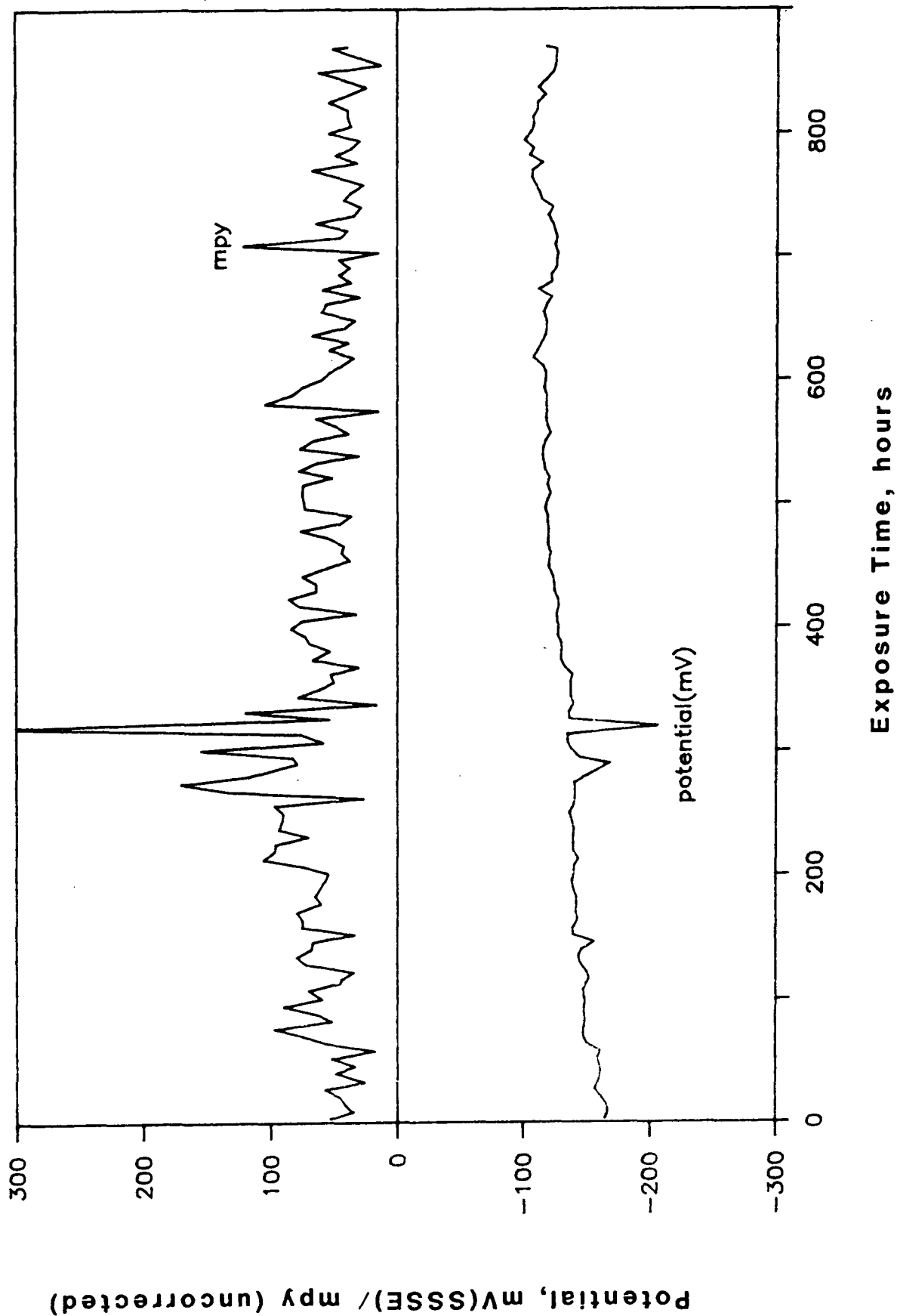
# Mill E9 - 1018 Electrode 1 Anodic



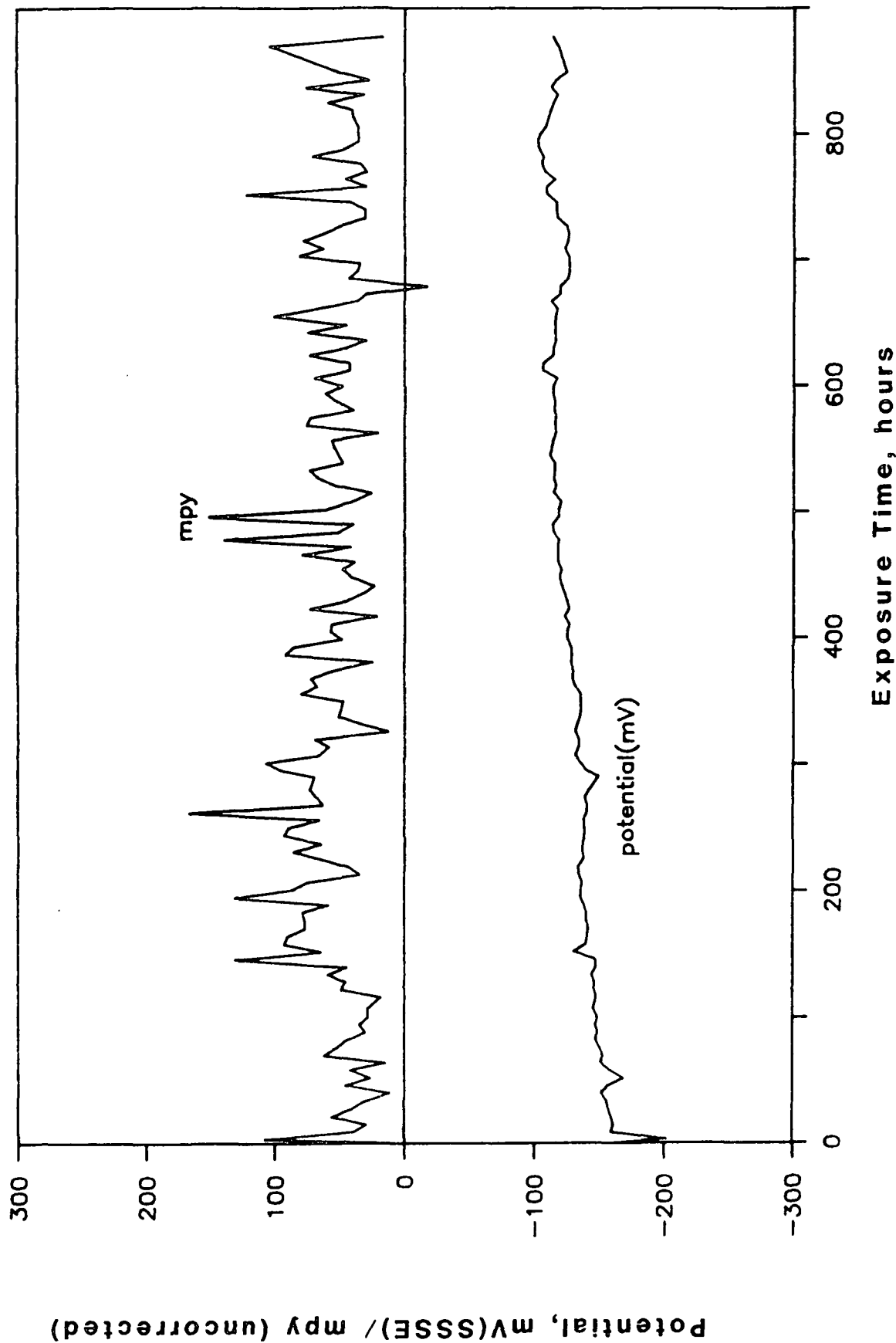
# Mill E9 - 1018 Electrode 1 Cathodic



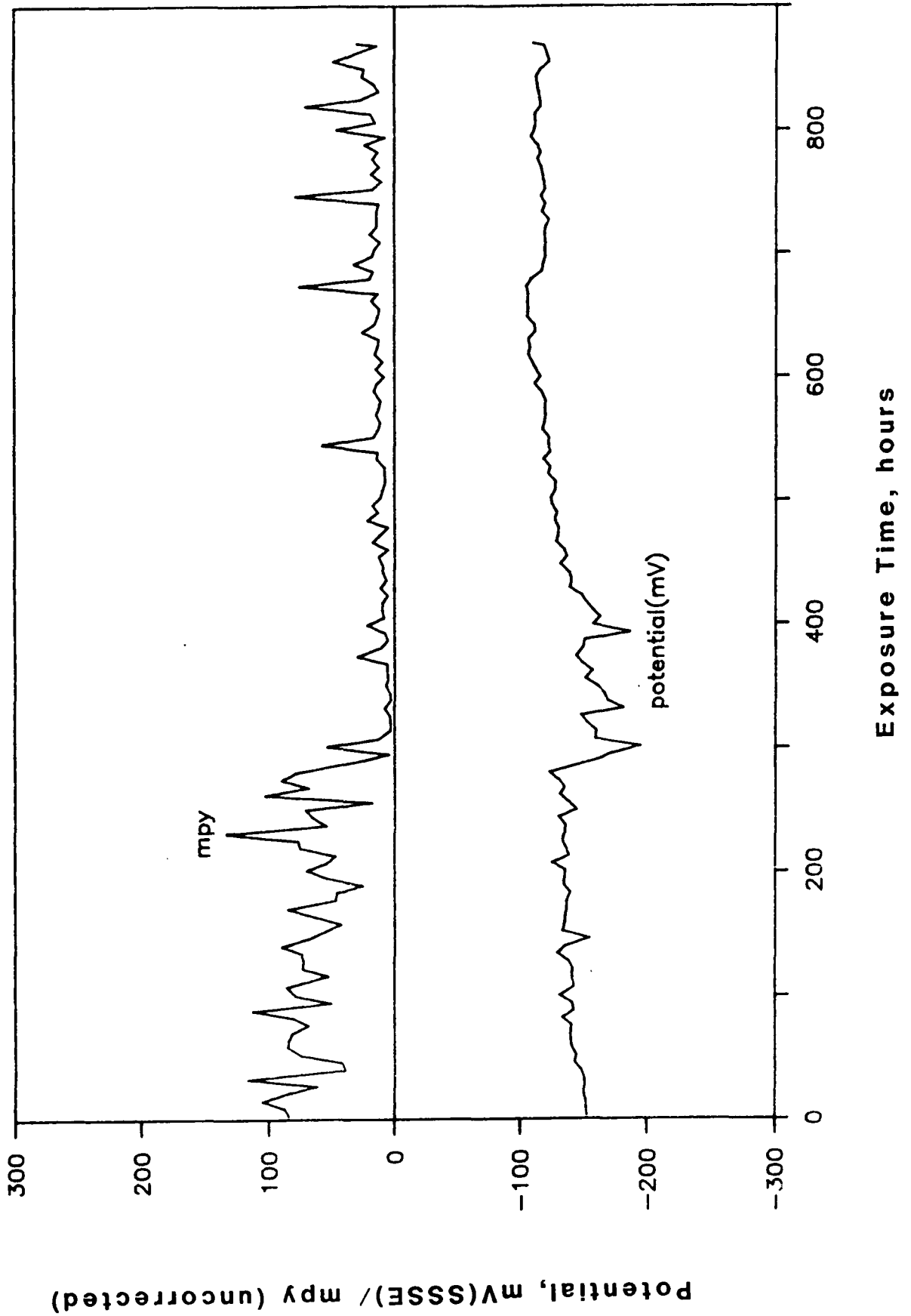
# Mill E9 - A285 Electrode 6 Anodic



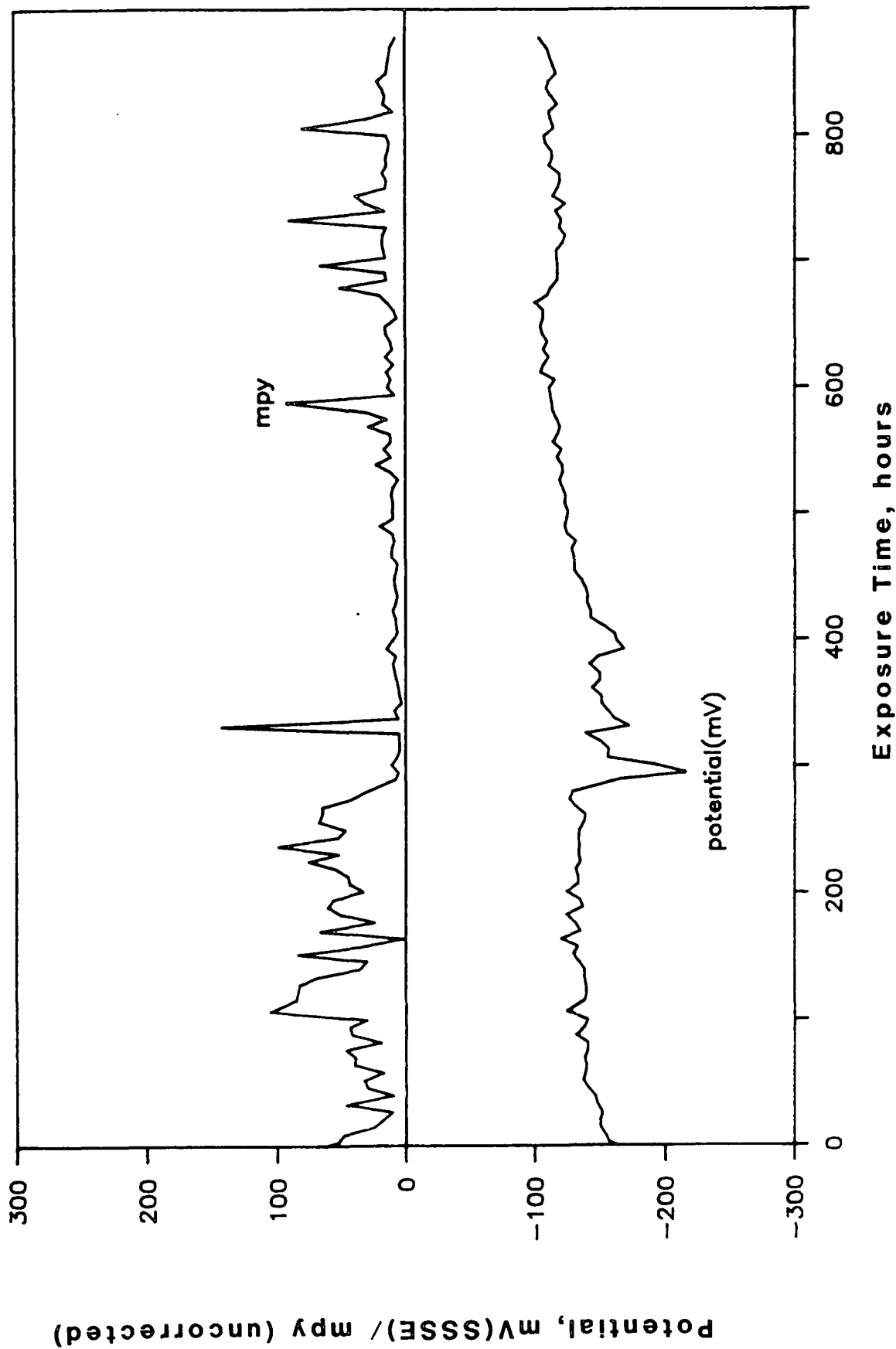
# Mill E9 - A285 Electrode 6 Cathodic



# Mill E9 - A285S Electrode 8 Anodic



# Mill E9 - A285S Electrode 8 Cathodic





THE INSTITUTE OF PAPER CHEMISTRY  
Appleton, Wisconsin

Status Report  
to the  
ENGINEERING PROJECT ADVISORY COMMITTEE

Project 3607  
EVALUATION OF STRUCTURAL COATINGS FOR PULP AND PAPER MILL SERVICE

October 22, 1986

## PROJECT SUMMARY FORM

DATE: September 20, 1986

PROJECT NO. 3607 - Evaluation of Structural Coatings for Pulp and Paper Mill Service

## IPC GOAL.

Increase the useful life of equipment by proper selection of materials of construction and by identifying suitable process conditions.

## OBJECTIVE:

Identify structural coatings which will offer optimal performance in challenging pulp and paper mill applications

BUDGET: \$25,000

## SUMMARY OF RESULTS:

This is a new project started in July, 1986. Plans have been made to prepare and expose standard coated coupons in the recovery, bleaching and papermaking areas at eight member company mills. Exposures are scheduled before the end of 1986.

## INTRODUCTION

Structural coatings are challenged by the aggressive environments encountered in the typical pulp and paper mill. A common sight in pulp and paper mills is the degradation of coatings on beams, handrails, grating, machine supports, and other structures which rely on protective coatings for rust prevention. Conditions encountered in the typical mill — including wetness and/or high humidity, aggressive gases, and salt deposits — combine to attack many of

the coatings in current use. Some areas where corrosion is particularly severe are in the recovery and recausticizing areas, the bleach plant, and the paper machine wet end.

The cost of coating application and maintenance is a significant expense for most pulp and paper mills. The premature failure of structural coatings, coupled with the difficulty of obtaining good coating repairs in mills, often jeopardizes the integrity of beams and other structural supports. Recoating is often unsatisfactory because abrasive blasting near motors and bearings is prohibited. In many cases, proper surface preparation is impeded by salt deposition that continues after surfaces are prepared or primer coatings placed. In some cases, particularly near the paper machine wet end, contamination of paper products by rust can be a significant concern.

An impediment to good coating practice is the lack of reliable information regarding the durability of coatings in the various pulp and paper applications. To a large extent, mills rely on information provided by different coating vendors whose information may be self-serving. Furthermore, direct comparisons of the performance of alternative coatings under identical controlled conditions are often unavailable. As a result, mills are forced to select coatings for structural applications with a very poor information base.

To remedy this situation, a project has been started to evaluate and rank coatings based on their durability in pulp and paper applications. This project involves the direct exposure of coated panels in various locations in selected pulp and paper mills to determine relative coating durability. This is viewed as a long-term project; however, most of the effort occurs in association with near-term preparation and installation of the coated panels.

## PROGRESS

Since this is a new project, most of the effort to date has focused on planning and arrangements for panel preparation and installation. Contacts are being made with coating vendors to solicit their participation in the program. Additional contacts are being made with various member company mills to arrange for coupon exposure over the long term.

In this phase of the project, the performance of coatings applied under ideal conditions is being evaluated. Consequently, coating vendors are being invited to select and apply their own coatings on standard panels provided by the Institute. Details of coating application procedure will be recorded. The panels used in the program are standard KTA paint test panels, each of which contains a hole, welds, and a welded channel attachment to challenge coating durability. To simulate actual service conditions, the coatings will be scored before exposure.

In the present plan, coating panels will be exposed in eight different mills in the recovery and recausticizing area, the bleach plant, and the paper machine wet end. The recovery and recausticizing panels will be exposed outdoors in locations where saltcake from the recovery boiler stacks, moisture droplets from the smelt dissolving tank stacks, lime from the lime kiln, dew and rainwater can contact the panels. In the bleach plant, exposures will be made where panels experience chlorine and/or chlorine dioxide gases entrained in the atmosphere, as well as moisture from various sources. In the paper machine, panels will be exposed to either a splash zone at the wet end of the machine, or in the rafters above the Fourdrinier section — both of which are notorious for severe corrosion problems.

The coatings will be ranked based on visual appearance after an extended exposure period, the length of which cannot be predicted at present. The performance of the various coatings will be monitored, presumably for a period of several years, and a photographic record of coating degradation will be made. If funds are available at the close of phase 1, a second phase will be initiated in which the coating vendors will be invited to re-coat panels with degraded coatings. This will provide an assessment of the ease of re-coating and the effectiveness of coatings applied under less than optimal conditions.

#### PLANS FOR THE NEXT PERIOD

In the next reporting period, all of the coupons will be coated by the vendors and installed in appropriate locations in selected mills. A long-term examination schedule will begin with installation of the coated coupon panels.

#### SIGNIFICANCE TO THE INDUSTRY

This project will provide mills with an independent, well-controlled assessment of the long-term reliability of structural coatings for pulp and paper mill applications, when applied under ideal conditions. This information will be invaluable for the selection of optimal coatings for challenging applications in the pulp and paper mill.

THE INSTITUTE OF PAPER CHEMISTRY  
Appleton, Wisconsin

Status Report  
to the  
ENGINEERING PROJECT ADVISORY COMMITTEE

Project 3606  
CORROSION IN HIGH YIELD PULPING PROCESSES

October 22, 1986

## PROJECT SUMMARY FORM

DATE: September 5, 1986

PROJECT NO.: 3606 - Corrosion in High Yield Pulping Processes

PROJECT LEADER: D. C. Crowe

IPC GOAL:

Increase the useful life of equipment by proper selection of materials of construction and by identifying suitable process conditions.

OBJECTIVE:

Use electrochemical methods to understand corrosion and corrosion-assisted cracking processes occurring in high yield pulping to identify potential problems and solutions.

CURRENT FISCAL BUDGET: \$40,000

INTRODUCTION:

1. Description of Chemistry of TMP, CTMP and CMP liquor.

Thermomechanical pulping (TMP), chemi-thermomechanical pulping (CTMP) and chemimechanical pulping (CMP) processes are mechanical pulping processes which employ chemicals or heat or both to assist the pulping. TMP processes typically use less than 1 % chemical, CTMP processes have 1-5 % chemical in the pulping solution and CMP processes use higher chemical concentrations.

A range of chemistries with a great variety of additives is found for these processes. For the purposes of this study these chemistries will be divided into three categories: alkaline sulfite, bisulfite and acid sulfite.

Alkaline sulfite chemistries may be neutral (pH 7) or alkaline (pH 11). Solutions contain sodium sulfite ( $\text{Na}_2\text{SO}_3$ ) with sodium bisulfite ( $\text{NaHSO}_3$ ) or sodium hydroxide ( $\text{NaOH}$ ) as principal components.

Bisulfite solutions contain approximately equal amounts of free and combined  $\text{SO}_2$ , to a total  $\text{SO}_2$  about 3%. These solutions have a pH of approximately 4-6. Vapor phase cooking is widely practiced in these processes.

Acid sulfite solutions are made by absorbing  $\text{SO}_2$  into a base such as limestone, milk of lime, magnesium hydroxide, sodium hydroxide or ammonia. Ammonium, sodium and magnesium based compounds are the most popular bases. The  $\text{SO}_2$  in solution forms a mixture of  $\text{H}_2\text{SO}_3$ ,  $\text{HSO}_3^-$  and  $\text{SO}_3^{2-}$ . The total  $\text{SO}_2$  in the liquor is about 6%. The pH of these solutions is very low: about 1.5 to 2.

## 2. Problems described in the literature.

Specific corrosive species in the process may cause corrosion in TMP and CTMP equipment. These species include chloride, hydrosulfite, organic acids, sulfuric acid and other inorganic acids.

A major source of problems is the sodium hydrosulfite (dithionite) used for bleaching (5). According to Laliberte (2), it decomposes to thiosulfate and bisulfite which stimulate corrosion of the paper machine. Barton (4) has claimed that 316 and 317 stainless steel are sufficiently corrosion resistant to the hydrosulfite bleaching environment in a refiner.

Sulfuric and sulfurous acids cause very serious problems in presteaming vessels. Charlton (1) has observed pitting of 316 stainless steel and has suggested that  $\text{Na}_2\text{SO}_3$  used in the process was decomposing at the high temperature in the refiner to form  $\text{SO}_2$  which was streaming back to the steaming



vessel to form  $H_2SO_3$ . There was evidence that acid was condensing on surfaces and streaming down the sides. Sulfurous acid solutions are oxidizing in nature and so 316 stainless steel should be fairly resistant, but sulfuric acid may dissolve the protective oxide film and cause rapid attack (11). Murarka (12) has described severe corrosion problems due to  $H_2SO_4$  formed in the digester vapor space of a bisulfite chemi-mechanical pulping process. The concentration of acid formed depended on the liquor pH and the amount of oxygen present in the reactor.

Chlorides, another corrosive species may be brought in with logs transported by sea or by brackish water. Evaporation may also concentrate small concentrations of salt. Laliberte (2) has noted the importance of chlorides to pitting and crevice attack in mechanical pulping. Charlton (1) has reported an instance of chloride stress corrosion cracking in a 316 stainless steel vertical expansion joint used in a TMP operation. Another source (3) has encountered failure of a 316 steaming vessel in a TMP plant due to chloride SCC. A replacement, constructed of 904L subsequently failed. Cracking was also observed in the refiner shroud of 17-4 pH stainless steel and in casings of CF8M.

Organic acids may also cause corrosion. Whitewater may have a pH of 4-6 due to fatty and resin acids (2). Franzen (6) has noted that the low pH of condensates indicates the presence of organic acids.

Higher temperature would be expected to increase corrosion rates. Temperatures of 40-60°C are encountered in grinding and 60-90°C in hot grinding. The maximum temperature is about 135°C in open discharge mechanical pulping but may be up to 160°C at 100 psi (2). High pressures are being used without knowledge of their influence on corrosion. General increases in temperature

accompany water recycling. Lower pH would also be expected to accelerate corrosion. Alum additions to control pitch may decrease the pH (2).

Some additions are made to reduce corrosion. Sodium sulfite is sometimes added to reduce refiner plate corrosion (5). Sodium carbonate additions are also made to control pH to about 6.

As would be expected, more corrosion is encountered in CMP processes. McGovern (7) has attributed most of the problems to sulfuric acid. Condensation of  $H_2SO_4$  from spent bisulfite liquor caused failure of 304 and 316 stainless steel storage tanks. It could also form from  $SO_3$  present due to excess oxygen being used in sulfur burning. Low pH and high temperature increased the corrosion. McGovern (8) noted that bisulfite decomposed to  $H_2SO_4$ , S and water in spent sulfite liquor. This problem could be anticipated even in weaker mechanical pulping liquors. Ahlers (9) has obtained results which indicate that steels remain passive to corrosion as long as there is some free  $SO_2$  present.

Chloride is the next most common problem (8). Laliberte (2) has noted that localized attack of 316 stainless steel can occur in sulfite processes with high chloride. Both 316 with 2.75% Mo and 317 may be satisfactory in some cases but severe localized attack and stress corrosion cracking have been observed on 317L in the presence of >1000 ppm chloride. Ahlers (9) has noted that chloride will cause activation and consequently higher corrosion rates.

McGovern (8) has reported intergranular corrosion in acid sulfite and bisulfite pulping digesters. Thorpe (10) and Potter, Kesler and Teeple (11) have also noted this problem if the alloy is sensitized. The extent of this problem in CMP or CTMP processes is unknown.

Corrosion and wear of refiner plates occurs through a combination of erosion accelerated by the corrosive environment, as well as cavitation caused by localized flashing of water to steam (1,2).

### 3. Problem areas to expect, need for further studies

Lower pH apparently leads to an increase in corrosion problems. Problems can also occur in the vapor phase, but the mechanism of vapor phase attack is not known. Chlorides in the process may have a significant negative effect on materials performance. Other additives, for example hydrosulfite, cause corrosive conditions but the sensitivity to these constituents is not known.

There is a need to define what corrosion problems are anticipated in different ranges of pH and sulfite or  $\text{SO}_2$  concentration. The chemistry and its influence on the corrosion are poorly understood from the corrosion standpoint. The conditions under which sodium sulfite is corrosive should be a focus of this study.

Condensation of sulfuric acid is known to be a serious problem but the conditions for its formation are not well defined. Polythionic acid cracking may be a serious problem in the vapor phase but virtually no information is available concerning it.

Some questions which we may be able to answer: What is the optimum chemistry, from a corrosion point of view? What operational problems can cause corrosion problems? Are the present materials of construction the best choice? What is the cause of stress corrosion in these processes?

## PROGRESS:

1. Samples of TMP, CTMP and CMP filtrate from mills are being collected for analysis to determine typical conditions.

2. Polarization curves of 316 and 304 stainless steel are beginning in acid sulfite, bisulfite and alkaline sulfite solutions of concentrations typical for CMP and CTMP. Some chemistries have been identified for exploratory investigation.

## Proposed chemistries of study:

## i) Alkaline Sulfite

- a) 65 g/L  $\text{Na}_2\text{SO}_3$   
     $\text{NaHSO}_3$  to adjust pH to 7
- b) 15 g/L  $\text{Na}_2\text{SO}_3$   
     $\text{NaHSO}_3$  to adjust pH to 7
- c) 12 g/L  $\text{Na}_2\text{SO}_3$   
     $\text{NaOH}$  to adjust pH to 10
- d) 8 g/L  $\text{Na}_2\text{SO}_3$   
     $\text{NaOH}$  to adjust pH to 10

## ii) Bisulfite

- a) 30 g/L  $\text{NaHSO}_3$   
     $\text{SO}_2$  to adjust pH to 4
- b) 12 g/L  $\text{NaHSO}_3$   
     $\text{SO}_2$  to adjust pH to 4

## iii) Acid Sulfite

- 30 g/L  $\text{NaHSO}_3$   
120°C  
 $\text{SO}_2$  to adjust pH to 1.5

3. A test cell for high temperature tests constructed of Hastelloy C276 has been designed and ordered. It will be resistant to the worst conditions we expect and will permit us to test performance of stainless steels.

#### FUTURE PLANS:

1. Weight loss and potential monitoring at 90 and 150°C (the temperature expected within a refiner) is planned. Stainless steel 304 and 316 will be tested in the liquid and vapor phases.

2. Slow strain rate tests will be performed at 150°C for 316 stainless steel to determine the susceptibility to stress corrosion cracking in the liquid and vapor phases.

3. The effects of various chemical additives on corrosion of plate and case materials will be studied in the most troublesome cases. Additives to be considered include  $\text{Na}_2\text{S}_2\text{O}_4$ ,  $\text{Na}_2\text{CO}_3$ ,  $\text{Al}_2(\text{SO}_4)_3$ ,  $\text{H}_2\text{O}_2$  and  $\text{NaCl}$ . Effects of  $\text{Na}_2\text{S}_2\text{O}_3$ , organic acids, carbonate and sulfide will also be investigated.

4. For the most aggressive environments, alternative materials which may be employed to solve a specific problem will be ranked.

## REFERENCES

1. Charlton, R. S. Materials Perf. 17(10): 27-35 (1978).
2. Laliberte, L. H. Pulp Paper Ind. Corr. Prob. 2: 1-11 (1977).
3. Private communication, April 1986.
4. Barton, R. W., Tredway, C. M. Pulp Pap. 53(6): 180-181 (1979).
5. Kindron, R. R. Pulp Paper 54(11):127-130 (1980).
6. Franzen, R. G. Pulp Paper 57(6):113-117 (1983).
7. McGovern, S. D. Matl.Perf. 18(1):27-31 (1979).
8. McGovern, S. D. Pulp Pap. Ind. Corr. Prob. 3:60-65 (1980).
9. Ahlers, P. -E. Pulp Pap. Ind. Corr. Prob. 3:66-71 (1980).
10. Thorpe, P.H. Pulp Pap. Ind. Corr. Prob. 4:48-52 (1983).
11. Potter, G. J. C., Kesler, R. B. Teeple,H.O., TAPPI 41(2):183A-195A (1958).
12. Murarka, S. K., Dwars, W. T. A., Langlois, J. F. Pulp Pap. Ind. Corr. Prob. 5:187-192 (1986).

THE INSTITUTE OF PAPER CHEMISTRY  
Appleton, Wisconsin

Status Report  
to the  
ENGINEERING PROJECT ADVISORY COMMITTEE

Project 3384  
REFINING OF CHEMICAL PULPS FOR IMPROVED PHYSICAL PROPERTIES

October 22, 1986

## PROJECT SUMMARY FORM

DATE: September 22, 1986

PROJECT NO. 3384 - Refining of Chemical Pulps for Improved Physical Properties

PROJECT LEADER: Ted Farrington

IPC GOAL: Develop ways to measure and control manufacturing processes.

OBJECTIVES:

1. To develop on-line techniques for measuring key process parameters controlling refiner performance with special emphasis on monitoring refining intensity.
2. To develop an understanding of relationships among fiber stock, refiner process variables (operational and design) and product physical properties which is sufficient to allow optimal control of the refining process.
3. Develop a refining model which can be used to predict the effect of refining and pulp variables on property development.

CURRENT FISCAL YEAR BUDGET: \$150,000

SUMMARY OF RESULTS SINCE LAST REPORT: (March, 1986 - September, 1985)

Approach

In current practice low intensity refining may lead to good fiber development, but is very energy intensive. High intensity refining is more energy efficient, but may lead to increased fiber cutting and fines production. A better understanding of factors which influence stresses seen by individual fibers, and fiber response, would allow us to determine optimal operating stress levels. Such information could lead to improved refiner design and operation.



When coupled with an "intensity sensor", this knowledge would improve control of fiber development and energy utilization, especially in the case of more sensitive pulps. Previous work on this project has been directed toward developing such a sensor for industrial use.

### Progress

At the last review a four-variable, orthogonal, rotatable experiment had been completed with the Valley beater. Control variables were load, beater speed, consistency, and time. Measured process variables included torque, gap, and pressure as seen by a small strain gage device placed within the beater bedplate. Pulp properties measured included freeness and fiber length distribution. Handsheets were produced and extensively tested for traditional physical and strength properties as well as all ultrasonic properties.

The goal of this study was to assess the utility of the embedded pressure transducer concept for monitoring pulp quality. Also, specific relationships among fundamental pulp properties, process variables, and final sheet properties were sought.

While sheet physical properties correlated well with such traditional performance measures as specific energy, any relationships between final properties and the pressure histogram data were questionable and usually not statistically significant. Correlations with fundamental fiber properties such as fiber length distribution and fines content were better than those with pressure histograms but still poorer than those with specific energy.

Two reasons were considered for the poor correlation between sheet properties or pulp quality and pressure histogram data. A piezoelectric transducer was obtained to increase signal to noise ratio as data from the "homemade"

strain gage device were quite noisy. While initial data from the PZ were much cleaner than from the strain gage, signal to noise ratio deteriorated with time until the point in a few hours when PZ data were no better than those from the strain gage.

Sample size was also considered as a possible cause of the poor correlation between physical properties and pressure histogram data. Each histogram shown at the last review represented 500 pressure readings taken one per revolution at the same physical location. This number was increased to 2000 in an attempt to decrease variability. The effect was not sufficient to significantly improve correlations of other parameters. Also, this approach became impractical as it required several minutes to acquire the data for one experimental point which should correspond to some moment in time.

In the final analysis, it was concluded that collecting 500 (or 2000) pressure readings once per revolution at one point in the Valley beater was not sufficient to characterize a process with so much inherent variability. Final sheet properties correlate best with measurements such as pulp freeness and specific energy which represent averages over millions of data points. Some correlation can be found with fundamental fiber properties which are typically averages over several thousand fibers. Correlations with measurements of such small sample size as the pressure data can be expected to be poor.

The possibility of placing several pressure transducers in the bedplate to increase statistical significance was considered. While this might prove an interesting experiment on the Valley beater, it was felt that ultimately the installation of such sensors on a commercial refiner would prove impractical. At this point Valley beater work to test pressure sensors for use on the 16-inch refiner was terminated.

Two activities have been pursued since the time of the last pressure transducer test. A significant amount of work has been done to complete development of the 16-inch double disk refiner system to provide a valuable research tool. Secondly, results of the first beater trials suggested a second set of tests to better understand the relationship between sheet properties and specific energy.

The first Valley beater tests showed that some specific energy parameter could be used to reduce essentially all the data obtained from a wide range of beater operating conditions to one operating curve. An important question to be answered on the 16-inch refiner is "Can some specific energy parameter be used here to correlate results taken over a wide range of operating conditions including variable plate design?" Obviously the range of operation of the Valley beater is quite limited compared to the refiner since "plate design" is fixed. As a preliminary test of the applicability of some specific energy parameter over a broader range of operating conditions some method was sought to significantly alter the normal operating mode of the Valley beater. This was accomplished through the addition of a chemical dispersing agent.

The final set of Valley beater trials is now complete and physical properties are being measured. A four-variable experiment very similar to the first set of tests has been conducted with and without the chemical dispersing agent. Two interesting hypotheses are being tested in this work. The first is that some specific energy parameter exists which is capable of reducing the data obtained at even these very different operating conditions. Secondly the addition of a dispersing agent may change the basic beating mechanism for one which works on fiber flocs to one which works on individual fibers. This may have some effect on the physical properties-operating variables correlation.

Work with the double disk refiner continues and will represent the major commitment of future time on this project. A significant amount of effort has gone to tightening the tolerances (such as plate gap variation) of the commercial refiner to turn it into a valuable research tool. The entire rotor positioning assembly was rebuilt to maintain parallelism of plate gap to within  $\pm 0.001$  inches. Several successful shakedown trials of the refiner have been conducted. Arrangements have been made to acquire refiner plates of several different designs for use in experiments. A very high speed data acquisition system will be connected to the many sensors on the machine in the next few weeks. A special full-stream sampling system, now verified as a very good system, will be automated shortly. Synchronization of the automatic sampling system and the data acquisition will permit rapid assessment of performance at a given operating condition. This will greatly reduce the cost and time for experimentation, major factors in the overall cost of refining research.

All future work will shift to the disk refiner with no further Valley beater work now planned. Progress in this area will depend on manpower availability.

THE INSTITUTE OF PAPER CHEMISTRY  
Appleton, Wisconsin

Status Report  
to the  
ENGINEERING PROJECT ADVISORY COMMITTEE

Project 3479  
HIGHER CONSISTENCY PROCESSING

October 22, 1986

## PROJECT SUMMARY FORM

DATE: September 1, 1986

PROJECT NO. 3479 - Higher Consistency Processing

PROJECT LEADER: Ted Farrington

IPC GOAL:

Reduction in complexity of forming systems.

OBJECTIVE:

To develop experimental and computational techniques necessary to better understand the behavior of fiber suspensions over a range of consistencies encompassing both current and potential future operations.

Ultimately to apply a better knowledge of fiber suspension micro-rheology to increase paper machine wet-end consistencies from current levels of 0.1-1.5% to 2.0-10%, depending on grade, without loss of machine speed or paper physical properties.

CURRENT FISCAL YEAR BUDGET: \$150,000

SUMMARY OF RESULTS SINCE LAST REPORT: (March, 1986 - September, 1986)

Approach

Our investigation of forming processes comprises three activities which when considered together will eventually produce a more fundamental understanding of the controlling mechanisms involved while also allowing for early testing of promising MC forming concepts. These three activities are as follows:

1. An experimental investigation of the microrheology of concentrated fiber suspensions during high speed flows - A major problem in all previous attempts at MC forming is lack of control of fiber orientation distribution within the MC headbox, and resulting sheets. Our basic strategy is to attack this problem from a more fundamental standpoint beginning with the development of some technique to actually observe fiber orientation in the bulk flow. This technique will then be used to study the fiber orientation distribution in concentrated suspensions during well controlled high speed flows.

At the last review, flash x-ray radiography was shown to be a technically feasible method for imaging tracer fibers in the high speed flow of concentrated fiber suspensions. More specifically, the ability to image 25 micron metal fibers in a 2% paper fiber suspension with a velocity on the order of 10 m/s was demonstrated with a commercial 300 kVp flash (30 ns) x-ray system from Hewlett Packard. An experimental system (150 kVp, 30 ns) at Lawrence Livermore National Laboratories (LLNL) demonstrated the ability to image under 12 micron diameter fibers.

As discussed at the time, while the technique has clearly demonstrated the potential to serve as a powerful tool for the investigation of MC forming and other processes, several technical issues must be resolved before the technique is proven. At the top of the list of issues is the need to identify believable tracer fibers which are imaged by x-ray but behave hydrodynamically as the bulk paper fibers.

2. Empirical testing of promising MC headbox designs - Our understanding of the problems involved in MC forming is largely secondhand and not based

on direct experience. To better understand these problems and allow testing of promising concepts in parallel with more fundamental studies, we are proceeding with empirical MC former trials.

3. Computer simulation of turbulent fiber suspension flows - This activity is directed toward a better understanding of the development of fiber orientation and structure at lower consistencies. Recent developments in computer technology and numerical techniques have produced the ability to dynamically simulate 3-dimensional turbulent fluid flows in several simple geometries. These Large Eddy Simulation (LES) techniques display many of the qualitative and quantitative features observed experimentally in turbulent flow studies. Our long-term objective is to employ this technique to give the first quantitative information regarding the relative importance of fiber-fiber and fiber-fluid interactions.

In summary, our approach is to attack the MC forming problem with parallel efforts taking more fundamental and empirical approaches. At the last review, the possible application of x-ray radiography to other problems was discussed and demonstrated a case of spray nozzle imaging. There appear to be several such applications of practical importance. Some time is being devoted to identifying a few of these and quickly assessing the potential utility of x-ray imaging.

#### Progress Since Last Review

Flash x-ray imaging at IPC - Results presented at the last review were obtained during visits to LLNL and to HP (with a portable flow loop). Results were sufficiently encouraging for us to put a high priority on obtaining one or both of these devices for use at IPC. Most of the effort since the last review



has gone into securing this capability. Both the LLNL and HP systems are now in place at IPC and undergoing preliminary testing. The HP system has been obtained via a lease agreement while the LLNL device was built by IPC personnel after visiting LLNL to obtain assembly experience.

Installation of these instruments at IPC is a major step forward for this project. A special radiation shielded room was required for operation. This facility was designed and drawings submitted to Wisconsin Department of Health for required approval prior to construction. In June IPC was issued a license for operation of flash x-ray devices. The HP system arrived in mid-August at approximately the same time the room and LLNL device construction were completed. The ability of this laboratory to perform high resolution flash x-ray imaging is matched in the U.S. by only LLNL.

Tracer fiber studies - A key technical issue concerning the flash x-ray technique is the availability of a tracer fiber system which is imaged by x-rays but behaves hydrodynamically as bulk paper fibers. Progress was made in this area by a visiting summer student. HP agreed to loan IPC a cabinet x-ray system for the summer. This was used to perform preliminary tracer studies and assess the potential use of very low energy x-rays for formation testing (discussed later).

By operating the cabinet (continuous source) system at energy levels roughly equivalent to that of the flash devices, we were able to assess the level of contrast to be expected from different tracer materials versus flow field depth. Among the approaches tested were:

1. very thin metal filaments which could be ultimately coated to appear as coarser paper fibers
2. synthetic films filled to various levels with fine metal powder

3. paper fibers lumen loaded with mercury
4. paper fibers lumen loaded with metal powders

Results of options 2 and 3 were particularly encouraging. In option 2, PVA films were loaded to 20 and 30% with 1-5 micron tungsten powder and clearly imaged in several centimeters of liquid. Finally, southern pine fibers were lumen loaded with mercury and imaged very clearly in several centimeters of water. Although the cabinet system is quite different from the flash devices, achievable contrasts should correlate. This effort served a very useful role in screening potential tracer systems and in overcoming the most significant technical hurdle in this work.

Empirical tests of MC former on pilot machine - Several options for getting hands-on exposure were considered. An experimental and untested headbox existed at IPC prior to this investigation which could be used. A second approach was to build a new headbox of traditional MC design. A final approach was to attempt to locate an existing headbox that had been used and proven in MC operations elsewhere.

Since our primary objective at this time was to gain some experience quickly and compare MC technology with conventional headbox performance, the last option was pursued. In the early 1980's a Department of Energy funded program in MC forming was conducted by the Thermo Electron Corporation. The objective of that work was not to improve the physical properties of MC sheets but rather to exploit the z-direction fiber orientation observed in such sheets to enhance drying. The headbox used in that work was successfully operated at consistencies in the 2-3% range at speeds of 500-1000 fpm.

Thermo Electron was approached and they agreed to give us the headbox used in that work on an extended loan basis. This device has been mounted on the pilot machine at IPC and preliminary trials are under way.

Simulation of fiber suspension flows - The potential use of LES techniques to dynamically simulate low concentration of fiber suspensions was discussed at the last review. Any such work requires supercomputer capabilities. At this time, little work has proceeded in this area with the exception of submission of a proposal to the National Science Foundation for 50 hours of Cray CPU time at the University of Minnesota.

Other potential applications of x-ray imaging - At the last review it was demonstrated that very soft flash x-rays can be employed to image fine low density liquid sprays. The realization that soft x-rays could be used in such cases for imaging low density objects has led to two brief investigations of other potential applications.

Black liquor spray nozzles - At the last review water spray images by x-ray were shown which had been obtained while at HP performing the fiber suspension investigations. It appeared that flash x-ray radiography might offer some unique capabilities for the study of large scale liquid sprays such as black liquor spray nozzles. Results were sufficiently encouraging that a short test with mill black liquor at operating temperatures was attempted in cooperation with the Recovery Systems Group. Although this experiment was funded by a project in the Chemical Sciences Division it is being mentioned here as an example of other potential uses for this novel imaging technology.

HP agreed to loan IPC a 150 kVp flash system for the month of August. Temporary shielding was set up in the Recovery Laboratory and a 30 day operating

license obtained from the state. A temporary flow loop was set up using existing pumps, tanks, and heat exchangers. Approximately 63% concentrated black liquor and a B&W nozzle were obtained from Thilmany Pulp and Paper Company.

Results were quite impressive. Concentrated black liquor sprays at normal operating conditions (230°F, 20 psig) were successfully imaged with approximately three days work with the x-ray apparatus. This short study has resulted in a proposal to the Department of Energy to purchase the equipment and required image analysis capability to execute a much needed study and developmental program in the area of improved black liquor delivery systems.

Sheet quality and formation via ultrasoft x-ray imaging - If sufficiently low energy levels are used, x-ray techniques can clearly image very low density objects such as paper sheets. Furthermore, since the relationships between object mass and x-ray absorption are well established, the technique gives true mass distribution (formation) within the sheet. The technique works regardless of basis weight and in the presence of additives or colorings. Again, very initial tests were performed during visits to HP to make fiber suspension studies.

HP agreed to loan IPC a cabinet x-ray system for some preliminary tests of this concept. Sheets up to 1000 g/m<sup>2</sup> have been successfully imaged with resolution on the order of few fiber diameters. Handsheets were made with basis weights ranging from 60 to 200 g/m<sup>2</sup> in which formation was modified by controlling suspension settling time. X-ray images clearly show variation in sheet formation.

The technique has definite promise for making quantitative determinations of sheet mass distribution as there is a simple relationship between image

gray level and mass present. It can also be used to identify contaminants such as stickies.

The cabinet system used here was also employed for the tracer studies discussed earlier. While this application is for continuous rather than flash x-rays, an interesting question is whether or not a flash device would allow on-line determinations. This idea was tested with the borrowed 150 kVp flash system and results were positive.

### Current Activities

Work is now proceeding in two major areas. The exact capabilities of each x-ray device are being assessed. The objective here is to develop an "operating manual" which can tell us exactly what resolution can be expected in flow fields of different dimensions. Armed with these results we will proceed to design and build specific flow devices for the investigation of concentrated fiber suspension flows in controlled high speed flows.

Work is proceeding with the experimental headbox. Activities in the near term are aimed toward comparing the performance of this headbox with that of a new narrow channel converflow headbox recently obtained from Beloit.

### PLANS FOR THE NEXT PERIOD:

1. A systematic assessment of each flash x-ray system's capabilities will be completed.
2. An investigation of concentrated fiber suspension microrheology in the case of converging channel flow will be undertaken with the appropriate flash x-ray system.
3. Capabilities of the Thermo Electron MC headbox and Beloit converflow headbox will be systematically investigated.

THE INSTITUTE OF PAPER CHEMISTRY  
Appleton, Wisconsin

Status Report  
to the  
ENGINEERING PROJECT ADVISORY COMMITTEE

Project 3470  
FUNDAMENTALS OF DRYING

October 22, 1986

## PROJECT SUMMARY FORM

DATE: September 1, 1986

PROJECT NO. 3470 - Fundamentals of Drying, and  
3595 - Advanced Water Removal Processes for Drying in the Pulp and  
Paper Industry

PROJECT LEADER: Hugh P. Lavery

IPC GOAL:

Reduction of the "necessary minimum" complexity (number and/or sophistication) of process steps.

OBJECTIVE:

To bring the impulse drying process to the point of commercial development by achieving the following subobjectives:

- To experimentally define the energy efficiency and properties enhancement possible with impulse drying on a range of important grades.
- To design, build, and operate rolling nip pilot equipment to demonstrate the feasibility of the process.
- To calculate the mill-wide economic incentives for the most suitable grades and process systems.

CURRENT FISCAL BUDGET:

\$100,000 for Project 3470, plus an additional \$350,000 under Project 3595 from a U. S. Department of Energy grant in the second year of a four-year, 1.5 million dollar total program.

SUMMARY OF RESULTS SINCE LAST REPORT: (February, 1986 - September, 1986)

Technical performance evaluation of impulse drying was extended to the measurement of the energy efficiency of the process. Energy aspects of impulse drying newsprint, linerboard, and high-yield CMP were investigated. Results confirm preliminary conclusions of very low BTU requirements per pound of water removed, typically less than one-half the heating demand of a conventional dryer section. The BTU/lb requirement decreases rapidly with increasing moisture ratio, and may permit economical implementation of impulse drying in typical pressing positions.

A pilot roll impulse dryer has been designed and is being built with the assistance of the DOE grant. The pilot machine will be ready for testing early in 1987.

A major progress report is being prepared and will be completed by the end of October.

## INTRODUCTION

Impulse drying has been a subject of research at the Institute of Paper Chemistry for the past five years as a promising alternative to conventional cylinder drying. The potential of the process was identified during the study of several novel drying and pressing processes, all of which had the common feature of improving dewatering by increasing the pressure driving forces for water removal from the sheet. This early comparative work was documented in Progress Report One for Project 3470, released in August, 1985. Work over the past year has involved an intense research program on impulse drying, with efforts proceeding on two fronts. First, an extensive database on properties response and energy requirements has been developed to support future economic analysis of the process. Second, a pilot roll impulse dryer has been designed and is presently under construction with the assistance of a major grant from the Department of Energy. This report will document progress in these two areas over the past six months. A comprehensive presentation of progress to date is being prepared as Progress Report Two, which will be complete by the end of October, 1986.

## IMPULSE DRYING

The characteristic features of impulse drying are the use of pressures and temperatures much above those normally used in paper drying, but with very short exposure times. The conditions required are all attainable by combinations of existing pressing and heat transfer technologies. This gives impulse drying an advantage over alternative processes, which require very long nip residence times. However, the conditions used in impulse drying promote transport and densification mechanisms which are very different from those found in conventional drying.



A conceptual sketch for a roll impulse dryer is illustrated in Fig. 1. This machine consists of a long-nip press with one of its rolls heated to between 400 and 700°F. This arrangement of equipment generates steam at high pressure at the surface of the sheet which is next to the heated surface. This burst of steam acts to displace liquid water through the sheet and into the felt. Simultaneously, sheet temperatures near the hot surface increase to levels which promote conformability and interfiber bonding. Impulse drying generally stops before the sheet is completely dry, and the vapor flashing in the sheet which results interrupts the densification process. The sheet is left with a distinctive density profile with a combination of surface density and mid-sheet bulk that is advantageous in the development of several important physical properties.

These new mechanisms of water removal and densification give impulse drying several advantages, including:

1. Drying rates 100 to 1000 times greater than in conventional can dryers. These high rates may translate into much smaller and less capital-intense dryer sections. An opportunity also is indicated for increased machine capacity through retrofit replacement of portions of existing drying sections or presses.
2. A significant component of liquid dewatering occurs, which reduces energy consumption to less than half that of a conventional dryer.
3. Excellent sheet densification. The extent of densification may be controlled by adjusting the impulse drying process variables. Densities above 1.0 gram/cc are easily attainable.

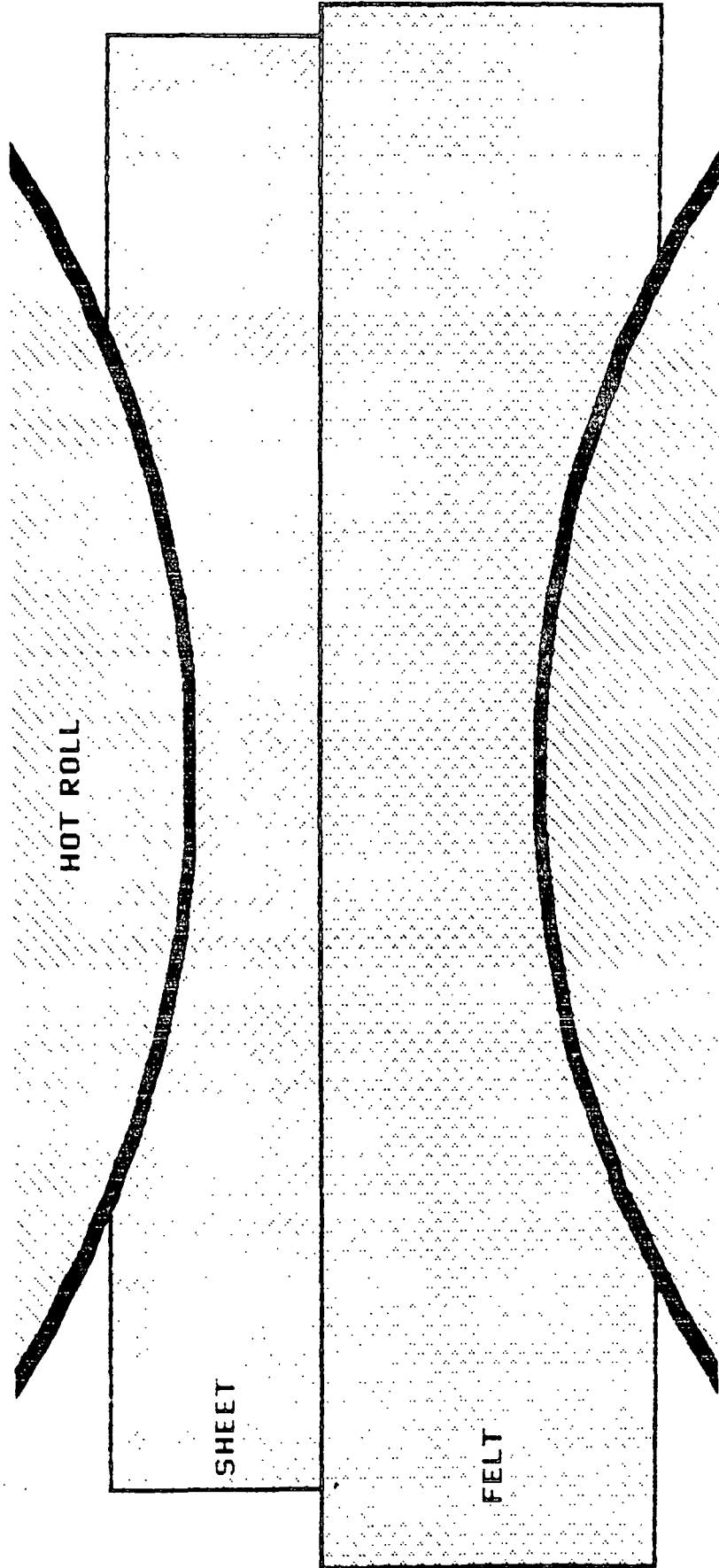


Figure 1. The impulse drying concept.

4. A unique density profile, with dense outer layers and a bulky inner layer. This structure protects optical and stiffness properties that would be lost in densification to comparable levels using conventional technology.

5. Significant improvements in surface properties including smoothness, pick resistance, air permeability, and water and ink penetration.

Most of these characteristic impulse drying advantages will be overviewed in this report; a comprehensive summary will be presented in the forthcoming Progress Report Two.

#### Project Plan

The primary objective of this project is to provide the data necessary to support and encourage commercial implementation of the impulse drying process. Figure 2 presents the project flowchart which has guided research in this area for the past two years. The program began with exploratory and feasibility work, which was completed in 1985 and documented in Progress Report One. Progress has also been made in the investigation of the fundamental processes behind impulse drying, with most of this work done in student theses. Student work completed during 1986 includes Chris Devlin's experimental study of water removal mechanisms in high-intensity drying and Steve Burton's work on sheet densification processes. These two theses provide a good quantitative description of transport and densification phenomena in impulse drying.

Recent work in the funded research area has been conducted with the support of both the Institute's dues-funded program and with a grant from the Department of Energy. The four-year, 1.5 million dollar DOE grant is being used

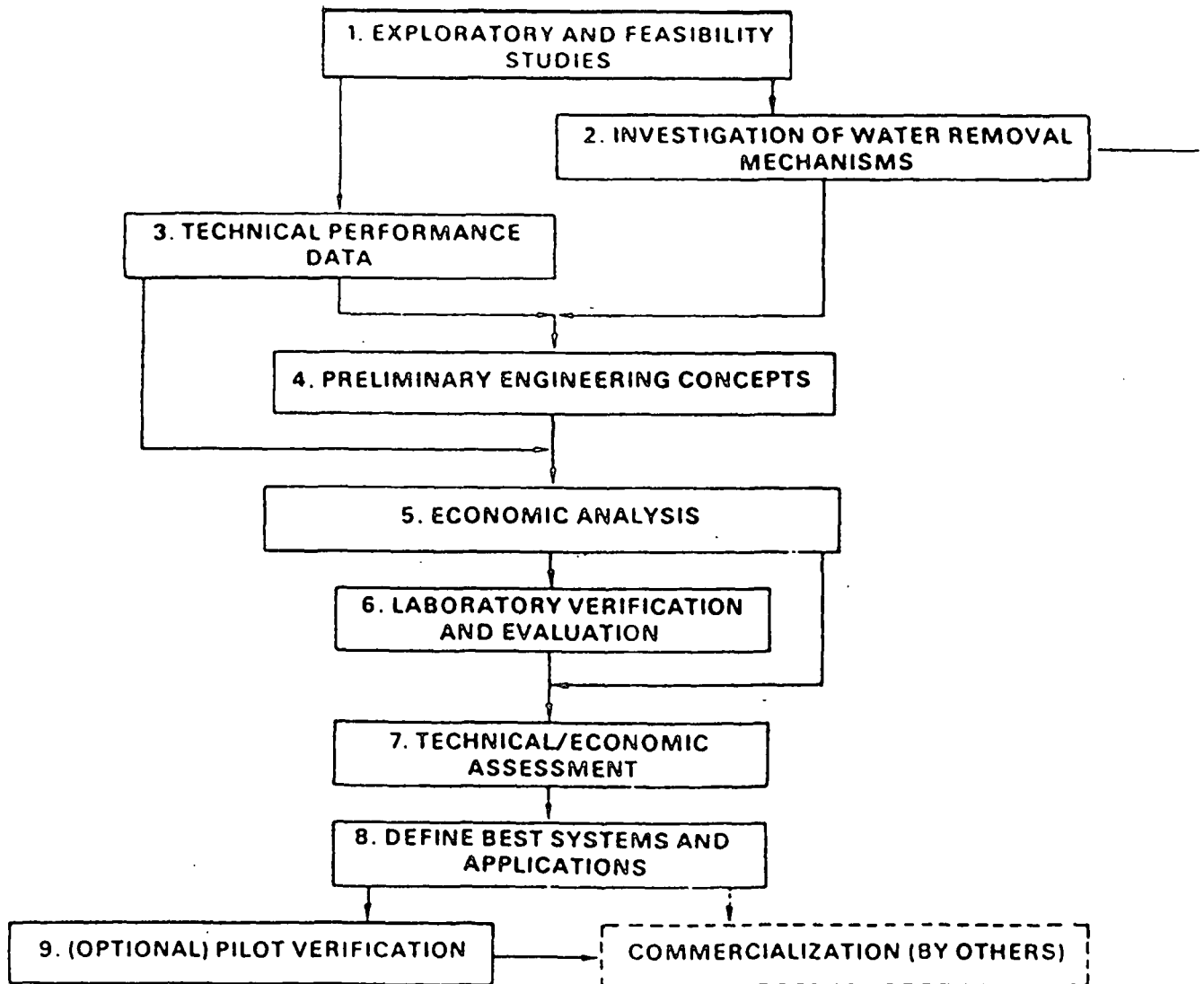


Figure 2. Project plan flowsheet.

largely in support of the design, construction and testing of a roll impulse dryer at the pilot scale. This pilot impulse dryer will be used in step 6, the laboratory verification and evaluation of the process, and has led us through the preliminary engineering concept stage planned as step 4.

The greatest amount of effort over the past year has gone into the technical performance evaluation experiments of step 3. An extensive database on properties development and energy use has been gathered on a variety of commercially important grades. The bulk of the properties results were reported in previous PAC meetings, and will be documented in Progress Report Two. This report will overview only typical results which illustrate process capabilities. New data in the performance area involve the energy effectiveness of the process and provide the data on utilities requirements which are a prerequisite for the economic analysis of the process (step 5). Some additional physical properties studies have been run, but the results have not yet been returned from physical testing. These experiments will be reviewed at the meeting.

#### PROGRESS ON TECHNICAL PERFORMANCE EXPERIMENTS

Impulse drying appears applicable to a wide range of commercially important grades. To understand the performance of impulse drying and to determine its best applications, a database covering a wide range of paper grades, furnishes, and operating conditions has been gathered. The data needed include water removal rates, densification, physical properties, and energy consumption. These data have been used directly in the design of the pilot roll impulse dryer mechanical and heating systems, and will find further use as we explore the economic consequences of impulse drying.

The studies as a whole have covered a selection of grades which represent over 70% of the total U.S. paper and board production. These grades are

summarized in Table 1. The recent studies on energy efficiency have been restricted to a further subset of these grades due to the experimental difficulty and time requirements of the methods used. Energy data is so far available only for linerboard, newsprint, and a high yield chemi-mechanical pulp.

Table 1. Grades tested to date.

- Lightweight Coating Rawstock
- Writing Papers
- Newsprint
- Tissue
- Corrugating Medium
- Linerboard - Virgin Kraft
  - Recycled Fiber (100% OCC)
  - CMP (74% & 88% Yield)

The properties and energy studies were both done on a bench-scale impulse drying simulator, which is illustrated in Fig. 3. This device consists of a heated upper platen and a Materials Testing Systems (MTS) electro-hydraulic system to deliver the pressure pulse which simulates the pressure history of a roll nip. With an actuator capacity of 22,000 lb force and simple adjustment of nip residence times from 10 milliseconds up, this device can simulate any impulse drying conditions desired. Standard five-inch handsheets are used, which are large enough for most standard test methods. A presteaming ring can be used to bring sheet temperatures to near 180°F.

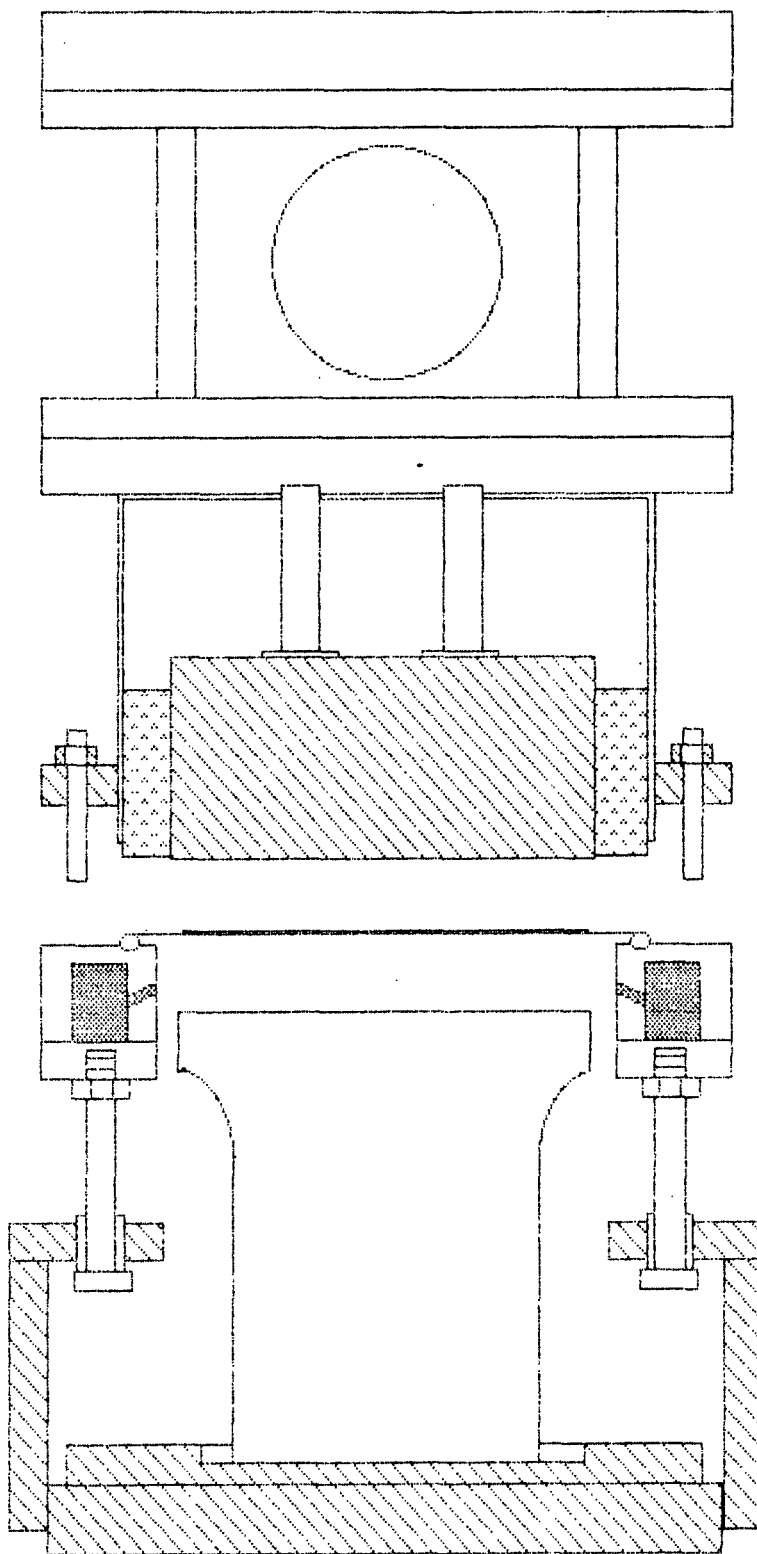


Figure 3. Sketch of bench scale impulse drying apparatus.

The procedures used in each series of physical properties tests follow a standard flowchart (Fig. 4). The energy use tests introduce a few variants into this flowchart, which will be reviewed in a subsequent section. Physical properties experiments begin with standard TAPPI handsheets made from the desired furnish. The sheets are stored at high moisture contents in refrigerated, sealed bags until they are used. Just before each impulse drying test, the sheets are wet pressed in a small roll press. Each sheet is placed between dry blotters, and passed through the press until the intended moisture ratio is reached. The wet weight is then recorded.

The sheets are then impulse dried using the equipment in Fig. 3. First, a dry, well-conditioned high-temperature Nomex press felt is placed on the lower platen. The sheet is then placed above the presteaming ring, supported by a coarse network of threads. The threads have been spaced so as not to interfere with later division of the sample for physical testing. If presteaming is used, a pre-determined pressure and steaming time is applied to bring the sheet to 180°F. The hydraulic system is then immediately activated to impulse dry the sheet. The sample is then removed, weighed, and finish dried in a low-intensity dryer which is controlled to conditions typical of conventional cylinder dryer operation. A few sheets from each pulp sample bypass the impulse drying step, and are conventionally dried in the low-intensity dryer to serve as controls on the experiment. The final sample is then conditioned and tested following standard TAPPI procedures

#### Summary of Physical Test Results

Before discussing the recent results on energy efficiency and the methodology of the energy experiments, let us briefly review the physical properties performance of impulse drying. More detailed properties data may be



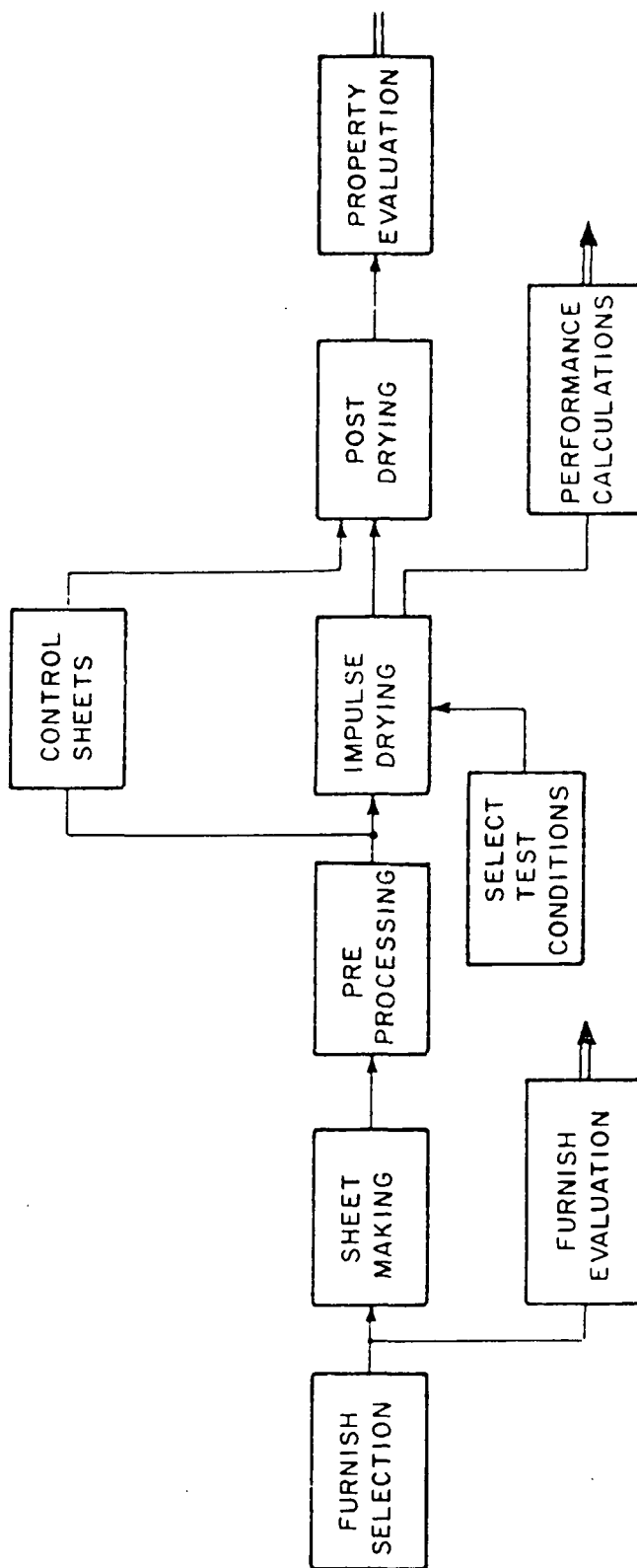


Figure 4. Elements of performance evaluation.

found in the October, 1985 PAC report, and a comprehensive presentation will be given in Progress Report Two.

### 1. Water removal rates.

Water removal rates for impulse drying are one to two orders of magnitude greater than for conventional cylinder dryers. The linerboard data in Fig. 5 is typical of all grades tested. Cylinder drying rates for this grade would be less than 10 lb/hr/ft<sup>2</sup>; impulse drying dewaterers at rates in the neighborhood of 1000 lb/hr/ft<sup>2</sup>. At any given basis weight, temperature is the dominant variable in determining water removal rates. Pressure influences the water removal rate, but its effect is relatively minor. Short nips produce higher water removal rates, but longer nips will give greater total water removal in proportion to the square root of the nip residence time. Pre-drying the sheet surface greatly reduces the water removal rate, indicating the need for water near the sheet surface in the impulse drying process. The water removal response of other grades follows the trends expected from their response to pressing. Recycled fiber linerboard dewaterers more readily, with 20% higher water removal rates. Medium, which is difficult to dewater, still exhibits impulse dried water removal rates in the 600 - 1000 lb/hr/ft<sup>2</sup> range. Implementation of impulse drying is projected to yield significant equipment simplification and capital cost reduction for all grades.

### 2. Densification

High levels of densification are easily achieved with impulse drying. Figure 6 compares the densification behavior of virgin kraft linerboard, linerboard made from old corrugated containers, and an 88% yield sulfonated chemical pulp. The excellent densification response of virgin linerboard is overshadowed by the performance of the recycled fiber and the high yield pulp,

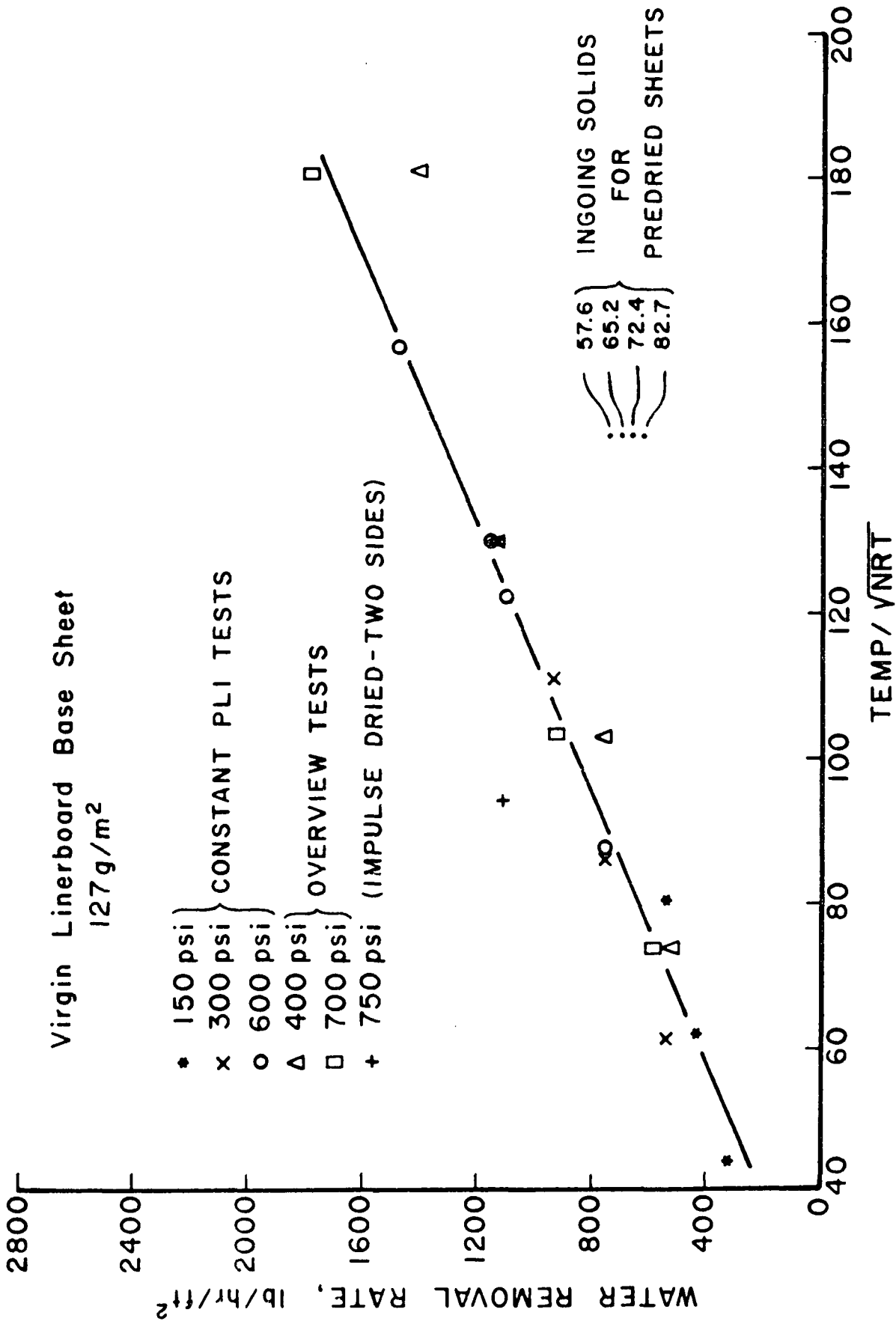


Figure 5. Water removal rates for virgin linerboard base stock.

both of which may be densified to levels comparable with conventional kraft practice. The opportunity to make equivalent product with lower quality furnishes is suggested by the density data of Fig. 6, and becomes evident when tensile strength development (Fig. 7) is considered. Other furnishes also respond well to impulse drying. The least responsive grade, corrugating medium, increased in density by about ten percent. Densification tends to vary directly with thermal impulse (temperature times nip residence time) for pressures above 300 psi; pressure has a significant effect on density development as well.

### 3. Properties development

The density increases do translate into improved strength properties, as would be expected. Figure 7 presents the tensile strength performance of the virgin kraft liner, the OCC liner, and the CMP liner. The lower-grade furnishes all may be brought to conventional kraft strengths using impulse drying. This behavior follows in other major properties, including burst and STFI index. All grades show similar significant improvements in fundamental strength properties.

The surface quality of the sheets is very good for all grades tested. Table 2 presents the qualitative response of sheet surface properties. The small effect on sheet optical properties (Fig. 8) is probably the result of the retention of bulk in the middle of the sheet. Much worse opacity losses would be anticipated, given the large increases in density. The effects on sheet brightness were minimal. The printing performance of these sheets should be excellent, but larger samples will be needed to do adequate print tests. The production of large samples for conversion tests is one of the principal goals of the pilot roll impulse dryer development effort.

Several unusual properties effects deserving further study were noted. Folding endurance of writing paper increased by a factor of two, (Fig. 9) indi-

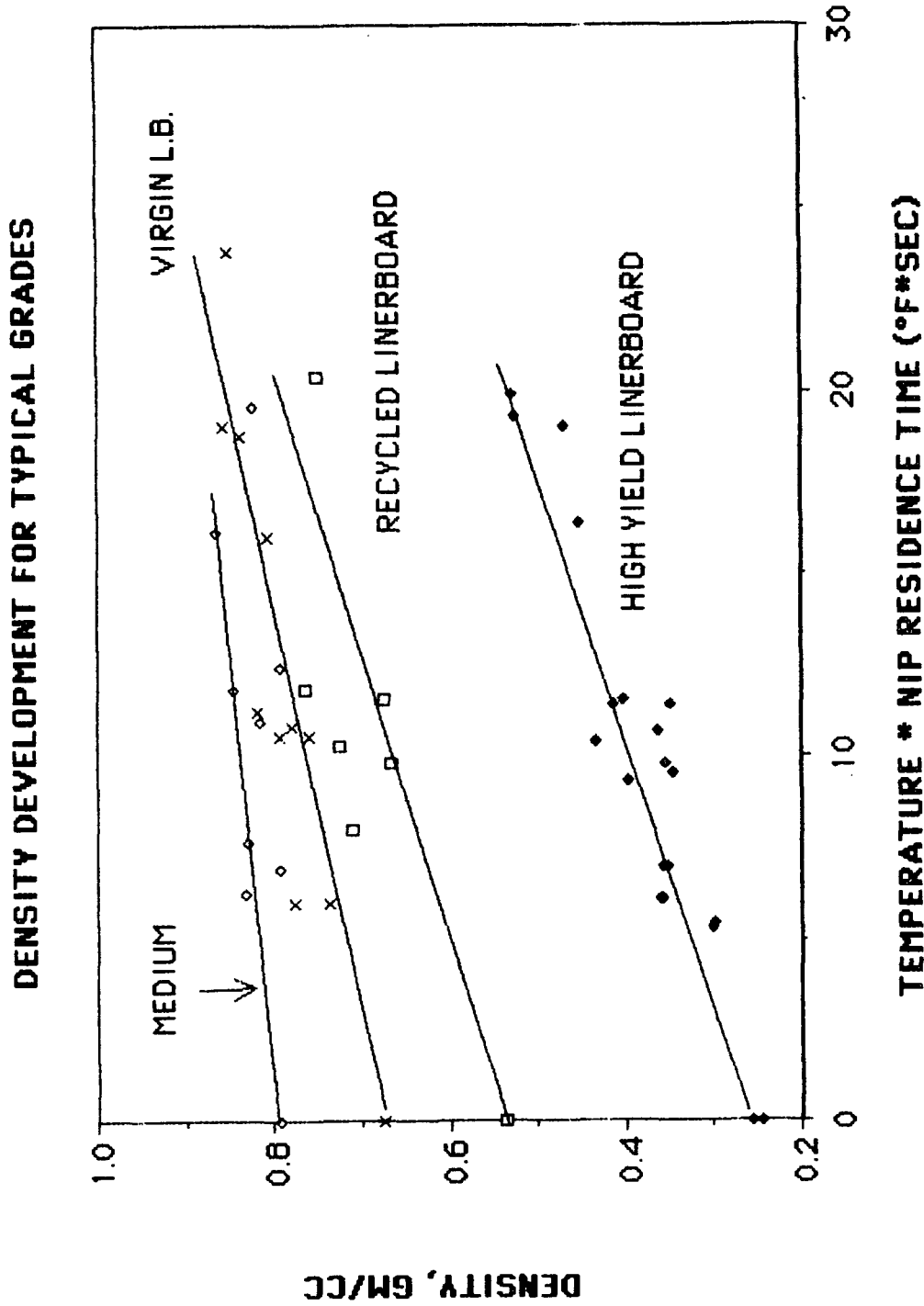


Figure 6. Density development for virgin linerboard base sheet.

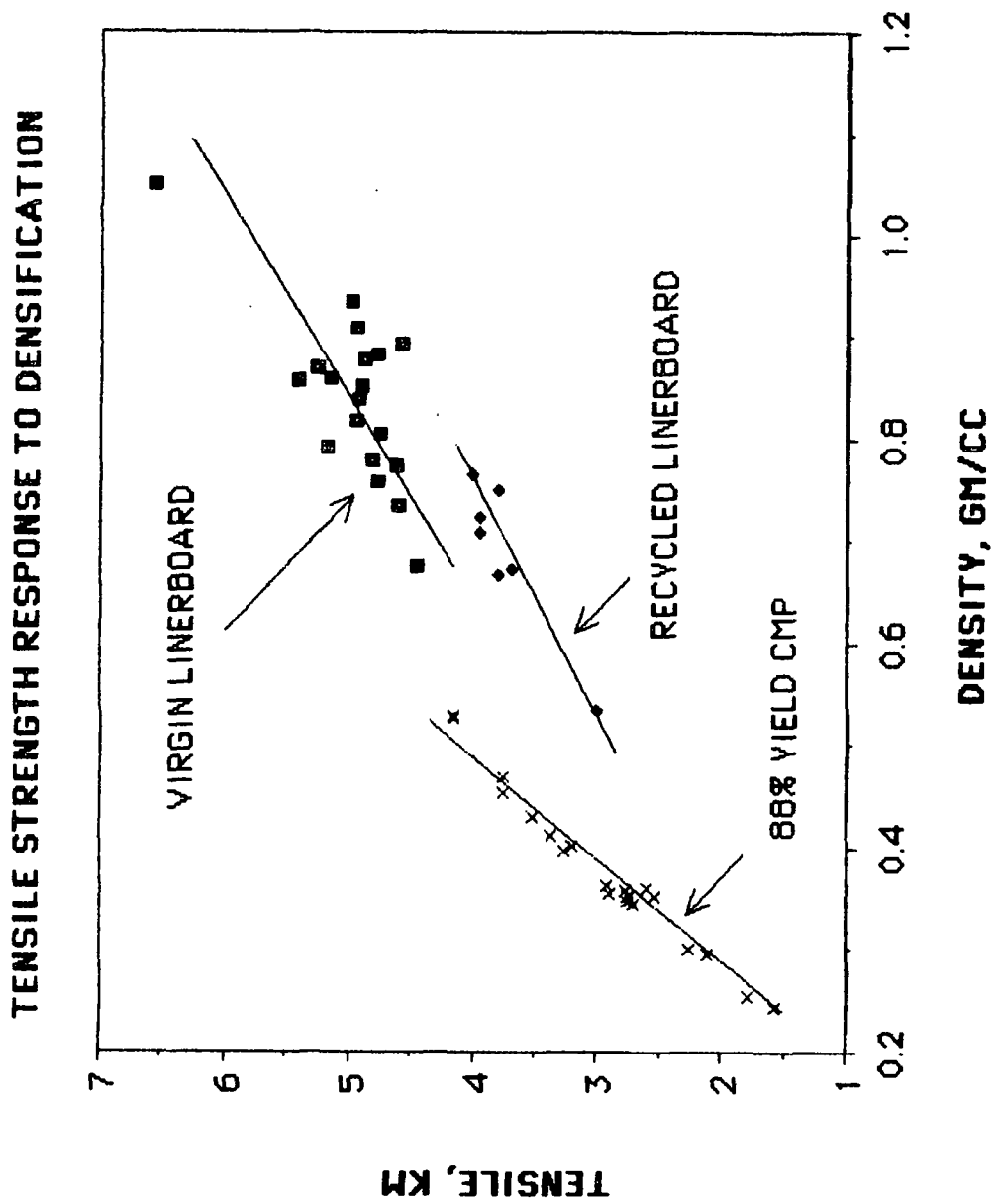


Figure 7. Tensile strength response to densification of virgin kraft, recycled OCC; and 88% CMP, all at 150 gm/cm<sup>2</sup> (25 lb/1000 ft.<sup>2</sup>).

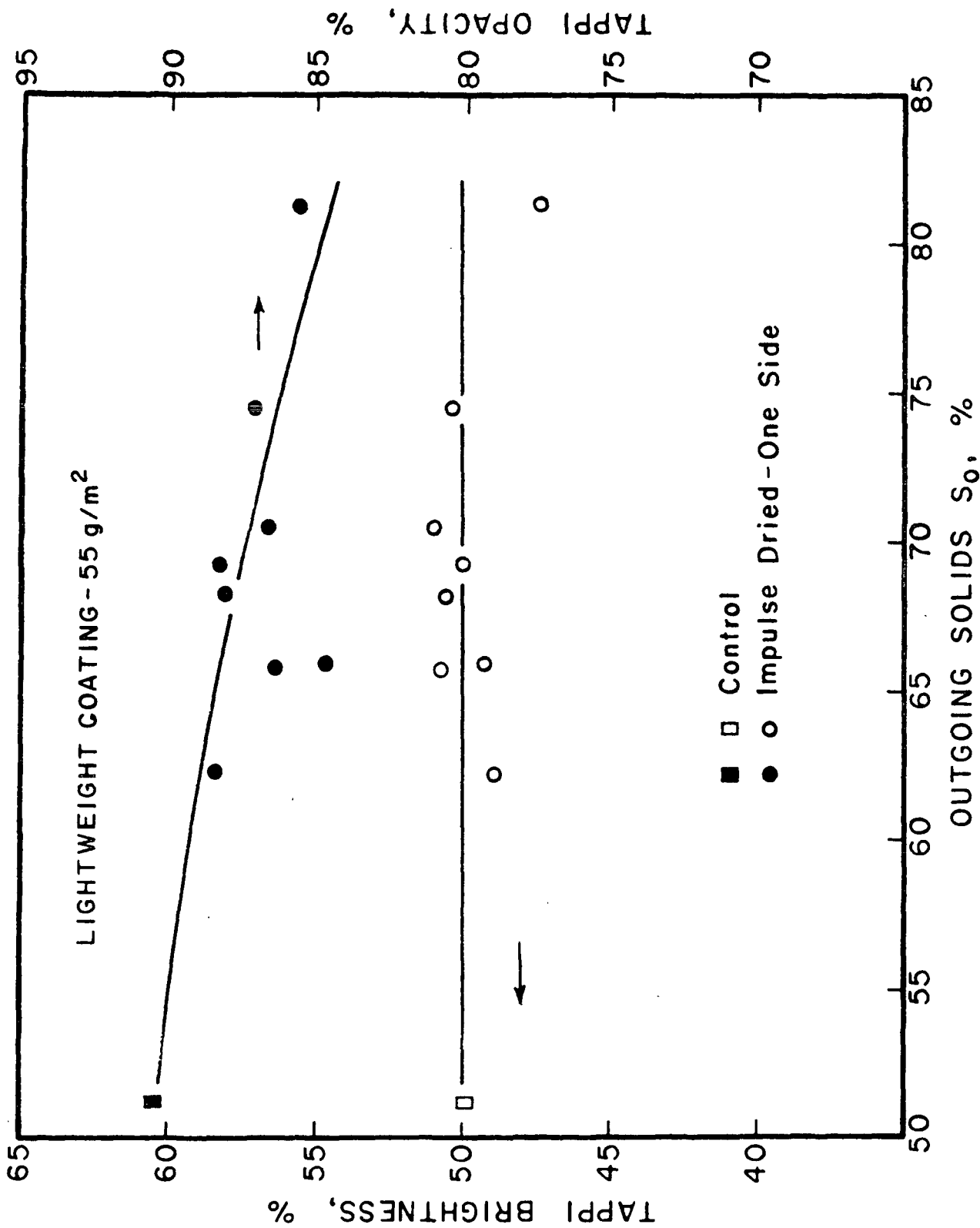


Figure 8. TAPPI brightness and pacity response to impulse drying. Coated paper rawstock.

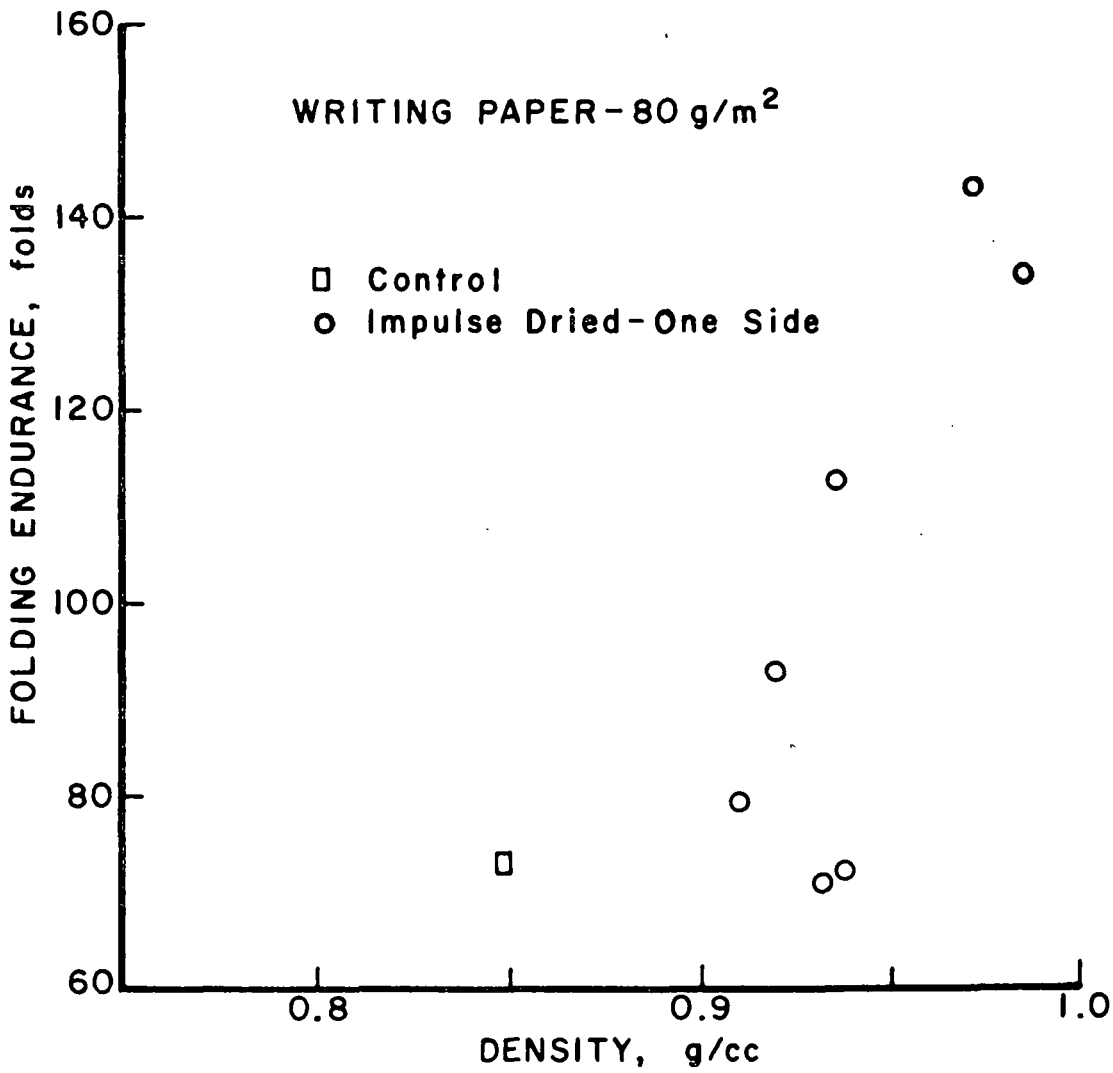


Figure 9. Fold endurance variations with density for writing paper.



cating that the sheet is not embrittled during impulse drying; this effect may derive from the unique sheet density profile. Two sided impulse drying increased newsprint tear along with the increase in tensile. Linerboard burst also showed a dramatic increase with two sided impulse drying. Further experiments to follow up on both these observations have been completed, but the results were not available at the time of this report.

Table 2. Impulse drying strongly influences a number of surface and bulk sheet properties, mostly in a beneficial and controllable fashion.

ADVANTAGE OF IMPULSE DRYING: PROPERTIES

Smoothness	↑
Porosity	↓
Absorbency	↓
Ink Penetration	↓
Pick Resistance	↑
Optical	→

CONVENTIONAL DRYING

IMPULSE DRYING

Summary Observations on Earlier Work

1. Impulse drying increases water removal rates on all grades studied to an extent that suggests major reductions in drying equipment size and cost may be possible.

2. Impulse drying increases density and strength properties to a degree that may allow significant substitution of lower cost furnishes while making equivalent product.

3. The impulse drying process can produce combinations of properties which are difficult to achieve with conventional processes. Significant opportunities for new product development are available using impulse drying.

Further Properties Studies

Additional work was performed over the past six months to expand the properties database on newsprint and linerboard. The experimental program included the effects of presteaming, two-sided impulse drying, and initial moisture ratios (0.8 and 1.2, plus lower ratios resulting from two-sided impulse drying experiments), all studied at the same two levels each of pressure, temperature and nip residence time used in the earlier experiments. The list of physical property data for each grade was also the same as in the earlier work.

The most important data from this experiment should be the confirmation of the increases in newsprint tear and linerboard burst in response to two-sided impulse drying. It will also be possible to see whether pre-steaming has an independent effect on strength development beyond what is expected from the increase in water removal. Finally, the initial moisture ratio effect on strength development can be defined, and design correlations established.

All impulse drying work on this study is completed, and the samples are being analyzed. The newsprint results should be available by the time of the October meeting.

## ENERGY EFFICIENCY STUDIES

The process of drying paper is energy intensive, and alterations in the way paper drying is done will have major impacts on mill energy balances and economics. Impulse drying demands the use of high grade energy, and will reduce or eliminate the demand for low pressure steam for paper drying. A thorough understanding of how these energy balances and cost trade-offs work is essential to the successful implementation of impulse drying. The necessary first step in developing this understanding is the measurement of the energy demands of impulse drying over the probable range of process operation.

A limited number of exploratory studies had been run in the past, which indicated that impulse drying removes substantial amounts of water in the liquid phase. Typical values for liquid water removal were in the range of 20 to 40 percent of the total water removed. However, this database was far from sufficient to support energy balance and economic calculations.

Therefore, a major series of experiments was undertaken to build a database of water removal rate data and specific energy demand (BTU/lb of water removed) from which multiple regression correlation equations could be developed for use in economic evaluations. The difficulty and cost of the experiments made it necessary to limit the grades investigated at this time. Attention was focused on linerboard, newsprint, and the high yield pulp grade which performed so well in the properties development studies.

The major goal of the studies - developing predictive equations for water removal and energy use over the likely range of operating conditions - was achieved. In addition, a surprising observation was made that the BTU/lb water removed energy costs of impulse drying decrease rapidly with increasing moisture ratio. This suggests that an earlier presupposition that impulse drying would be most economical after the press section had removed as much water as possible may not be correct. There may be economic justification for considering impulse drying for last-press rebuilds as well as for replacement of portions of conventional dryer sections. A further experimental study at high moisture ratios will be necessary to demonstrate the truth of this proposition.

#### Experimental Methods

Two independent techniques were tried for measuring heat flow to the sheet. The more successful method measured liquid water displacement into the felt using a lithium tracer technique, which will be described below. Heat

requirements were calculated from an energy balance on the sheet, given the amount of liquid water removed. This technique is reliable and gives reasonably consistent results. A second technique used a surface-junction thermocouple to measure the temperature history of the heated platen surface. Heat flow from the platen to the sheet could be calculated from the temperature history using a mathematical model of heat transfer in a semi-infinite slab initially at constant temperature. The results from this technique were not satisfactory, due to the experimental difficulty of bringing the heated platen to a true constant initial temperature. Results were erratic and generally gave very low BTU/lb values. All data reported here were gathered using the lithium tracer technique.

The lithium chloride tracer method for measuring liquid water removal was developed in its present form in Chris Devlin's recently completed PhD thesis, where a thorough analysis of its performance may be found. The flowsheet for the method is presented in Figs. 10 and 11. The pulp slurry is first treated with aluminum nitrate and the pH adjusted to 4.1 with nitric acid, if necessary. The intention of this step is to saturate the negative sites on the fibers with aluminum ions to prevent subsequent adsorption of lithium tracer ions. After allowing 12 hours for this to occur at all possible sites, a lithium chloride solution is added to the slurry. Handsheets are then formed, using dilution water made up to the same concentration of aluminum nitrate and lithium chloride as in the slurry. The handsheets are pre-pressed to the desired moisture ratio and impulse dried using the same equipment and procedures described above in the description of the physical properties experiments. After the impulse drying pulse, the felt is removed and extracted in one liter of boiling water for 12 hours. The resulting weak solution is then analyzed for its lithium content using flame emission analysis. Any lithium in the felt was

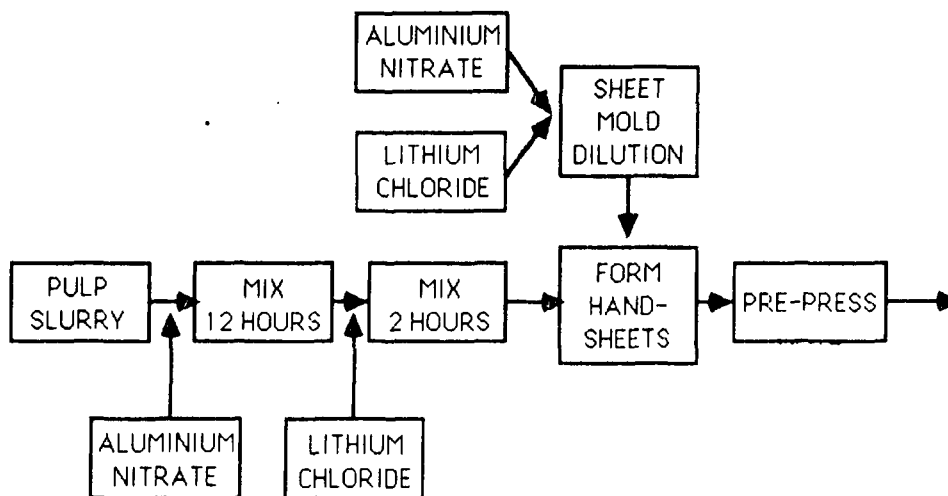


Figure 10. Preparation of high LiCl handsheets.

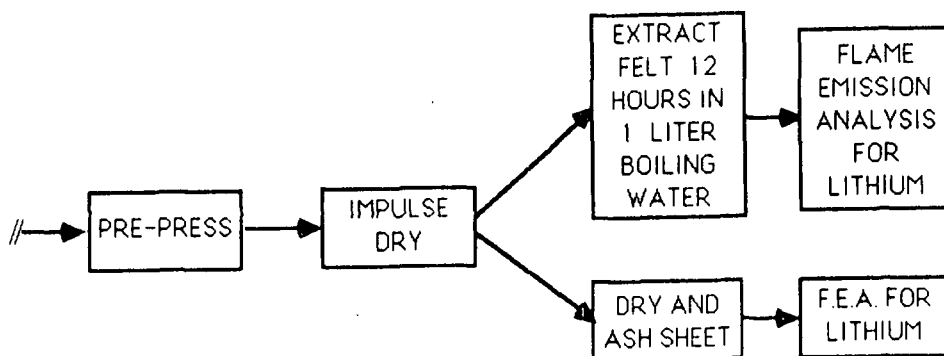


Figure 11. Impulse drying extraction and analysis of LiCl.

carried there by water, and the amount of water needed to transport the lithium is readily calculated from the initial lithium concentration in the handsheet liquid phase. It is also possible to analyze the sheet for its lithium content, but the processes of ashing the sheet and re-dissolving the ash make this approach much less reproducible.

Once the amount of liquid water removed is known, the heat required to bring the sheet to its final state may be calculated from the simple energy balance shown in Table 3.

Table 3. Specific energy transfer estimate.

$$e_{\min} = \frac{E_{\min}}{(RMR)m_{w_0}} = \underbrace{\left( \frac{C_f}{m_{r_0}} + \frac{C_w}{RMR} \right) (T_B - T_0)}_{\text{Initial sensible heating of wet web}} + \underbrace{(1 - \alpha_L)\Delta h_B}_{\text{Latent heat}} + \underbrace{\frac{C_f(T_H - T_B)}{2m_{r_0}}}_{\text{Final sensible heating of "dry zone"}}$$

- where  $C_f$  = specific heat of fiber BTU/lb/°F  
 $C_w$  = specific heat of water BTU/lb/°F  
 $e_{\min}$  = BTU/lb water removed  
 $E_{\min}$  = BUT/lb fiber heat transfer to paper  
 $\Delta h_B$  = latent heat of vaporization  
 $RMR$  = water removed/initial water content  
 $m_{r_0}$  = lbs water removed/lb fiber -  $m_{w_0} * RMR$   
 $m_{w_0}$  = initial moisture ratio (lb water/lb fiber)  
 $T_B$  = boiling temperature, °F  
 $T_H$  = final hot sheet temperature, °F  
 $T_0$  = initial sheet temperature, °F  
 $\alpha_L$  = fraction of water removed as liquid

Chris Devlin was able to directly compare the lithium chloride tracer technique and the surface thermocouple technique, which was much better behaved in his relatively slow experiments. Agreement was very good. Note that all the probable errors in the lithium chloride technique - adsorption of lithium by the sheet and felt, lithium losses in handling the samples, transport of lithium to the evaporation front by the capillary movement of water - will all tend to reduce the amount of lithium in the final analysis. These errors, if they actually occur, will make the calculated liquid water removal low and the BTU/lb values high. The technique is, therefore, conservative.

Water removal rates and energy use data were measured on the same linerboard, newsprint and high yield pulp furnishes used in the properties studies.

The range of variables studied included:

- Temperatures of 400 and 600°F.
- Pressures of 400 and 700 psi.
- Nip residence times of 15 and 25 milliseconds.
- Initial moisture ratios of 1.2 and 0.8 on the first side tested, with many lower initial moisture ratios from two-sided impulse experiments.
- One and two-sided impulse drying histories.

Most of the data was taken on sheets presteamed to 170°F.

Statistical analysis of the data was performed using the personal computer software package STATVIEW-512 for the Apple Macintosh computer.

#### Energy Use Experiment Results

The energy requirements for impulse drying linerboard, newsprint, and high yield pulp are shown in Figs. 12, 13, and 14, respectively. In these plots, BTU/lb is graphed against ingoing moisture ratio, which was the most sen-

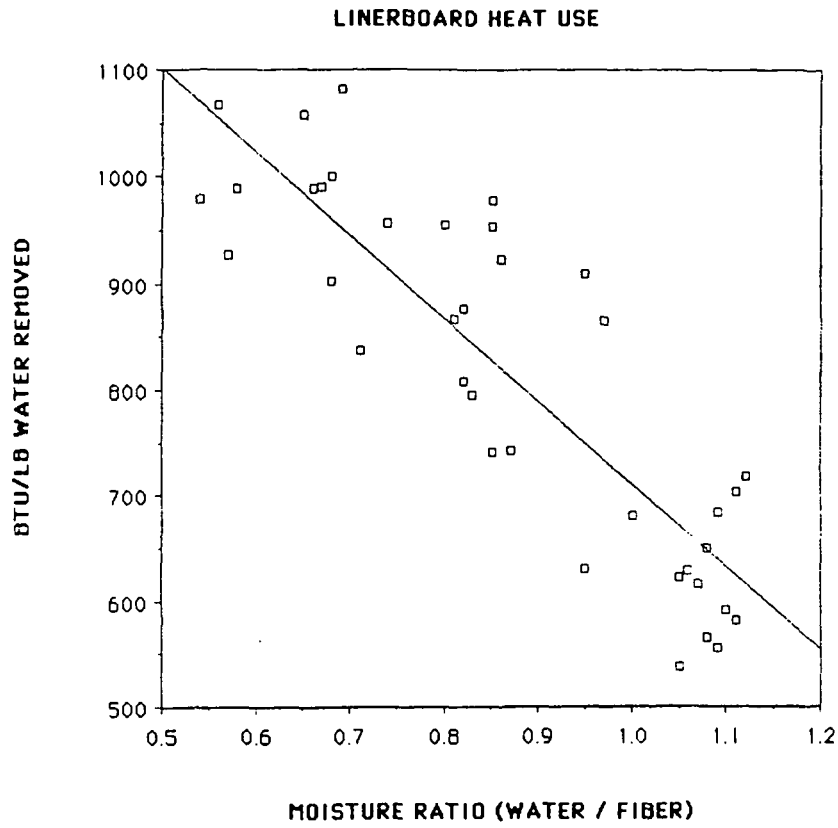


Figure 12. Linerboard energy use.

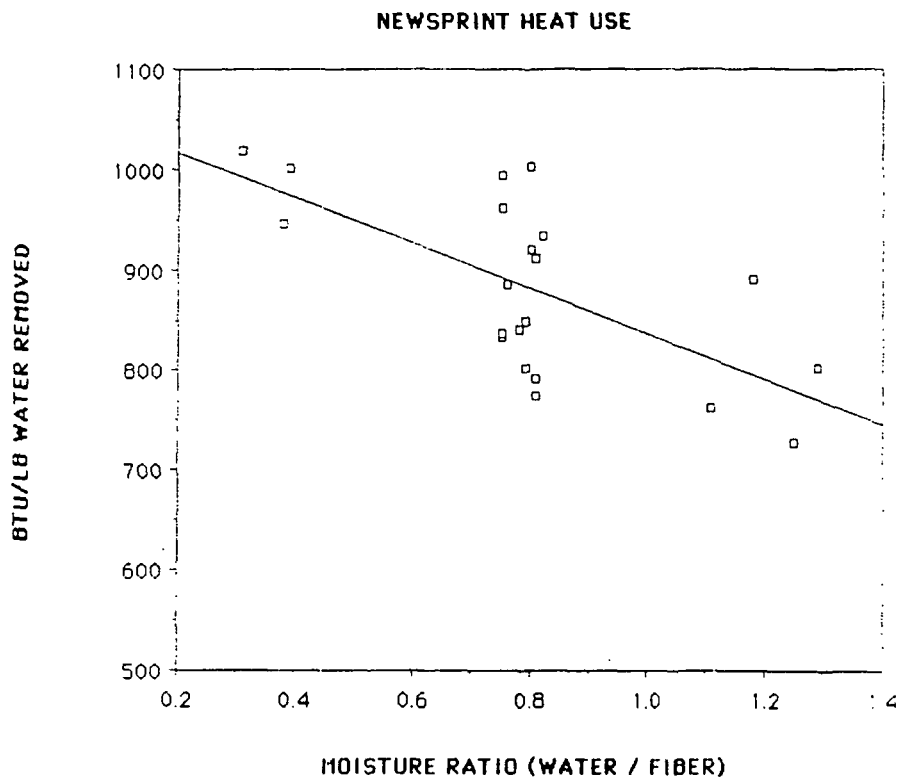


Figure 13. Newsprint energy use.



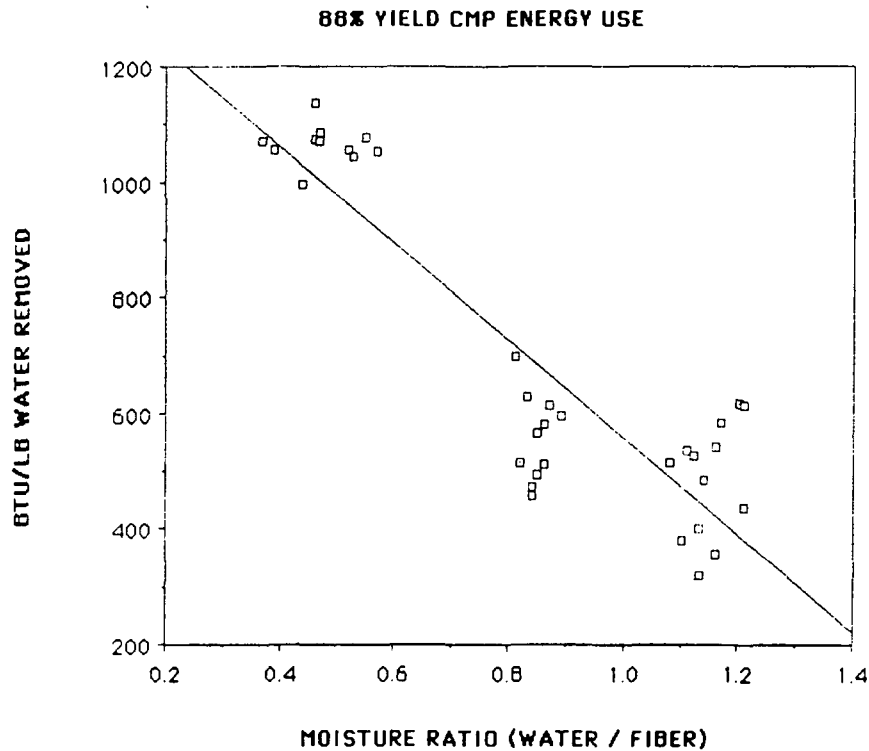


Figure 14. High yield pulp energy use.

sitive variable. The apparent scatter in the data is due to the temperature, pressure, and nip residence time range of the experiments, which can be taken into account through multiple regression analysis.

Energy requirements are all very low relative to conventional drying performance. For example, the energy balances indicated in Table 3 can be done for comparable sheets undergoing the conventional drying process. For a 125 gm/m<sup>2</sup> linerboard sheet at an initial moisture ratio of 1, energy requirements of 1013 BTU/lb are predicted for conventional drying, neglecting process inefficiencies. In practice, values closer to 1600 to 1800 BTU/lb would be observed. At moisture ratios near one, impulse drying requires 60 percent as much energy under most conditions.

The data all show the common feature of a rapid decline in the BTU/lb requirement with increasing moisture ratio. If these trends continue to hold at higher moisture ratios, impulse drying may have a role in third press rebuilds, as well as its original conceptual place as a dryer section replacement. Note that impulse drying becomes less economical at very low moisture ratios, which may indicate a lower limit of applicability of the process.

All the moisture ratio data below a moisture ratio of 0.8 were obtained by impulse drying sheets a second time on their reverse side. For linerboard and newsprint, both single sided and two sided data fall on the same line. This indicates that the sheet surface which was consolidated during the first impulse drying nip does not present a significant impediment to liquid water removal in the second nip. The high yield pulp data exhibit some curvature which suggests that its densified layer may pose more resistance to flow, but the effect is relatively minor.

Total water removal rate was also calculated from the results of the energy use experiments. These data differ from earlier results, such as those in Fig. 5, in that the sheets were preheated and a wide range of moisture ratios in the experimental design allowed moisture ratio to be included in the regression analysis. The results of the multiple regression analysis on this database is presented in Table 4. Water removal rate decreases as nip residence time increases, and increases with increasing temperature. Pressure is the least sensitive of the variables, except in the case of the high yield pulp, which probably represents an extreme case of web compressibility.

Moisture ratio has a strong effect on water removal rates. The correlation for newsprint in Table 4 has been used to construct Fig. 15, which shows the exit solids leaving an impulse dryer under the most severe conditions in the

**LINERBOARD, 125 GM/M<sup>2</sup>**  
**700 PSI, 600°F, 25 MILLISECONDS**

**PREDICTED LINERBOARD RESPONSE**

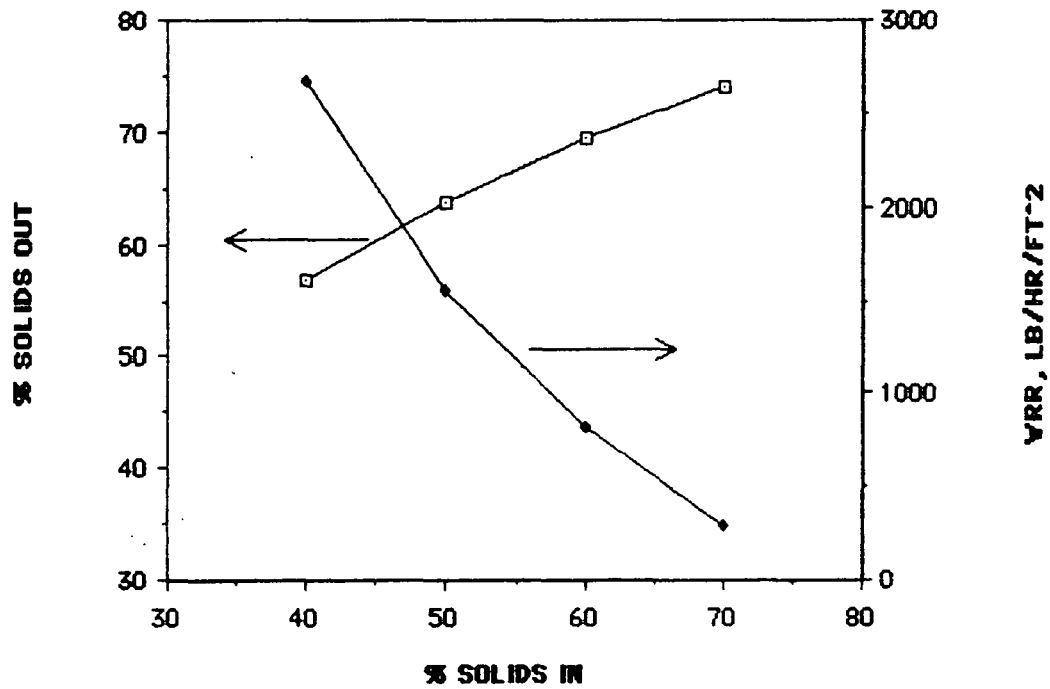


Figure 15. Linerboard response to impulse drying at varied initial % solids.

experimental plan (700 psi, 600F, 25 ms) for a range of entering moisture ratios. The moisture ratio effect on water removal tends to produce similar levels of exit dryness regardless of ingoing moisture content. This may translate to moisture-profile leveling on machine, and also suggests that a last-press position impulse dryer might do much the same job in terms of water removal as a post-press impulse dryer. Further experimentation at higher moisture ratios is required to demonstrate that this potential can be actualized.

Table 4. Multiple regression correlations for water removal rate.

$$WRR (LB/HR/FT^2) = A + B * P (PSI) + C * T (°F) + D * NRT (MS) + E * MR$$

GRADE	A	B	C	D	E	R <sup>2</sup>
NEWSPRINT	-448	.401	1.574	-30.2	1000	0.953
LINERBOARD	-2237	.804	2.218	-13.0	2223	0.922
88% YIELD CMP	-1112	1.473	.917	-71.4	3494	0.902

For purposes of impulse dryer design and economic evaluation the energy use data is more conveniently presented as BTU's required per square foot of paper processed. Multiple regression correlations for BTU/ft<sup>2</sup> are presented in Table 5. Increasing any of the experimental variables acts to increase the energy transfer to the sheet, although moisture ratio is again dominant. Figure 16 presents a preliminary calculation of the BTU/ADT requirements of impulse drying based on these correlations. The energy requirement for impulse drying increases very gradually with decreasing percent solids in comparison with the rapid increases for conventional drying. Again, installing impulse

**LINERBOARD, 125 GM/M<sup>2</sup>  
700 PSI, 600°F, 25 MILLISECONDS**

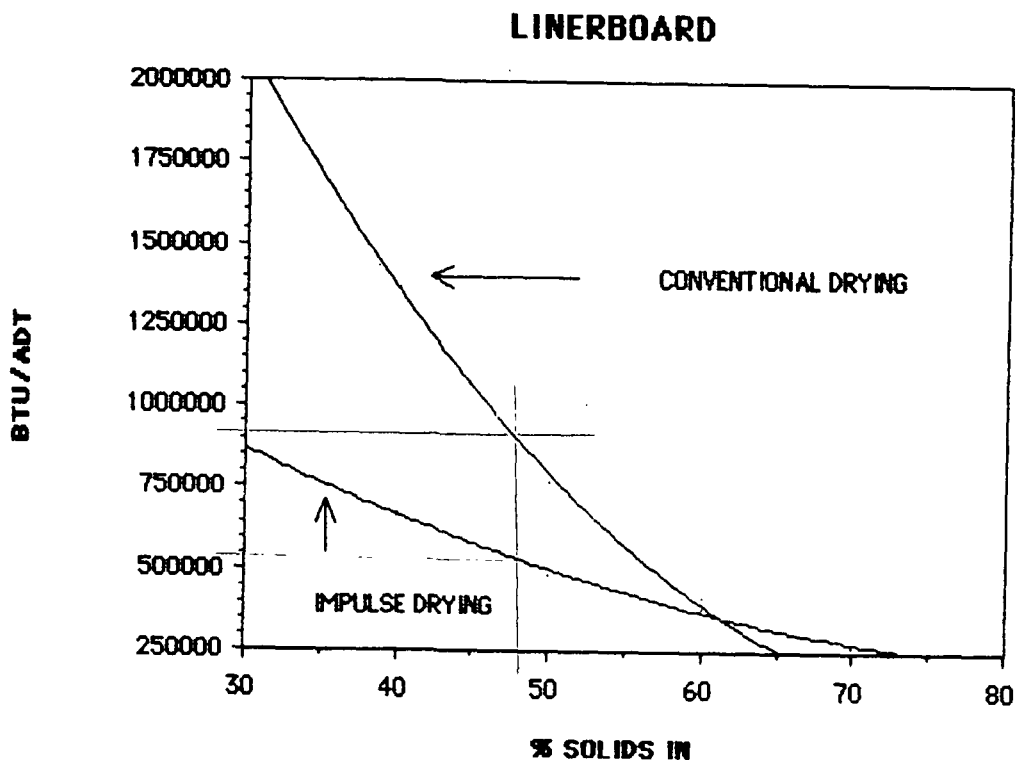


Figure 16. Effects of initial % solids on the energy use of impulse drying, compared with conventional drying to the same exit dryness attained by impulse drying.

dryers in the last-press position may make sense when a press rebuild is necessary, given the modest additional energy costs involved. Further detailed economic analysis is necessary, and will be undertaken during the coming year.

Table 5. Multiple regression correlations for energy use (BTU/ft.<sup>2</sup> of paper).

$$\text{BTU/FT}^2 \text{ PAPER} = A + B * P \text{ (PSI)} + C * T \text{ (}^\circ\text{F)} + D * \text{NRT (MS)} + E * \text{MR}$$

<u>GRADE</u>	<u>A</u>	<u>B</u>	<u>C</u>	<u>D</u>	<u>E</u>	<u>R<sup>2</sup></u>
NEWSPRINT	-4.782	.00232	.00642	.017	4.285	0.909
LINERBOARD	-7.042	.00127	.00727	.128	4.953	0.897
88% YIELD CMP	-4.880	.00379	.00205	.054	6.805	0.741

#### ROLL IMPULSE DRYER DESIGN

The other major project activity during the past six months has been the design and initial construction of a pilot roll impulse drier. This pilot scale equipment is essential in the development of impulse drying, as there are a number of important process and product performance questions that can not be addressed in the bench-scale geometry and with its sample size limits. These questions include:

1. Will the water removal and densification performance be the same in the roll geometry as in a flat press?
2. What will the energy efficiency of the process be in this geometry?
3. Will there be process problems such as sticking or delamination that will show up in a roll geometry? What will we do to correct them?

4. How will the heated roll perform metallurgically under these harsh, cyclical conditions? How will the felt perform?

5. How do impulse dried sheets perform when converted? Large samples are necessary to do meaningful evaluations of

- coating
- printing
- corrugation of medium
- combined board conversion and performance

To address these questions, a pilot roll impulse dryer is being built with the assistance of a 1.5 million dollar grant from the Department of Energy.

A sketch of the pilot unit is presented in Figure 17. The ultimate design of the dryer includes two nips, however, the first nip will be built and tested before the second nip is ordered. An unwind and rewind stand and slitter system have also been ordered, although they are not shown in the sketch.

The current status of the pilot unit is that the design and equipment ordering phase is essentially complete. Parts for most major systems have been received, and construction is underway. Startup is expected by the first of the year.

The rest of this section will give a brief description of the specifications for this device.

#### Specifications for the Pilot Roll Impulse Dryer

##### 1. Size, load and speed.

The pilot roll impulse dryer has been designed to process sheets from The Institute of Paper Chemistry web-former. These sheet samples will be delivered in roll form, with a total length of a few thousand feet. The limited sample availability makes high speed operation inadvisable, and this option was elimi-

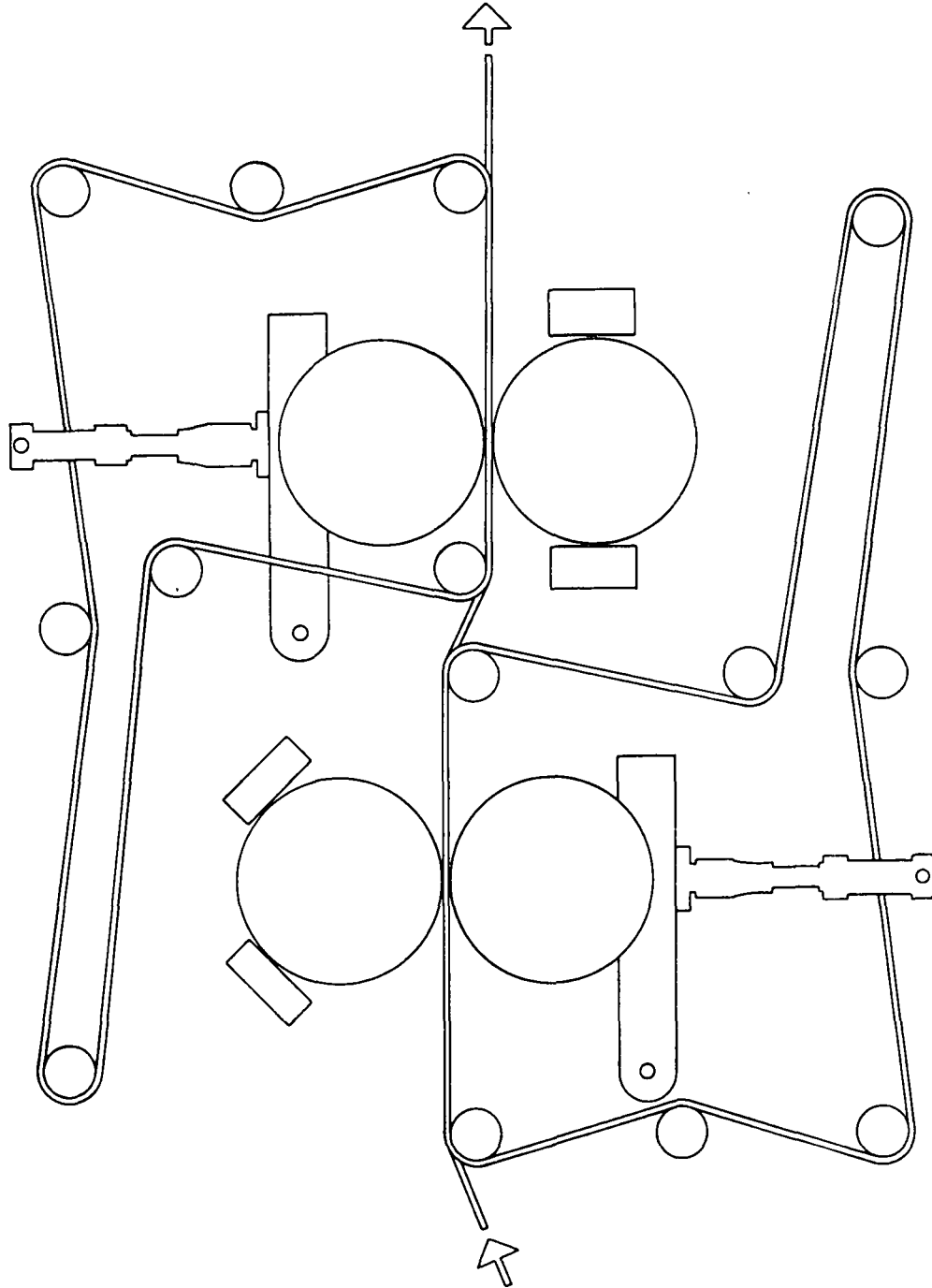


Figure 17. Pilot impulse dryer.



nated early in the design process. The web-former sheets are 12 inches or less wide, and the impulse dryer rolls were designed with a face width of 24 inches to minimize end effects. Without the constraint of high speeds, a simple nip geometry with two rolls gives adequate nip width, eliminating the mechanical complexity of long-nip press technology in this laboratory device. Calculation of the roll diameters required to give a nip width of one inch using a press felt similar to the Nomex/nylon felt used in our bench-scale studies, and loads in the 400 to 700 psi range indicated that 24 inches in diameter would be a good size for both rolls. The final size, load and speed specifications were:

- Size: 24 inch diameter main rolls with 24 inch face width.
- Speed: 350 fpm initially, which can be increased to 700 fpm with a simple belt ratio change.
- Load: Up to 1500 pli over 24 inches (hydraulic load specification will permit the pilot dryer to serve as a pilot press later, if necessary, with some modification to the rolls).

## 2. Heating system.

Although gas infrared or hot gas impingement heaters are more likely choices for mill systems, the pilot dryer will use electrical infrared. This choice was made because the easier control and turndown of electrical IR is desirable in a laboratory device. The equipment selected is of the high-temperature (4000F) lamp type; a maximum rating of 100 kw per foot of face width was chosen. This heat input is twice as high as the highest requirements calculated from our experimental data, which provides a large margin of error. Roll temperatures of 700F at the maximum expected heat load will be sustainable. The heaters are controlled in two zones across the roll face, which will make it possible to keep an even temperature profile across the roll. Temperature control will be done using the signal from surface junction thermocouples imbedded in the hot roll. The temperature controller is independent from the overall machine control system and is supplied by the heating system vendor.

### 3. Construction details.

Rolls are plain carbon steel, of hollow shell construction with bolted end plates. The roll bearings are oil-cooled spherical roller bearings. Each roll will have one oscillating doctor blade of a material softer than the roll shell at temperature.

The frame is welded and bolted construction, with machined pads for all bolted surfaces. All felt rolls, etc. can be re-positioned by changing their attachment points.

Nip pressure will be supplied by a hydraulic system. A large surge tank has been designed into the lines to permit rapid nip opening in the event of a sheet break.

### 4. Drive System

A line-shaft drive system has been designed. Variation in hot and cold roll surface speeds can be compensated for by slippage in the roll clutch as the nip is closed. A D-C drive motor will be used for speed control.

### 5. Felt runs and felts

Each felt run will include an automatic tracking system, automatic tensioning, a lubricating shower, and a vacuum box to remove excess water from the felt. The control system is designed to allow felt conditioning by continuous running through the press nip at ambient temperature. The felts will be slightly narrower than the test sheets, to protect them from the hot rolls.

### 6. Instrumentation

Control instrumentation includes surface thermocouples inside the roll for heater control, a rotational speed tachometer on each roll, load cells on each nip loading cylinder and a transducer for roll rotational position.

Additional research instrumentation includes surface thermocouples to provide temperature histories of the hot roll metal surface. A cross-shaped array of 9 thermocouples will be used to monitor cross-machine and machine-direction temperature variations. Total nip pressure will be measured by strain gage transducers in the cool roll. Five transducers will be used in a single C.D. line. Signals from all these in-roll sensors will be brought out through slip rings.

#### 7. Control and data acquisition.

Basic machine control will be accomplished through a programmable controller donated to the project by Westinghouse. This powerful device will be able to integrate all control functions required to operate the pilot roll impulse dryer.

A high-speed data acquisition system will record process data so that detailed temperature and pressure histories can be obtained for each test

#### FUTURE WORK

The pilot roll impulse dryer is expected to consume most of the project hours over the coming year. The sequence of events is difficult to predict, given the novelty of the process, but we will plan to cover the following topics:

1. Complete construction — by early January, 1987.
2. Debugging — through late March, 1987.
3. Initial tests of agreement with MTS results, probably using linerboard — through early May, 1987.
4. Top priority experiments — balance of the 1987.
5. Decision on second nip — April 1987.
6. Final design, purchase, and construction of second nip — balance of 1987.

The priority experiments would begin with those grades having significant conversion issues which we have not been able to address on the small samples available to date:

Linerboard - print quality, coefficient of friction, glueability.

Coating rawstock - drawdown performance, print quality.

Newsprint - print quality.

Corrugating medium - corrugation performance.

Water removal rates, densification, and important physical properties will be measured in each experiment.

These experiments are major efforts, involving pulp procurement, sheet forming, impulse drying, properties tests, and conversion work.

Water removal and densification data can be easily gathered over a range of pressures, temperatures, nip residence times and initial moisture ratios once a sample is available on the impulse dryer. However, we will need to be selective in the conditions sent on for physical testing and conversion. These selections will have to be made on the basis of the performance we observe on the pilot impulse dryer.

The important issue of impulse dryer performance at high moisture ratios (2.0) deserves early evaluation. This continuation of the bench-scale research program will fit into the last months of this year before the pilot scale work intensifies.

Economic evaluation of impulse drying in a whole-mill context is also a high priority for next year. One simple version - the effects of impulse drying on the economics of a simple newsprint mill using groundwood and purchased Kraft pulp - is presently being evaluated by students in a Process Design class. In addition, work will be done in this project to evaluate the economics of a simple linerboard mill.